JEFFERSON SANTANA DA SILVA CARNEIRO

BIOCHAR-BASED FERTILIZERS AS TECHNOLOGY TO IMPROVE NUTRIENT USE EFFICIENCY IN TROPICAL SOILS

LAVRAS – MG
2022

JEFFERSON SANTANA DA SILVA CARNEIRO

BIOCHAR-BASED FERTILIZERS AS TECHNOLOGY TO IMPROVE NUTRIENT USE EFFICIENCY IN TROPICAL SOILS

Thesis presented to the Federal University of Lavras, as part of the requirements of the graduate program in Soil Science, concentration area in Soil Fertility and Plant Nutrition, to earn the title of Doctor.

Dr. Leônidas Carrijo Azevedo Melo
Advisor

Dr. Juliano Elvis de Oliveira
Co-advisor

LAVRAS – MG
2022

Catalog sheet prepared by the Catalog Sheet Generation System of the UFLA University Library, with data informed by the author himself.

Carneiro, Jefferson Santana da Silva.
Biochar-based fertilizers as technology to improve nutrient use efficiency in tropical soils / Jefferson Santana da Silva Carneiro. - 2022.
185 p. : il.

Advisor: Leônidas Carrijo Azevedo Melo.
Co-advisor: Juliano Elvis de Oliveira.
Thesis (Doctor's degree) - Federal University of Lavras, 2022.
Bibliography.

1. Biochar. 2. Graphene oxide. 3. Soil fertility. I. Melo, Leônidas Carrijo Azevedo. II. Oliveira, Juliano Elvis de. III. Título.

JEFFERSON SANTANA DA SILVA CARNEIRO

BIOCHAR-BASED FERTILIZERS AS TECHNOLOGY TO IMPROVE NUTRIENT USE EFFICIENCY IN TROPICAL SOILS

FERTILIZANTES À BASE DE BIOCARVÃO COMO TECNOLOGIA PARA MELHORAR A EFICIÊNCIA DE USO DE NUTRIENTES EM SOLOS TROPICAIS

Thesis presented to the Federal University of Lavras, as part of the requirements of the graduate program in Soil Science, concentration area in Soil Fertility and Plant Nutrition, to earn the title of Doctor.

Approved on February 24th.

Dr. Carlos Alberto Silva	DCS, ESAL/UFLA
Dr. Cícero Célio de Figueiredo	FAV, UNB
Dr. Paulo Sergio Pavinato	LSO, ESALQ/USP
Dr. Leonardus Vergütz	CESFRA, UM6P

Dr. Leônidas Carrijo Azevedo Melo
Advisor

Dr. Juliano Elvis de Oliveira
Co-advisor

LAVRAS – MG
2022

To God for allowing me to realize another dream and for never forsaking me;
To my parents, Gilvan Dias Carneiro and Luciene da Silva Carneiro, and to my siblings Janaina da Silva Carneiro (*in memorian*) and Julio Cesar da Silva Carneiro, by the immense and unconditional love and incentive, especially in moments of uncertainties and difficulties;
To my wife, Dagna Ariele da Costa Leite, by all the love, support and trust you always had for me.
I DEDICATE

ACKNOWLEDGMENTS

To God, for giving us life, health and wisdom to carry out our work.

To the Federal University of Lavras (UFLA), in particular, to the Soil Science Department (DCS), at School of Agricultural Sciences (ESAL), by providing all the necessary structure for this achievement, as well as the Graduate Program in Soil Science, by the opportunity.

To the National Council of Scientific and Technological Development (CNPq), by the grant of the PhD scholarship.

To the Coordination of Improvement of Higher Education Personnel (CAPES) and to the Foundation for Research Support of Minas Gerais (FAPEMIG), by the financial subsidy to our research group.

To professor Dr. Leônidas Carrijo Azevedo Melo, my advisor, and professor Dr. Juliano Elvis de Oliveira my Co-advisor, by the support, patience, generosity and collaboration at all times.

To the members of the examining board, composed of Dr. Carlos Alberto Silva, Dr. Cícero Célio de Figueiredo, Dr. Paulo Sergio Pavinato, and Dr. Leonardus Vergütz, by the willingness to participate, by contributions and, by extreme competence in the evaluation of this thesis.

To all professors of the Soil Science Department, with whom I have learned a lot and will serve as a reference throughout my life.

To the staff of the Soil Science Department laboratories, by the spirit of solidarity, promptness, and contribution in carrying out the analyzes, in special Livia Botelho, and the secretaries who are always attentive and cordial, doing an efficient job, in special Dirce C. C. Macedo.

To all the colleagues of the program that I had the pleasure to live with, whose friendship I will take for a lifetime.

To my research group team - Aline A. Leite, Bárbara O. Nardis, Bruno C. Lago, Cristiane F. Barbosa, Dehon A. Correa, Evanise S. Penido, Gustavo M. Castro, Ivan C. A. Ribeiro, José F. Lustosa Filho, Kallil T. S. Almeida, and to my wife Dagna A. C. Leite - who contributed to the execution of these works and made it possible to obtain high-quality results based on their contributions.

To my parents, Gilvan Dias Carneiro and Luciene da Silva Carneiro, by all the support they gave me during this journey, and mainly by the trust and all the love they have always shown for me, even being so far away from home.

In general, I thank all those who helped me in the realization of this dream, and I apologize to those whom I have not mentioned since they are no less important.

Finally, to all who, directly and indirectly, contributed to the conclusion of this important journey.

♪ […] always be grateful for everything HE gave you!

It has never been luck; it was always GOD [...] ♫

(@wagaomusic)

GENERAL ABSTRACT

Highly weathered soils under natural conditions have low macro and micronutrient availability and very low efficiency for most soluble fertilizers used to overcome this issue. Therefore, we sought to develop new fertilizers technologies to increase the nutrient use efficiency, such as phosphorus (P), copper (Cu), and zinc (Zn) in tropical soils. Two studies were carried out, the first with P and the second with micronutrients (Cu and Zn). It is known the incorporation of phosphorus (P) into an organic matrix may be an effective strategy to increase plant P use efficiency in high P-fixing soils. Therefore, the objective of the first study was to evaluate the effect of biochar-based fertilizers (BBFs), produced from poultry litter (PLB) and coffee husk (CHB) enriched with phosphoric acid and magnesium oxide, in combination with triple superphosphate (TSP) on plant growth and soil P transformations. Treatments were prepared as: TSP, CHB, PLB, CHB + TSP [1:1], CHB + TSP [3:1], PLB + TSP [1:1] and PLB + TSP [3:1]; with numbers in brackets representing the proportion of BBF and TSP on a weight basis. Cultivations were: Mombasa grass, maize, and common bean interspersed with fallow periods. After cultivations, a sequential extraction procedure was employed to determine P distribution among different P pools. A kinetic study was performed and revealed that TSP released approximately 90% of total P, and BBFs less than 10% in the first hour. BBF alone or in combination with TSP presented higher or similar biomass yields, relative agronomic effectiveness, and P uptake when compared with TSP. As for the soil, BBFs increased non-labile P fractions, which can be due to pyrophosphate formed during pyrolysis. According to these results, BBFs could totally or partially replace conventional soluble P fertilizers without compromising crop yield either in the short and long-term. In the second study the effect of poultry litter biochar-graphene oxide composite (PLB-GO) as a novel adsorbent for copper (Cu) and zinc (Zn) was evaluated, as well as fertilizing effects on plant growth, nutrient use efficiency and soil fertility. In order to do so, poultry litter biochar (PLB) and PLB-GO were produced, characterized and evaluated by isotherm adsorption and kinetics to evaluate their Cu and Zn sorption and desorption properties. Cu and Zn loaded to PLB and PLB-GO as biochar-based fertilizers (BBF) were researched. PLB-GO showed higher adsorption capacity for Cu (16.2%) and Zn (17.7%) than pristine PLB and in both cases < 0.5% of the sorbed metal content was released in water. Plant effects on growth, nutrient uptake and nutrient use efficiency were, in general, as shown in the following order both for Cu and Zn: PLB-GO ≥ PLB ≥ Sulfates. PLB increased Cu availability while PLB-GO increased Zn availability after cultivation, even after increasing nutrient uptake and being little soluble in water. Addition of small amounts (≤ 0.5%) of graphene oxide in biochar has potential to increase its properties to retain micronutrients and enhance fertilizer use effectiveness in highly weathered soils. In general, both biochar-based fertilizers studied showed promising results when applied to highly weathered soils with high fixation capacity. The use of these materials increased the nutrient use efficiency by plants, showing that they have the potential for use in agriculture.

Keywords: Biochar. Graphene oxide. Soil fertility. Phosphorus. Micronutrient. Highly weathered soil.

RESUMO GERAL

Solos altamente intemperizados em condições naturais têm baixa disponibilidade de macro e micronutrientes. Fertilizantes solúveis usados para superar esse problema, em geral, apresentam baixa eficiência de uso dos seus nutrientes. Portanto, buscou-se desenvolver novas tecnologias de fertilizantes para aumentar a eficiência do uso de nutrientes, como fósforo (P), cobre (Cu) e zinco (Zn) em solos tropicais. Foram realizados dois estudos, o primeiro com P e o segundo com micronutrientes (Cu e Zn). Sabe-se que a incorporação de P em uma matriz orgânica pode ser uma estratégia eficaz para aumentar a eficiência do uso de P pelas plantas em solos de alta fixação de P. Portanto, o objetivo do primeiro estudo foi avaliar o efeito de fertilizantes à base de biocarvão (BBF), produzidos a partir de cama de frango (BCF) e casca de café (BCC) enriquecidos com ácido fosfórico e óxido de magnésio, em combinação com superfosfato triplo (SFT) no crescimento das plantas e nas transformações do P do solo. Os tratamentos foram preparados como: SFT, BCC, PLB, BCC + SFT [1:1], BCC + SFT [3:1], BCF + SFT [1:1] e BCF + SFT [3:1]; com números entre parênteses representando a proporção de BBF e SFT com base em peso. Os cultivos foram: capim Mombaça, milho e feijão-comum intercalados com períodos de pousio. Após os cultivos, um procedimento de extração sequencial foi empregado para determinar a distribuição de P entre diferentes frações de P. Um estudo cinético foi realizado e revelou que SFT liberou aproximadamente 90% do P total, e BCF e BCC menos de 10% na primeira hora. BBF sozinho ou em combinação com SFT apresentou rendimentos de biomassa maiores ou semelhantes, eficácia agronômica relativa e absorção de P quando comparados com SFT. Quanto ao solo, os BBFs aumentaram as frações de P não lábeis, o que pode ser devido ao pirofosfato formado durante a pirólise. De acordo com esses resultados, os BBFs podem substituir total ou parcialmente os fertilizantes fosfatados solúvel convencional sem comprometer a produtividade da cultura a curto e longo prazo. No segundo estudo, avaliou-se o efeito do composto de biocarvão de cama de frango e óxido de grafeno (BCF-OG) como um novo adsorvente para cobre (Cu) e zinco (Zn), bem como os efeitos da fertilização no crescimento das plantas, eficiência no uso de nutrientes e fertilidade do solo. Para tanto, foram produzidos biocarvão de cama de frango (BCF) e BCF-OG, caracterizados e avaliados por meio de isotermas e cinética de adsorção para avaliar suas propriedades de sorção e dessorção de Cu e Zn. BCF e BCF-OG adsorvidos com Cu e Zn foram avaliados como fertilizantes à base de biocarvão (BBF). BCF-OG apresentou maior capacidade de adsorção de Cu (16,2%) e Zn (17,7%) do que BCF puro e em ambos os casos < 0,5% do teor de metal sorvido foi liberado em água. Os efeitos no crescimento das plantas, absorção de nutrientes e eficiência de uso de nutrientes foram, em geral, na seguinte ordem tanto para Cu como Zn: BCF-OG ≥ BCF ≥ Sulfatos. O BCF aumentou a disponibilidade de Cu enquanto o BCF-OG aumentou a disponibilidade de Zn após o cultivo, mesmo após aumentar a absorção de nutrientes e ser pouco solúvel em água. A adição de pequenas quantidades (≤ 0,5%) de óxido de grafeno no biochar tem potencial para aumentar suas propriedades de retenção de micronutrientes e aumentar a eficácia do uso de fertilizantes em solos altamente intemperizados. Em geral, ambos os fertilizantes à base de biocarvão estudados apresentaram resultados promissores quando aplicados em solos altamente intemperizados e com alta capacidade de fixação. O uso desses materiais aumentou a eficiência do uso de nutrientes pelas plantas, mostrando que eles têm potencial para uso na agricultura.

Palavras-chave: Biocarvão. Óxido de grafeno. Fertilidade do solo. Fósforo. Micronutriente. Solo altamente intemperizado.

LIST OF FIGURES

Article 1

Article 2

LIST OF TABLES

Article 1

Article 2

LIST OF ABBREVIATIONS AND ACRONYMS

a.u.	Arbitrary unit
AFNU	Apparent fertilizer nutrient uptake
AIC	Akaike information criterion
Al	Aluminum
ANOVA	Analysis of variance
ANUE	Apparent nutrient use efficiency
ASAP	Accelerated surface area and porosimetry system
ASTM	American Society for Testing and Materials
B	Boron
BBF	Biochar-based fertilizer
C	Carbon
Ca	Calcium
$Ca(H_2PO_4)_2 \cdot H_2O$	Calcium phosphate
$Ca_2P_2O_7$	Calcium pyrophosphate
$CaCO_3$	Calcium carbonate (Calcite)
CAPES	Coordination for the Improvement of Higher Education Personnel
CHB	Coffee husk biochar
CHB100	Coffee husk biochar alone (100%)
CHB50	Coffee husk biochar (50%) + triple superphosphate (50%)
CHB75	Coffee husk biochar (75%) + triple superphosphate (25%)
cm	Centimeter
$cmol_c$	Centimol of charge
CNPq	National Council for Scientific and Technological Development
cos	Cosine
CO_3^{2-}	Carbonates
Cu	Copper
$Cu(CH_3COO)_2 \cdot H_2O$	Hoganite
$CuSO_4 \cdot 5H_2O$	Copper sulfate pentahydrate
d	Day(s)
dag	Decagram
DM	Dry mass
doi	Digital object identifier
Dr.	Doctor
e.g.	Example
EC	Electric conductivity
EDS	Energy dispersive spectroscopy
EDX	Energy-dispersive X-ray spectroscopy
Eq.	Equation
equiv.	Equivalent

Fe	Iron
Fig.	Figure
Fig. S	Supplementary figure
FTIR	Fourier transform infrared
g	Gram(s)
GO	Graphene oxide
h	Hour(s)
H	Hydrogen
H+Al	Potential acidity (Hydrogen + Aluminum)
H_2O_2	Hydrogen peroxide
H_2SO_4	Sulfuric acid
H_3PO_4	Phosphoric acid
HCl	Hydrochloric acid
HNO_3	Nitric acid
ICP-OES	Inductively coupled plasma optical emission spectrometry
K	Potassium
kg	Kilogram(s)
$KMnO_4$	Potassium permanganate
KNO_3	Potassium nitrate
KOH	Potassium hydroxide
kV	Kilovolt
L	Liter
m	Meter(s)
M	mol L^{-1}
m%	Aluminum saturation index
mA	Milliampere
MAP	Monoammonium phosphate
Mg	Magnesium
mg	Milligram(s)
MG	Minas Gerais
$Mg_2P_2O_7$	Magnesium pyrophosphate
$MgCO_3$	Magnesium carbonate
MgO	Magnesium oxide
min	Minute(s)
mL	Milliliter
mm	Millimeter(s)
Mn	Manganese
MNT	Calcium-montmorillonite
Mo	Molybdenum
Ms.	Miss

Msc.	Master
n	Replicates
N	Nitrogen
N_2	Nitrogen
$Na_2Cr_2O_7$	Sodium dichromate
NAC	Neutral ammonium citrate
$NaHCO_3$	Sodium bicarbonate
NaOH	Sodium hydroxide
Ni	Nickel
No	Number
Nº	Number
NU	Total nutrient uptake by plants from fertilized treatments
NUF	Total nutrient uptake by plants from unfertilized treatments
O	Oxygen
O.M.	Organic matter
P	Phosphorus
P_{BBF}	Dry matter production by plants under biochar-based fertilizer
PC	Principal components
PCA	Principal component analysis
pH	Hydrogen potential
PhD	Doctor
Pi	Inorganic phosphorus
PLB	Poultry litter biochar
PLB100	Poultry litter biochar alone (100%)
PLB50	Poultry litter biochar (50%) + triple superphosphate (50%)
PLB75	Poultry litter biochar (75%) + triple superphosphate (25%)
PLB-Cu	Poultry litter biochar loaded with copper
PLB-GO	Graphene oxide enriched poultry litter biochar
PLB-GO-Cu	Graphene oxide enriched poultry litter biochar loaded with copper
PLB-GO-Zn	Graphene oxide enriched poultry litter loaded with zinc
PLB-Zn	Poultry litter biochar loaded with zinc
Po	Organic phosphorus
P-Rem	Remaining phosphorus
Pt	Total phosphorus
PTFE	Teflon Polytetrafluoroethylene
P_{TSP}	Dry matter production by plants under triple superphosphate fertilizer
PV	Pore volume
r	Correlation coefficient
R5	Pre-flowering period (secondary branches and flower buds)
RAE	Relative agronomic effectiveness
rpm	Rotation per minute

S	Sulphur
SB	Sum of exchangeable bases
SDM	Shoot dry mass
SE	Standard errors for the estimative of the models
SEM	Scanning electron microscopy
Si	Silicon
SiO_2	Quartz
SIPS	Langmuir-Freundlich isotherm model
SMP	Shoe-Maker, Mclean & Pratt solution
SSA	Specific surface area
t	Effective cation exchange capacity
T	Cation exchange capacity at pH 7
Treat.	Treatments
TSP	Triple superphosphate
U.S.	United States
UFLA	Federal University of Lavras
v	Volume
V%	Base saturation index
V2	Developmental stage (opening of primary leaves)
V4	Developmental stage (third leaf trifoliate fully open)
w	Weight
wt.	Weight
XRD	X-ray diffraction
Zn	Zinc
$ZnSO_4 \cdot 7H_2O$	Zinc sulfate heptahydrate

LIST OF SYMBOLS

^{o}C	Degrees celsius
%	Percentage
^{o}	Degrees
'	Coordinates in minutes
"	Coordinates in seconds
µm	Micrometer
a	Initial desorption rate
$\sum$	Sum
$>$	Larger
$<$	Smaller
k_1	First order rate constant
k_2	Second order rate constant
t	Time
Q_t	Amount release or adsorbed measured
Q_e	Amount released or adsorbed at equilibrium
β	Desorption constant
ln	Natural logarithm
b	Desorption rate coefficient
R	Diffusion rate constant
N	Number of measurements
Q'_t	Amount release or desorbed predicted
$LL(\theta\|y,M_i)$	Log-likelihood
M_i	Model
K_i	Number of free parameters in model
ns	Not significant
$\geq$	Higher or equal
C_i	Initial solution concentration
C_e	Concentration at equilibrium
m	Mass
v	Volume
L	Crystallite size
Å	Angstrom
θ	Theta
q_m	Maximum adsorption capacity
n	Freundlich nonlinearity constant
K_f	Freundlich equilibrium constant
K_L	Langmuir equilibrium constant
K_s	Langmuir-Freundlich constant
n_s	Langmuir-Freundlich constant
R_i	Initial factor for intraparticle diffusion model
$=$	Equal

K_p	Intraparticle diffusion rate constant
exp	Exponential
C	Constant for any experiment in intraparticle diffusion model
q_{ref}	Solid phase concentration at time $t = t_{ref}$ for an adsorption system
t_{ref}	Longest time in the adsorption process
K	Scherrer constant
λ	Radiation wavelength used for analysis
τ	Width at half the height of the diffraction peak
θ	Bragg angle

SUMMARY

FIRST PART

GENERAL INTRODUCTION

Most tropical soils are highly weathered, which generally results in low natural soil fertility, low pH, high aluminum toxicity, high phosphorus (P) fixation capacity and low levels of soil organic matter (LOPES; GUILHERME; RAMOS, 2012). These characteristics are major constraints for food production in this region.

In order to achieve profitable yields in these soils it is necessary first to correct soil acidity by using lime (ALLEONI *et al.*, 2010; CAIRES *et al.*, 2001) and gypsum (CAIRES *et al.*, 2001), and also to apply large amounts of fertilizers containing either macro and micronutrients. Fertilizers are typically applied to soil by either surface broadcasting, subsurface placement, or fertigation (RALIYA *et al.*, 2018). However, the high solubility and fast release of most conventional fertilizers, generally make them prone to losses resulting in low plant use efficiency of nutrients (DIMKPA; BINDRABAN, 2018; KAH *et al.*, 2018; RALIYA *et al.*, 2018), which is compensated by the application of larger amounts (KABIRI *et al.*, 2017).

The low nutrient use efficiency is a result of several transformations that occur when fertilizers are applied in the soil, such as immobilization reactions in clay minerals and organo-mineral complex in soil, formation of precipitates and losses due to leaching or volatilization (e.g. nitrogen - N) (ANDELKOVIC *et al.*, 2018; CARDOSO; KUYPER, 2006; LOPES; GUILHERME; RAMOS, 2012). It is estimated that around 40–70% of N, 80–90% of P and 50–90% of potassium (K) content applied via fertilizer are lost into the environment (DEROSA *et al.*, 2010; LIU; LAL, 2017; SOLANKI *et al.*, 2015), while plant use efficiency of micronutrients using soluble fertilizers sources to soil is much lower (< 5%) than macronutrients (MONREAL *et al.*, 2016).

Most of the current fertilizer technologies are unable to synchronize the release of nutrient from fertilizer according to crop demand during the growing season (MONREAL *et al.*, 2016). Consequently, it is essential to reduce nutrient losses in fertilization, increase nutrient use efficiency, and develop fertilizers with higher plant uptake to increase crop productivity (JANMOHAMMADI *et al.*, 2016; LIU; LAL, 2015; RALIYA *et al.*, 2018). In such scenario, it is important to develop new strategies to improve nutrient use efficiency in agricultural soils, mainly for P and zinc (Zn) that are naturally low in soils of tropical regions (LAVRES JUNIOR *et al.*, 2012; LOPES; GUILHERME; RAMOS, 2012; MOUTA; SOARES; CASAGRANDE, 2008).

Currently, biochar has emerged as a candidate to produce enhanced efficiency fertilizers. Biochar is a stable and carbon-rich byproduct synthesized by pyrolysis/carbonization of plant- or animal-based feedstock under limited oxygen conditions, which is environmentally friendly and renewable material that help increase carbon sequestration in soil as well as soil fertility (HUANG *et al.*, 2017; LEHMANN; JOSEPH, 2015; ZHANG *et al.*, 2018). Furthermore, it is a porous substance with multiple functional groups which might be an effective sorbent and a suitable material for efficient nutrient retention and delivery (GHAFFAR; YOUNIS, 2014; GWENZI *et al.*, 2018; LIU *et al.*, 2016).

The biochar ability to improve crop productivity varies from positive (JEFFERY *et al.*, 2011; 2017) to negative responses (JEFFERY *et al.*, 2017). The main barrier, however, are the high application rates required for significant improvements in crop productivity that might not be economical (JOSEPH *et al.*, 2013), mainly due to the low nutrient content in some feedstocks. Thus, creating biochar-based fertilizers (BBF), which is enriching biochar with nutrients by different methods is an alternative to reduce biochar application rates and increase nutrient use efficiency beyond that of conventional fertilizers. In a recent meta-analysis was shown a 10% increase in crop productivity by using BBF when compared with conventional fertilizers (MELO *et al.*, 2022).

In pre-pyrolysis methods, a mixture of biomass, ground rocks or minerals and nutrients is subjected to slow and relatively low pyrolysis temperature, while in post-pyrolysis methods, biochar is mixed with ground rocks or minerals, nutrients and/or manures (JOSEPH *et al.*, 2013; YAO *et al.*, 2015), or even mixed with conventional fertilizers as a blend or coated material (POGORZELSKI *et al.*, 2020). Recent results showed promising results regarding the use of BBF as carriers of nutrients (e.g. N, P, and K) with slow-release characteristics (AN *et al.*, 2020; CHEN *et al.*, 2017; GWENZI *et al.*, 2018; LUSTOSA FILHO *et al.*, 2017).

The pre-pyrolysis of feedstock with soluble sources of P was shown to produce a slow-release P material (LUSTOSA FILHO *et al.*, 2017; ZHAO *et al.*, 2016). These fertilizers are typically poorly soluble in water, and the P availability is low in the short-term, but can increase over time due to fertilizer dissolution (DEGRYSE *et al.*, 2017; LUSTOSA FILHO *et al.*, 2020). Besides that, BBFs produced by pre-pyrolysis treatment with phosphate sources can increase labile, and moderately labile P in soil, demonstrating higher residual effect of fertilization (LUSTOSA FILHO *et al.*, 2020). However, these studies are conducted in the short-term, and the BBFs residual effect on different crops cultivated in successive cycles as well as P transformation in soil have not been studied yet.

Recently, graphene oxide (GO) has also been proposed as a nutrient carrier (KABIRI *et al.*, 2017). Graphene oxide is a water-dispersible material produced through the chemical oxidation of graphite that presents a high density of oxygen functional groups, surface area, hydrophilicity, and good biocompatibility (MA *et al.*, 2021; MARCANO *et al.*, 2010; WANG *et al.*, 2013). Its high surface area and unique 2-d structure, make them an ideal candidate for processes involving adsorption or surface reactions (SITKO *et al.*, 2013; ZHAO, GUIXIA *et al.*, 2011), because it shows great binding affinity to metal and metalloid ions in aqueous solutions (DING *et al.*, 2014; TIAN *et al.*, 2012), being an ideal platform for nutrient loading, with the potential of being employed in the manufacture of slow-release fertilizers (ANDELKOVIC *et al.*, 2018; GHAFFAR; YOUNIS, 2014).

Graphene oxide has also been employed as a carrier for nutrients, such as P (ANDELKOVIC *et al.*, 2018), Cu and Zn (KABIRI *et al.*, 2017; WATTS-WILLIAMS *et al.*, 2020), and as an improver of the physical/chemical properties and the nutrient release rate of conventional fertilizers (KABIRI *et al.*, 2018; YUAN *et al.*, 2018; ZHANG *et al.*, 2014). Phosphorus use efficiency was improved when graphene oxide was coated to monoammonium phosphate granules, which slightly delayed the release of P, decreasing the diffusion and increasing the physical strength of granules (KABIRI *et al.*, 2018). Graphene oxide-modified polyacrylate polymer exhibited great performance as coating materials for controlled-release fertilizers, decreasing N release from 87.3% to 59.7% after 28 days (YUAN *et al.*, 2018). KNO_3 pellets also exhibited slow-release behavior of K when coated by graphene oxide (ZHANG *et al.*, 2014). Graphene oxide can also improve micronutrient use efficiency by decreasing the release and diffusion of Cu and Zn, increasing wheat grain production and micronutrient uptake (KABIRI *et al.*, 2017).

Despite the excellent results of graphene oxide as a nutrient carrier, its use at large scale is restricted due to high costs (HUANG *et al.*, 2017). Therefore, combining biochar with graphene oxide is a promising strategy aiming to improve the physicochemical properties of both materials, while still maintaining low productions costs (GHAFFAR; YOUNIS, 2014). Graphene oxide enriched biochar has been used to adsorb cadmium, lead (LIU *et al.*, 2016; ZHANG *et al.*, 2018), chromium (IV) (SHANG *et al.*, 2016), as well as organic chemicals, such as atrazine (ZHANG *et al.*, 2018), imidacloprid (MA *et al.*, 2021) and sulfamethazine (HUANG *et al.*, 2017). However, to our current knowledge, there has not been any study so far concerning graphene oxide enriched biochar for Cu and Zn adsorption, as well as its reusability as biochar-based fertilizers.

The absence of long-term studies with BBF containing P, and the absence of studies with biochar enriched with graphene oxide loaded with micronutrients as a fertilizer was the motivation for the studies that compose this thesis, which was organized in four parts: general introduction (First part), article 1 (Second part), article 2 (Third part) and final remarks (Fourth part).

In the general introduction (First part), we present the central theme of the thesis, as well as the gaps that led to these studies. We also present the main novelty of each study. The first article (Second part) was about evaluation of BBFs containing P as fertilizer. In this study we hypothesized that P-enriched BBFs provides available P to plants longer than triple superphosphate (TSP). In addition, increases of the organic P fractions in soil, and its combination with TSP can promote better results than TSP alone. Thus, the objectives of this study were to evaluate the use of P-enriched BBF in successive crops (grass, maize, and common beans) to assess its long-term residual effect. The second article (Third part) was about the evaluation of graphene oxide enriched biochar for Cu and Zn adsorption and their use as fertilizer. In this study we hypothesized that graphene oxide enriched biochar increases Cu and Zn adsorption when compared to pristine biochar, as well as increases its effectiveness as BBFs when applied to soil for plant growth. The objectives of this study were to evaluated the use of BBF enriched with graphene oxide loaded with micronutrients (Cu and Zn) as a fertilizer for the cultivation of common beans. In the final remarks section (Fourth part) we close the thesis with some remarks about the studies, main conclusions, and give suggestions for future works related to these researches.

REFERENCES

ALLEONI, L. R. F. *et al.* Acidity and Aluminum Speciation as Affected by Surface Liming in Tropical No-Till Soils. *Soil Science Society of America Journal*, v. 74, n. 3, p. 1010–1017, 2010.

AN, X. *et al.* Copyrolysis of Biomass, Bentonite, and Nutrients as a New Strategy for the Synthesis of Improved Biochar-Based Slow-Release Fertilizers. *ACS Sustainable Chemistry and Engineering*, v. 8, n. 8, p. 3181–3190, 2020.

ANDELKOVIC, I. B. *et al.* Graphene oxide-Fe(III) composite containing phosphate – A novel slow release fertilizer for improved agriculture management. *Journal of Cleaner Production*, v. 185, p. 97–104, 2018.

CAIRES, E. F. *et al.* Crescimento radicular e nutrição da soja cultivada no sistema plantio direto em resposta ao calcário e gesso na superfície. *Revista Brasileira de Ciência do Solo*, v. 25, n. 4, p. 1029–1040, 2001.

CARDOSO, I. M.; KUYPER, T. W. Mycorrhizas and tropical soil fertility. *Agriculture, Ecosystems and Environment*, v. 116, n. 1–2, p. 72–84, 2006.

CHEN, L. *et al.* Environmental-friendly montmorillonite-biochar composites: Facile production and tunable adsorption-release of ammonium and phosphate. *Journal of Cleaner Production*, v. 156, p. 648–659, 2017.

DEGRYSE, F. *et al.* Dissolution rate and agronomic effectiveness of struvite fertilizers – effect of soil pH, granulation and base excess. *Plant and Soil*, v. 410, n. 1–2, p. 139–152, 2017.

DEROSA, M. C. *et al.* Nanotechnology in fertilizers. *Nature Nanotechnology*, v. 5, n. 2, p. 91, 2010.

DIMKPA, C. O.; BINDRABAN, P. S. Nanofertilizers: New Products for the Industry? *Journal of Agricultural and Food Chemistry*, v. 66, p. 6462–6473, 2018.

DING, Z. *et al.* Filtration and transport of heavy metals in graphene oxide enabled sand columns. *Chemical Engineering Journal*, v. 257, p. 248–252, 2014.

GHAFFAR, A.; YOUNIS, M. N. Adsorption of organic chemicals on graphene coated biochars and its environmental implications. *Green Processing and Synthesis*, v. 3, n. 6, p. 479–487, 2014.

GWENZI, W. *et al.* Synthesis and nutrient release patterns of a biochar-based N–P–K slow-release fertilizer. *International Journal of Environmental Science and Technology*, v. 15, n. 2, p. 405–414, 2018.

HUANG, D. *et al.* Sorptive removal of ionizable antibiotic sulfamethazine from aqueous solution by graphene oxide-coated biochar nanocomposites: Influencing factors and mechanism. *Chemosphere*, v. 186, p. 414–421, 2017.

JANMOHAMMADI, M. *et al.* Impact of nano-chelated micronutrients and biological fertilizers on growth performance and grain yield of maize under deficit irrigation condition. *Biologija*, v. 62, n. 2, p. 134–147, 2016.

JEFFERY, S. *et al.* A quantitative review of the effects of biochar application to soils on crop productivity using meta-analysis. *Agriculture, Ecosystems and Environment*, v. 144, n. 1, p. 175–187, 2011.

JEFFERY, S. *et al.* Biochar boosts tropical but not temperate crop yields. *Environmental Research Letters*, v. 12, 053001, 2017.

JOSEPH, S. *et al.* Shifting paradigms: development of high-efficiency biochar fertilizers based on nano-structures and soluble components. *Carbon Management*, v. 4, n. 3, p. 323–343, 2013.

KABIRI, S. *et al.* Cogranulation of Low Rates of Graphene and Graphene Oxide with Macronutrient Fertilizers Remarkably Improves Their Physical Properties. *ACS Sustainable Chemistry and Engineering*, v. 6, p. 1299–1309, 2018.

KABIRI, S. *et al.* Graphene Oxide: A New Carrier for Slow Release of Plant Micronutrients. *ACS Applied Materials and Interfaces*, v. 9, n. 49, p. 43325–43335, 2017.

KAH, M. *et al.* A critical evaluation of nanopesticides and nanofertilizers against their conventional analogues. *Nature Nanotechnology*, v. 13, p. 677–684, 2018.

LAVRES JUNIOR, J. *et al.* Deficiency symptoms and uptake of micronutrients by castor bean grown in nutrient solution. *Revista Brasileira de Ciência do Solo*, v. 36, n. 1, p. 233–242, 2012.

LEHMANN, J.; JOSEPH, S. (Org.). *Biochar for Environmental Management: Science, Technology and Implementation*. 2nd. ed. London and New York: Routledge: Taylor and Francis group, 2015. 944 p.

LIU, R.; LAL, R. Nanofertilizers. In: LAL, R. (Org.). . *Encyclopedia of Soil Science*. Third Edit ed. [S.l.]: CRC Press, Taylor & Francis, 2017. p. 1511–1515.

LIU, R.; LAL, R. Potentials of engineered nanoparticles as fertilizers for increasing agronomic productions. *Science of the Total Environment*, v. 514, p. 131–139, 2015.

LIU, T. *et al.* Biochar-supported carbon nanotube and graphene oxide nanocomposites for Pb(II) and Cd(II) removal. *RSC Advances*, v. 6, n. 29, p. 24314–24319, 2016.

LOPES, A. S.; GUILHERME, L. R. G.; RAMOS, S. J. The saga of the agricultural development of the brazilian cerrado. *International Potash Institute, Research Findings*, v. 32, p. 29–56, 2012.

LUSTOSA FILHO, J. F. *et al.* Co-Pyrolysis of Poultry Litter and Phosphate and Magnesium Generates Alternative Slow-Release Fertilizer Suitable for Tropical Soils. *ACS Sustainable Chemistry and Engineering*, v. 5, n. 10, p. 9043–9052, 2017.

LUSTOSA FILHO, J. F. *et al.* Aging of biochar-based fertilizers in soil: Effects on phosphorus pools and availability to Urochloa brizantha grass. *Science of the Total Environment*, v. 709, 136028, 2020.

MA, Y. *et al.* A novel, efficient and sustainable magnetic sludge biochar modified by graphene oxide for environmental concentration imidacloprid removal. *Journal of Hazardous Materials*, v. 407, 124777, 2021.

MARCANO, D. C *et al.* Improved Synthesis of Graphene Oxide. *ACS Nano*, v. 4, n. 8, p. 4806–4814, 2010.

MELO, L. C. A. *et al*. Biochar-based fertilizer effects on crop productivity: a meta-analysis. *Plant and Soil*, 2022.

MONREAL, C. M. *et al.* Nanotechnologies for increasing the crop use efficiency of fertilizer-micronutrients. *Biology and Fertility of Soils*, v. 52, n. 3, p. 423–437, 2016.

MOUTA, E. R.; SOARES, M. R.; CASAGRANDE, J. C. Copper adsorption as a function of solution parameters of variable charge soils. *Journal of the Brazilian Chemical Society*, v. 19, n. 5, p. 996–1009, 2008.

POGORZELSKI, D. *et al.* Biochar as composite of phosphate fertilizer: Characterization and agronomic effectiveness. *Science of the Total Environment*, v. 743, p. 140604, 2020.

RALIYA, R. *et al.* Nanofertilizer for Precision and Sustainable Agriculture: Current State and

Future Perspectives. *Journal of Agricultural and Food Chemistry*, v. 66, p. 6487–6503, 2018.

SHANG, M. R. *et al.* A novel graphene oxide coated biochar composite: Synthesis, characterization and application for Cr(VI) removal. *RSC Advances*, v. 6, n. 88, p. 85202–85212, 2016.

SITKO, R. *et al.* Adsorption of divalent metal ions from aqueous solutions using graphene oxide. *Dalton Transactions*, v. 42, n. 16, p. 5682–5689, 2013.

SOLANKI, P. *et al.* Nano-fertilizers and Their Smart Delivery System. In: RAI, M. *et al.* (Org.). *Nanotechnologies in Food and Agriculture*. [S.l.]: Springer International Publishing, 2015. p. 81–101.

TIAN, Y. *et al.* Methods of using carbon nanotubes as filter media to remove aqueous heavy metals. *Chemical Engineering Journal*, v. 210, p. 557–563, 2012.

WANG, H. *et al.* Adsorption characteristics and behaviors of graphene oxide for Zn(II) removal from aqueous solution. *Applied Surface Science*, v. 279, p. 432–440, 2013.

WATTS-WILLIAMS, S. J. *et al.* Potential of zinc-loaded graphene oxide and arbuscular mycorrhizal fungi to improve the growth and zinc nutrition of Hordeum vulgare and Medicago truncatula. *Applied Soil Ecology*, v. 150, 103464, 2020.

YAO, C. *et al.* Developing More Effective Enhanced Biochar Fertilisers for Improvement of Pepper Yield and Quality. *Pedosphere*, v. 25, n. 5, p. 703–712, 2015.

YUAN, W. *et al.* Application of Graphene-Oxide-Modified Polyacrylate Polymer for Controlled-Release Coated Urea. *Coatings*, v. 8, n. 64, p. 1–10, 2018.

ZHANG, M. *et al.* Slow-release fertilizer encapsulated by graphene oxide films. *Chemical Engineering Journal*, v. 255, p. 107–113, 2014.

ZHANG, Y. *et al.* Biochar-supported reduced graphene oxide composite for adsorption and coadsorption of atrazine and lead ions. *Applied Surface Science*, v. 427, p. 147–155, 2018.

ZHAO, G. *et al.* Few-layered graphene oxide nanosheets as superior sorbents for heavy metal ion pollution management. *Environmental Science and Technology*, v. 45, p. 10454–10462, 2011.

ZHAO, L. *et al.* Copyrolysis of Biomass with Phosphate Fertilizers to Improve Biochar Carbon Retention, Slow Nutrient Release, and Stabilize Heavy Metals in Soil. *ACS Sustainable Chemistry and Engineering*, v. 4, n. 3, p. 1630–1636, 2016.

SECOND PART

ARTICLE 1

Long-term effect of biochar-based fertilizers application in tropical soil: agronomic efficiency and phosphorus availability

Published in the *Science of the Total Environment Journal*, 760 (2021) 143955.

https://doi.org/10.1016/j.scitotenv.2020.143955

Long-term effect of biochar-based fertilizers application in tropical soil: agronomic efficiency and phosphorus availability

Jefferson Santana da Silva Carneiro [a], *Ivan Célio Andrade Ribeiro* [a], *Bárbara Olinda Nardis* [a], *Cristiane Francisca Barbosa* [a], *José Ferreira Lustosa Filho* [b], *Leônidas Carrijo Azevedo Melo* [a, *]

[a] Federal University of Lavras, Soil Science Department, Lavras, 37200-900, Minas Gerais, Brazil.

[b] Federal University of Viçosa, Department of Soils, Viçosa, 36570-900, Minas Gerais, Brazil.

*Corresponding author

Leônidas Carrijo Azevedo Melo

E-mail: leonidas.melo@ufla.br

Highlights

- Pyrolysis of biomass enriched with phosphorus generates fertilizer with slow-release profile.

- Biochar-based phosphate fertilizer is efficient in the short- and long-term.

- Biochar-based phosphate fertilizer increases soil P reserves on soil.

- Biochar-based phosphate fertilizer can replace conventional P fertilizer.

Graphical Abstract

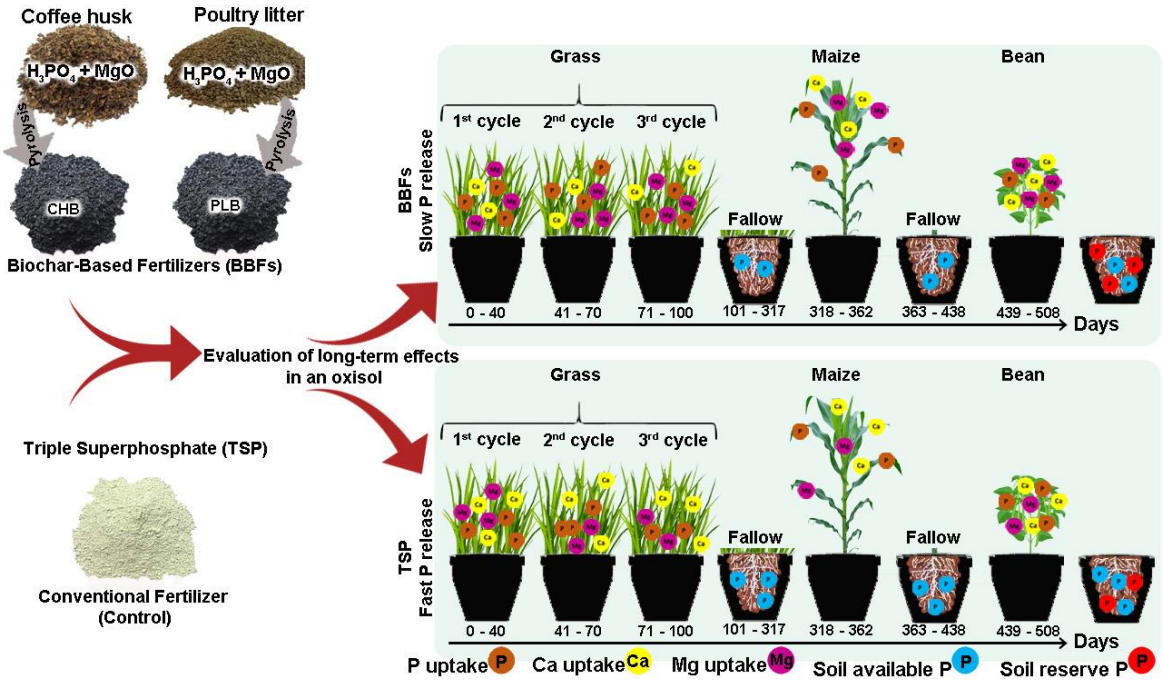

Abstract

Incorporation of phosphorus (P) into an organic matrix may be an effective strategy to increase plant P use efficiency in high P-fixing soils. The objective of this work was to evaluate the effect of biochar-based fertilizers (BBFs), produced from poultry litter (PLB) and coffee husk (CHB) enriched with phosphoric acid and magnesium oxide, in combination with triple superphosphate (TSP) on plant growth and soil P transformations. Treatments were prepared as: TSP, CHB, PLB, CHB + TSP [1:1], CHB + TSP [3:1], PLB + TSP [1:1] and PLB + TSP [3:1]; with numbers in brackets representing the proportion of BBF and TSP on a weight basis. Cultivations were: Mombasa grass, maize, and common bean interspersed with fallow periods. After cultivations, a sequential extraction procedure was employed to determine P distribution among different P pools. A kinetic study was performed and revealed that TSP released approximately 90% of total P, and BBFs less than 10% in the first hour. BBF alone or in combination with TSP presented higher or similar biomass yields, relative agronomic effectiveness, and P uptake when compared with TSP. As for the soil, BBFs increased non-labile P fractions, which can be due to pyrophosphate formed during pyrolysis. According to these results, BBFs could totally or partially replace conventional soluble P fertilizers without compromising crop yield either in the short and long-term.

Keywords: Nutrient-enriched biochar; Slow-release fertilizer; Plant use efficiency; Soil nutrient reserve; Fertilizer residual effect.

1. Introduction

Most tropical soils are highly weathered and acidic, presenting low available P (Lopes et al., 2012). These soils also present high P fixation capacity due to the predominance of low-activity clay minerals and (hydr)oxides of Fe and Al in the clay fraction (Lopes and Guilherme, 2016; Novais and Smyth, 1999). Therefore, addition of large amounts of phosphate fertilizers

was needed in order to achieve profitable yields in these soils (Baligar and Bennett, 1986; Sanchez and Uehara, 1980). In Brazil, for instance, the current average P fertilizers rate for all crops is ca. 25 kg P ha^{-1} $year^{-1}$ (which is twice plant demand), but P fertilizer rate can double in some areas where soils are still P deficient (Withers et al., 2018).

Phosphate fertilizers employed in agriculture are derived from phosphate rock, which is a finite, non-renewable resource that need to be managed wisely with regards to its sustainable use (Scholz et al., 2013), which includes efficient ways of P recycling and reuse (Peng et al., 2019; Yang et al., 2019; Zhang et al., 2020). Phosphate rock is mainly converted to highly water-soluble sources presenting low efficiency, which represents a threat to a sustainable crop production (Withers et al., 2018). Only around 10 to 20% of P applied via fertilizer is effectively taken up by plants in the first season after application (Khan and Rizvi, 2017; Li et al., 2020; Solanki et al., 2015). Surplus P application of soluble sources constitute a legacy of P reserve in the long-term, which is difficult to be mobilized for in a timely manner to meet crop nutrition requirements (Rodrigues et al., 2016). Therefore, some strategies and technologies are required to create phosphate fertilizers with lower solubility and improve P management in tropical soils.

An alternative can be incorporation of P into an organic matrix, such as in biochar-based fertilizers (BBFs) through pre- or post-pyrolysis treatments (Joseph et al., 2013; Yao et al., 2015). Biochar is a stable and carbon-rich byproduct synthesized by pyrolysis/carbonization of plant- or animal-based biomasses under low or limited oxygen conditions (Lehmann and Joseph, 2015). In the pre-pyrolysis methods, a mixture of biomass, ground rocks, minerals and nutrients is subjected to slow and relatively lower pyrolysis temperature, while in post-pyrolysis methods biochar is mixed with ground rocks or minerals, nutrients and/or manures (Joseph et al., 2013; Yao et al., 2015).

The approach of using nutrient-enriched biochar has been increasing in recent years. Lustosa Filho et al. (2019) observed a slow release of P in poultry litter biochar that was treated

with H_3PO_4 and MgO. This caused similar maize yield but preserved higher P concentration in the granules after cultivation when compared with the soluble P source (TSP). Sahin et al. (2017) observed higher maize yield when biochar was post-treated with H_3PO_4 and HNO_3 in a calcareous soil. Using post-pyrolysis treatment with TSP peletization in different biochars, Santos et al. (2019) did not observe higher P use efficiency than TSP, while Pogorzelski et al. (2020), reported that TSP coated with 15% biochar increased plant P uptake, but higher crop yield was not obtained. Conversely, Borges et al. (2020) observed higher sugarcane yield using a biochar fertilizer enriched with H_3PO_4 and KOH in comparison to TSP fertilizer. In most cases total P content from BBFs are comparable with soluble P sources. The increased efficiency of P-enriched biochar as compared with soluble fertilizers is argued to be mainly due to P protection in the carbon matrix, which prevents the fast P sorption sites on the soil surface and also due to the pH buffering capacity caused by biochar, making P more available over time and favoring plant uptake. However, these studies were performed in very short-term greenhouse studies (typically just one cultivation).

Pre-pyrolysis treatment to soluble P sources was shown to produce a slow release P material (Lustosa Filho et al., 2017; Zhao et al., 2016). These fertilizers are typically poorly soluble in water, and the P availability is low in the short-term, but can increase over time due to fertilizer dissolution (Degryse et al., 2017; Lustosa Filho et al., 2020). On the other hand, soluble phosphate fertilizers release most P immediately after soil application, and have their availability for plants reduced over time due to contact with soil particles and conversion to less soluble forms (Everaert et al., 2016; Rivaie et al., 2008). Besides this, BBFs produced by pre-pyrolysis treatment with phosphate sources can increase labile, and moderately labile P in soil, demonstrating higher fertilization residual effect (Lustosa Filho et al., 2020). Sequential chemical fractionation that identifies several soil P fractions has been widely used to understand soil P transformations (Lustosa Filho et al., 2020; Pavinato et al., 2009). However, BBFs

residual effect on different crops cultivated in successive cycles, as well as P transformation in the soil have not been studied yet.

In this study, we hypothesized that BBFs provides available P to plants longer than TSP. In addition, increases of the organic P fractions in soil, and its combination with TSP can promote better results. The objectives of this study were (i) to evaluate the effect of BBF produced from poultry litter and coffee husk enriched with H_3PO_4 and MgO on the P supply to different crops (Mombasa grass, maize, and common bean) in successive cultivations, (ii) to evaluate the effect of BBF and TSP in different combinations over plant growth and soil fertility, and (iii) to investigate the long-term effect of the BBF application on transformations of soil P fractions.

2. Material and methods

2.1. Production and characterization of biochar-based fertilizers

Coffee husk and poultry litter biomasses were collected on farms near Lavras, Minas Gerais, Brazil (21°13′34″ S and 44°58′31″ W). Samples were air-dried at room temperature and ground to pass through a 1.00 mm sieve. Biomasses were mixed with concentrated phosphoric acid (H_3PO_4) (95 - 98%) and magnesium oxide (MgO) to achieve a ratio of biomass:H_3PO_4 of 1:0.5 (w/w) and to achieve a P:Mg molar ratio of 1:1, as described in the literature (Lustosa Filho et al., 2017). MgO was added to neutralize H_3PO_4 acidity. After thorough mixing, pretreated samples were moistened by adding water, in order to reach 100% of the water holding capacity of each biomass, for better homogenization. Samples were then left to rest for 16 h. After this period, materials were oven-dried at 60 °C to a constant mass to be pyrolyzed. Pyrolysis was performed in an adapted muffle furnace by adjusting the temperature to 500 °C at a heating rate of approximately 10 °C min^{-1}, maintaining the target temperature for 2 h. This was enough time for complete carbonization as described by Zhao et al. (2014) and Lustosa

Filho et al. (2017). BBFs obtained were identified as CHB (coffee husk biochar + H_3PO_4 + MgO) and PLB (poultry litter biochar + H_3PO_4 + MgO).

Total nutrient contents (Table 1) were determined according to Enders and Lehmann (2012). For this, 0.20 g of BBF were ashed in a muffle furnace for 8 h at 500 °C. After ashing, nitric acid was added and the samples were taken for digestion at 120 °C with H_2O_2 addition in the final digestion step to oxidize all organic carbon. Finally, the digested material was dissolved in 20 mL of 5% (v/v) HCl solution using sonication. Contents of the tubes were filtered in membranes (< 0.45 μm) and elements were quantified by ICP-OES (Model Blue, Germany).

Table 1. Biochar-based phosphate fertilizers and TSP characterization.

Total content[a] (g kg^{-1})	CHB	PLB	TSP
P	201 ± 3.22	178 ± 3.28	204
K	25.3 ± 0.38	26.4 ± 0.69	-
Ca	6.76 ± 1.12	17.2 ± 0.17	100
Mg	105 ± 1.21	95.7 ± 1.12	-
S	0.22 ± 0.11	0.50 ± 0.23	-
Cu	0.02 ± 0.01	0.03 ± 0.00	-
Fe	2.51 ± 0.14	1.05 ± 0.14	-
Mn	0.10 ± 0.00	0.49 ± 0.02	-
Ni	0.01 ± 0.00	0.01 ± 0.00	-
Zn	2.13 ± 0.03	4.01 ± 0.12	-
P solubility[b] (g kg^{-1})			
Water soluble P	1.74	1.75	157
Citric acid soluble P	83.7	117[d]	193[d]
NAC + water-soluble[c] P	123	147[d]	200
SSA (m^2 g^{-1})[e]	124.5[f]	114.0[f]	-

[a] Mean ± standard deviation (n=3); [b] Solubility determinate according to Brasil (2017); [c] Neutral ammonium citrate + water; [d] Adapted from Lustosa Filho et al. (2019); [e] SSA = specific surface area; [f] Adapted from Carneiro et al. (2018).

Microscopic features and morphology of each material were characterized using scanning electron microscopy (LEO EVO 40 XVP - Carl Zeiss) equipped with energy-dispersive X-ray spectroscopy (Brunker - Quantax EDX).

2.2. Kinetics of phosphorus release

Kinetics of phosphorus release by BBFs and TSP were performed according to Lustosa Filho et al. (2017) with some modifications. Briefly, 0.25 g of sample were mixed with 50 mL of deionized water (pH of approximately 6.5) in falcon tubes and then shaken in a reciprocating shaker at 120 rpm for up to 240 h at 25 °C. Samples were then collected at 0.25, 0.5, 1, 3, 6, 12, 24, 48, 72, 120, and 240 h. Triplicate tubes were taken out in each sampling time. Solids in the suspension were rapidly separated from the liquid phase, after passing through 0.45 µm Millipore filters. Solutions were analyzed for P by using ICP-OES. Kinetics of P release were determined as "changes in P concentrations" over time, and the release of P as a function of sampling time was fitted using models presented on Table S3.

2.3. Greenhouse pot experiments

2.3.1. Soil samples and preparation

Samples of an Oxisol were collected from 40 - 100 cm layer at the Campus of the Federal University of Lavras, Minas Gerais, Brazil (915 m altitude, 21°13'34" S and 44°58'31" W), air dried and passed through a 2-mm sieve for further chemical and textural characterization (Silva, 2009). This soil was chosen due to its representativeness of important Brazilian cultivation areas and worldwide as well, and also due to its low P availability (0.77 mg kg^{-1}) (Table S1). The subsurface layer was chosen in order to reduce the influence of soil organic matter and to evaluate the role of BBFs treatments on the interaction of P and soil mineral phase (Lustosa Filho et al., 2020).

Three kg of soil were placed in plastic bags and mixed with $CaCO_3$ + $MgCO_3$ in a Ca/Mg molar ratio of 3:1, with the goal of rising soil cation saturation to 70% in order to neutralize soil acidity and provide adequate levels of Ca and Mg to plants. The soil was then kept at 80% humidity for 30 days. After this incubation period, samples were air dried, homogenized, and

fertilized according to Malavolta (1980) and Novais et al. (1991) to reach the ideal fertility condition for plants growth in pots (Table S2). The P dose (240 mg kg^{-1} of soil) was applied only in the first planting to evaluate its residual effect over time.

2.3.2. Experimental design and plant growth

Experimental design was completely randomized, with four replicates. Seven treatments were used varying the proportion between BBFs and TSP as shown in Table 2.

Table 2. Experimental setup

Treatments	CHB	PLB	TSP	BBF:TSP
	% of P dose[a]			
CHB100	100	-	-	1:0
CHB75	75	-	25	3:1
CHB50	50	-	50	1:1
PLB100	-	100	-	1:0
PLB75	-	75	25	3:1
PLB50	-	50	50	1:1
TSP	-	-	100	0:1

[a]P dose of 240 mg kg^{-1} of soil based on NAC + water-soluble P content.

Three successive cultivations were performed as follows: in the first planting, ten Mombasa grass seeds (*Megathyrsus maximus* cv. Mombasa) were sown in each pot and thinned 10 d after emergence, maintaining three plants per pot, which was cultivated for three cycles. The first crop cycle was conducted for 40 d, and the second and third crop cycles for 30 d, totaling 100 d of cultivation followed by 217 d of fallow period. Four maize seeds (*Zea mays*) were sown in the second planting in each pot, and thinned to one plant per pot 10 d after emergence, which was cultivated for 45 d with another fallow of 76 d. In the third planting, six common bean seeds (*Phaseolus vulgaris* L. cv. BRSMG UAI) were sown in each pot and thinned to two plants per pot 10 d after emergence. These plants were cultivated for 70 d until grain production.

These three crops were selected in order to simulate crops in an integrated system, in which a pasture for animal consumption is grown in the off-season. Then this pasture was replaced by a grain crop in the first harvest (represented by maize) and another crop (represented by common beans) in second harvest, thus simulating a sequence of crops under the same phosphate fertilization.

2.3.3. Plant and soil analysis

After each Mombasa grass crop cycle the plants were harvested at the height of 10 cm from the soil level in the pot (to allow regrowth). For maize growth, the plants were harvested close to the soil surface. For both crops, harvested shoots were washed with distilled water, placed into paper bags, and dried at 65 °C until weight stabilization (approximately 72 h), weighed, and milled for chemical analysis. For common bean analysis, senescent leaves were collected in a paper bag until plant maturity when the grains were harvested. After this, leaves were mixed with shoots and pods to determine shoot dry mass (SDM) and grain yield, separately. Then, all plant samples were ground and digested using nitric-perchloric acid mixture (Malavolta et al., 1997), and P, Ca, and Mg were then measured in the extract by ICP-OES. These values were used to calculate the nutrient accumulation in each plant, taking into account the yields. After each planting, 30 g of soil were collected from each pot to determine the pH in water and available P using Mehlich-1 solution and resin as described by Silva (2009) and Raij et al. (1986), respectively. Phosphorus was determined colorimetrically (Murphy and Riley, 1962) following the recommendations of these standard methods.

Relative agronomic effectiveness (RAE) was calculated by comparison of each treatment to the reference fertilizer (TSP) added at the same fertilization dose, following the equation:

$$\text{RAE } (\%) = \left(\frac{P_{BBF}}{P_{TSP}}\right) \text{ x } 100$$

Where P_{BBF} is the dry matter production by plants in a given BBFs fertilization treatment (g plant^{-1}); P_{TSP} is the dry matter production by plants in the reference treatment (TSP).

2.3.4. Phosphorus fractionation procedure

A sequential chemical fractionation was performed as proposed by Hedley et al. (1982) and modified by Condron et al. (1985) to evaluate the influence of BBFs and TSP in soil P transformation. Phosphorus fractions [organic (Po), inorganic (Pi) and total P (Pt)] were extracted in the following order: anion exchange resin membrane (resin-Pi), 0.5 mol L^{-1} $NaHCO_3$ ($NaHCO_3$-Pi and Po), 0.1 mol L^{-1} NaOH (0.1 mol L^{-1} NaOH-Pi and Po), 1.0 mol L^{-1} HCl (HCl-Pi) and 0.5 mol L^{-1} NaOH (0.5 mol L^{-1} NaOH-Pi and Po). Phosphorus fractions obtained were then grouped according to their plant availability, as suggested by Cross and Schlesinger (1995): labile (resin-Pi + $NaHCO_3$-Pi + $NaHCO_3$-Po); moderately labile (0.1 mol L^{-1} NaOH-Pi + 0.1 mol L^{-1} NaOH-Po + HCl-Pi); and non-labile (0.5 mol L^{-1} NaOH-Pi + 0.5 mol L^{-1} NaOH-Po + residual-P).

2.4. Statistical analysis

Data were subjected to analysis of variance (one-way ANOVA, $p < 0.05$) and when significant difference ($p < 0.05$) was observed, the means were compared by the Tukey test ($p < 0.05$) using the *emmeans* package (Lenth et al., 2019). Additionally, the data of the shoot dry mass, P uptake, and P fractions by sequential fractionation were submitted to principal component analysis (PCA) using the *ggbiplot* function from the *ggbiplot* package (Vu, 2011). Kinetics data for P release were fitted to nonlinear models using the *nlstools* package (Baty et al., 2015). All analyzes were performed using the R software version 3.6.1 (R Core Team, 2019).

3. Results and discussion

3.1. Scanning electron microscopy (SEM) and energy dispersive spectroscopy (EDS)

Scanning electron microscopy images from BBFs in different magnifications are shown in Fig. 1. SEM images show differences in particles sizes and the surface morphology of CHB (Fig. 1a, b, and c) and PLB (Fig. 1d, e, and f). These changes occur due to enrichment with H_3PO_4 and MgO in co-pyrolysis for the production of the biochar fertilizer.

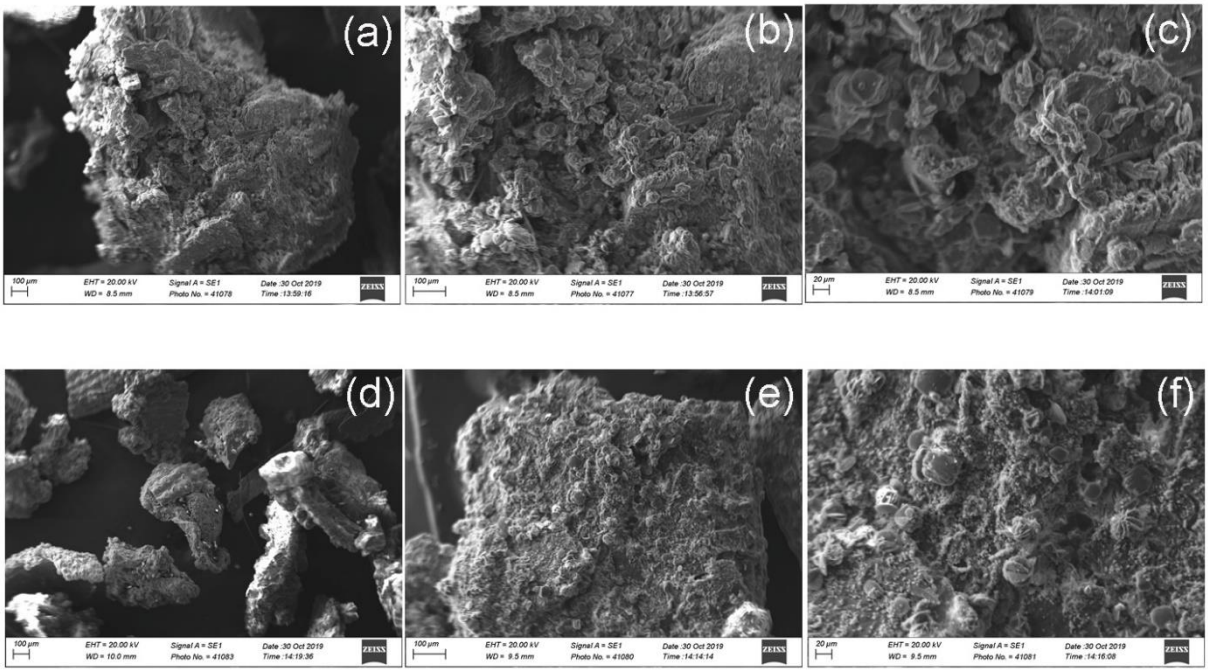

Fig. 1. SEM images of BBFs. Figures a, b and c for CHB, and figures d, e and f for PLB, at 100, 200, and 500 times enhancement, respectively.

Addition of P and MgO affects the microstructure and the surface structure, presenting a degraded matrix with lower crystallite size, and higher specific surface area and porosity (Carneiro et al., 2018; Penido et al., 2019). By analyzing SEM images, it was possible to observe precipitates on the BBFs surface (Fig. 1c and 1f), probably due to the formation of P and Mg compounds during pyrolysis, such as magnesium pyrophosphate ($Mg_2P_2O_7$) (Lustosa Filho et al., 2017).

EDS mapping (Fig. S1) revealed a uniform distribution for P (Fig. S1b and S1f), Ca (Fig. S1c and S1g), and Mg (Fig. S1d and S1h) on the surface of each material. It was observed that P was closely associated with Mg distribution, mainly in the precipitates on the BBFs surface. Fig. S1i and S1j showed the peaks of the main elements found on the BBFs surface by SEM-EDX. The main peaks observed in the BBFs were in accordance with total concentration (Table 1).

Oxygen presented the highest composition in both BBFs (Fig. S1i and S1j), probably due to the functional groups containing O present in this BBFs binding to carbon (C) and/or P, such as C−O, C=O, −CHO, −COO, P−O−P, P=O, P−O, P−O−C and others groups (Carneiro et al., 2018; Lustosa Filho et al., 2017). P and Mg were added to the biomasses increasing their contents on BBFs. The K present in CHB and PLB was very similar (Table 1, and Fig. S1i and S1j). The higher Ca observed in the PLB was due to poultry diets that include $CaCO_3$ in their feeding, and the Si was due to quartz in the poultry litter as observed by other authors (Domingues et al., 2017; Nardis et al., 2020).

3.2. Phosphorus release kinetics

The P release behavior of the BBFs and TSP is shown in Fig. 2. BBFs show a quick P release on the first 3 h of test followed by a slight and constant release until the final time evaluated (240 h). P release from BBFs did not stabilize over the sampling period, while TSP reached the maximum after the first hours. As expected, TSP released much more P when compared to BBFs and reached 186 g kg^{-1} of P in the first hour, which represents 91.2% of the total P. The BBFs released only between 13 and 16 g kg^{-1}, which represents 6.47 and 8.99% of all P in CHB and PLB, respectively. According to the second order model (Table S4), TSP released all neutral ammonium citrate + water-soluble P (200 g kg^{-1}) (Table 1).

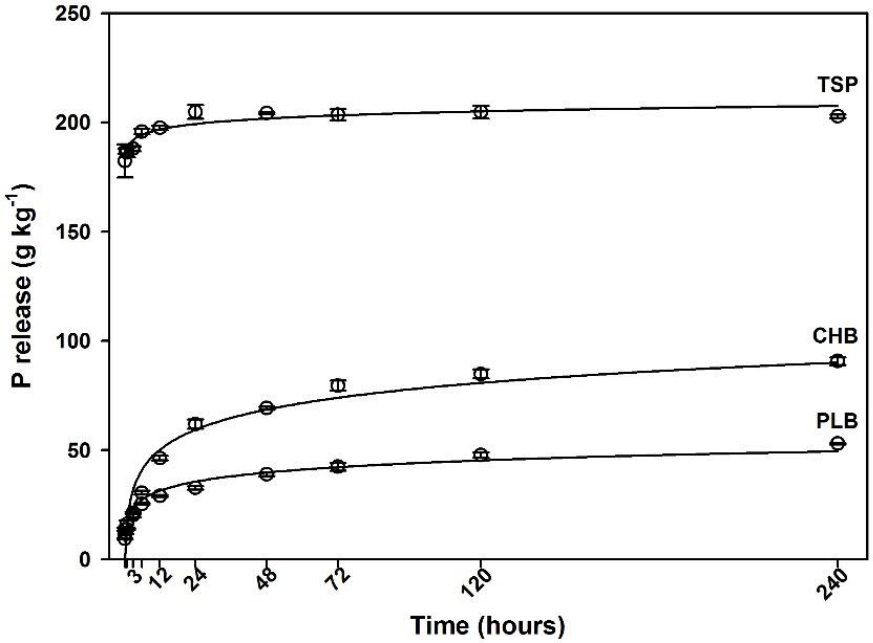

Fig. 2. Kinetics of P release in water from BBFs and TSP. CHB – coffee husk biochar + H_3PO_4 + MgO, PLB – poultry litter biochar + H_3PO_4 + MgO, and TSP – triple superphosphate.

Standard errors for the estimative of the models (SE) (Shariatmadari et al., 2006) and Akaike information criterion (AIC) (Akaike, 1974; Kingdom and Prins, 2016) were used to describe the quality of data fitting and selection the best models (More information are given in the supplementary materials). The lower the parameters SE and AIC the better is the fitting and model. Kinetics of P released from TSP was better fitted to the Power function (SE: 3.067; AIC: 59.67) and Elovich models (SE: 3.002; AIC: 59.20) (Table S4). Similar results were also observed by Lustosa Filho et al. (2017), in which P release data from TSP presented a better fit to the Elovich model. The fast P release within the first hour for TSP was probably attributed to the ion desorption process and/or dissolution of some crystalline phosphates such as $[Ca(H_2PO_4)_2 \cdot H_2O]$ (Lustosa Filho et al., 2017). Fast P release from TSP ensures P supply to plants. However, the amount that is not absorbed is then rapidly adsorbed onto Fe and Al (hydr)oxides through monodentate bindings, which evolves to bidentate binding and causes high P fixation in tropical soils (Abdala et al., 2015b).

Second order (SE: 4.658; AIC: 68.86) and power function (SE: 1.191; AIC: 38.84) models showed the best fit for CHB and PLB (Table S4). The second order model indicates that the P release of CHB is a combined process of dissolution and diffusion (Zhao et al., 2016). The CHB (91.6 g kg^{-1}) released more P than PLB (45.1 g kg^{-1}), which represents about 74% and 30% of the NAC + water-soluble P, respectively. The initial P desorption rate (*a*) estimate of power function (Table S4) was 24.4 (CHB) and 16.6 g P kg^{-1} h^{-1} (PLB), while TSP was 188 g P kg^{-1} h^{-1}. The higher P release observed from CHB when compared to PLB was probably due to the differences between feedstocks and also to their higher specific surface area (Table 1), which allowed higher dissolution of the fertilizer, thus releasing more P to the solution.

These results show that the BBFs have a pattern of P slow-release, which might be due to conversion of P into pyrophosphates (Sahin et al., 2017), such as calcium pyrophosphates ($Ca_2P_2O_7$) and magnesium pyrophosphates ($Mg_2P_2O_7$) (Lustosa Filho et al., 2017). These compounds have low water-soluble P (Lustosa Filho et al., 2017; Sahin et al., 2017) when compared to the main P form [$Ca(H_2PO_4)_2 \cdot H_2O$] present in TSP.

Biochar enriched with TSP or bone meal had a lower P release rate than TSP or bone meal alone (Zhao et al., 2016). In addition, P enriched biochars displayed a better match to the power function and parabolic diffusion models, indicating that extra energy is needed for breaking C-O-P or C-P bonds for releasing the P (Zhao et al., 2016). Besides, this could explain the lower P release rate of PLB, which was better fitted to the power function model (Table S4).

The slow and steady release of P by these BBFs may result in a more efficient P uptake by plants when compared with the highly water-soluble P fertilizers due to fast P adsorption onto soil surface particles (Abdala et al., 2015b). In addition, the longer-term P release was supposedly an advantage of the BBF over conventional soluble P sources for plant nutrition (Lustosa Filho et al., 2017; Zhao et al., 2016).

3.3. Plant growth and biomass production

Response from grass, maize, and common bean plants in successive cultivations in regards to BBFs and TSP fertilization are shown in Figs. 3, S2, and S3. Grass height in the first (Fig. S2a) and second (Fig. S2b) cropping cycles was affected by treatments, while the height in the third cropping cycle of grass (Fig. S2c) and maize (Fig. S2d) was not affected.

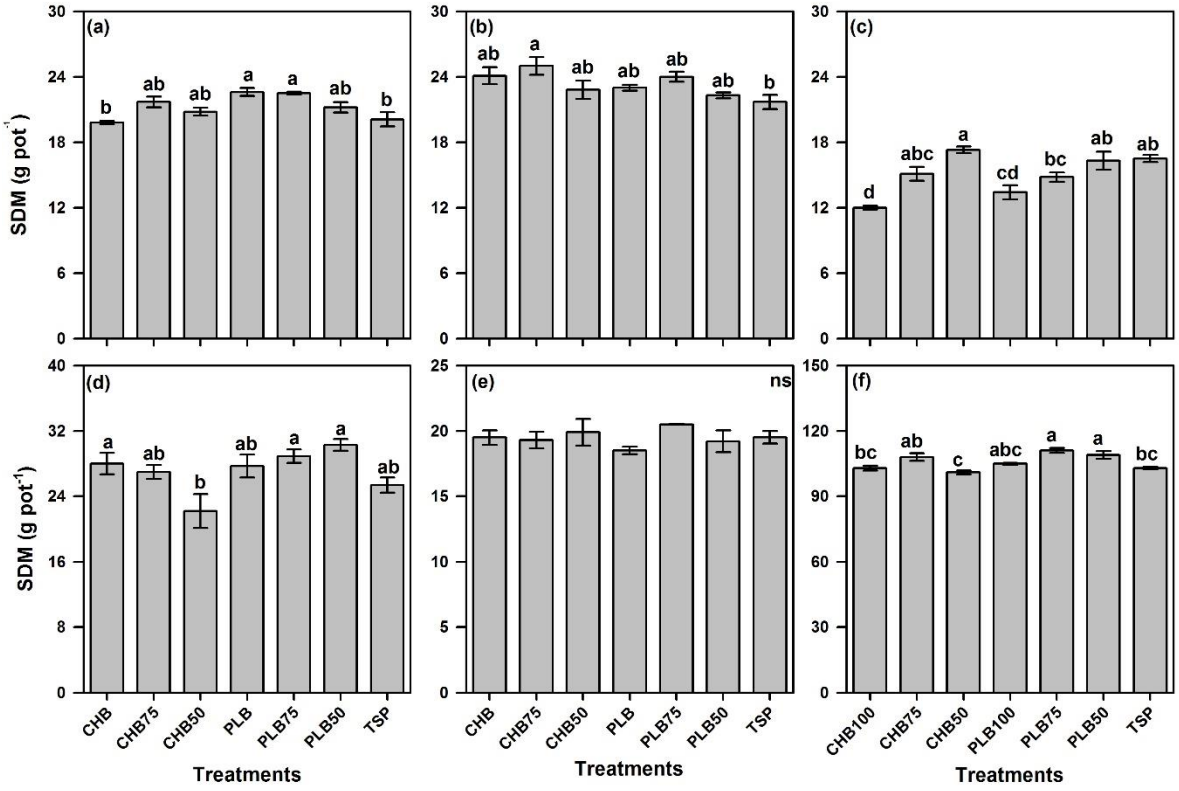

Fig. 3. Shoot dry mass (SDM) of Mombasa grass in the first cropping cycle (a), second cycle (b), and third cycle (c), maize plants (d), common bean plants (e) and shoot dry mass total (f) of plants under BBFs and TSP fertilization. Dry mass total = ∑ of dry mass production of Mombasa grass, maize and bean. ^{ns} Means of the treatments do not differ from each other by the Tukey test ($p > 0.05$). Mean followed by the same letters in the bars do not differ from each other by the Tukey test ($p < 0.05$); Error bars represent standard error (n = 4).

In the first cropping cycle, plants height using the BBFs or in combination with TSP was higher than TSP fertilizer alone about from 7% to 17%, except for CHB100 and PLB50 which presented similar results. In the second and third cropping cycles of grass and maize plants the

BBFs did not differ from TSP fertilization presenting heights of approximately 79 and 140 cm respectively.

The shoot dry mass (SDM) of grass (Fig. 3a, b, and c) and maize plants (Fig. 3d) were affected by treatments, while the SDM of common bean (Fig. 3e) was not affected. The SDM of grass was better (about from 12% to 15%) or equal to results obtained with TSP fertilization in the first and second cropping cycles (until 70 days). In the third cropping cycle, the CHB (CHB100) and PLB (PLB100) alone presented lower SDM production than TSP (70 - 100 days), about of 19% and 27%, respectively.

There was a decrease observed in the SDM production by grass in the third cropping cycle compared to the first and second cycles. This lower production probably occurred due to the extractions of successive cultivations that caused a decrease in the available P (Sá et al., 2017) as well as the longer-term P contact with soil which caused higher adsorption and reduced its availability (Abdala et al., 2015a) leading to lower plant P uptake (Table S5), but without causing negative effects to crop yield. This probably occurred due to the efficiency of this grass in dealing with P depletion (Carneiro et al., 2017). After grass cultivation, applied P aged for 217 d, which might have caused soil P fixation and allowed the evaluation of the residual fertilization effect by growing maize and subsequently common bean plants. Maize plants (Fig. 3d) and common bean (Fig. 3e) presented SDM productions similar to TSP when BBF was used for fertilization, with SDM productions of approximately 27 and 19.5 g per pot for maize and common bean plants respectively. The grain yield of common bean (Fig. S3) was similar to production obtained with TSP fertilization (approximately 17.2 g per pot), while the total SDM (Fig. 3f) was better when PLB50 and PLB75 was used in about of 6% and 8%, respectively. These BBFs have high carbon stability (Carneiro et al., 2018) and low carbon contents were added via BBFs, therefore their carbon content has negligible effect on plant production.

Soil application of BBF as fertilizer to maize crop cultivated for 35 – 40 days increased the SDM when compared to the unfertilized soil, when P was added in pre-pyrolysis or post-pyrolysis. However, when compared to TSP fertilizer the SDM was lower or similar, likely due to restrictive access to P in the short-term as compared with the highly water soluble fertilizer (Lustosa Filho et al., 2019, 2017; Santos et al., 2019). In a study with sugarcane production, the effect of biochar fertilizer was 35% higher than the TSP in a clayey soil and showed no difference in sandy and loam soils (Borges et al., 2020), which evidenced the effect of biochar fertilizer, that is influenced by soil texture, by protecting P from soil sorption in a high P buffering capacity soil.

In a study evaluating the effect of aging P into the soil for 100 d before planting Marandu grass (*Urochloa brizantha* cv. Marandu), Lustosa Filho et al. (2020) verified that TSP presented better shoot dry mass production only in the first cropping cycle. However, in the second and third cropping cycles, the BBFs were higher than TSP and in the sum of production the BBF was higher than TSP by 6% to 13%. When a BBF containing Bayovar rock phosphate as P source associated with selected bacterial strains to P solubilization was used as fertilizer, it presented lower maize biomass production when compared with the same P dose applied using TSP (Leite et al., 2020), which was attributed to the very low P solubility from this BBF, not able to supply P to maize in the short-term.

3.4. Phosphorus, calcium and magnesium uptake by plants

The P uptake by plants is shown in Fig. 4. In the first cropping cycle of grass (Fig. 4a) there was no difference between BBF and TSP fertilization, while in the second and third cycles BBFs were higher than TSP. The CHB100 and CHB75 were better than TSP in the second cycle by 22.4% and 21.7%, and CHB100 and PLB100 in the third by 30.5% and 32.1% respectively. This indicated that in the short-term the effect of BBFs and TSP were similar.

However, in the long-term the BBF increased the plant P uptake, although it might not result in greater dry mass production.

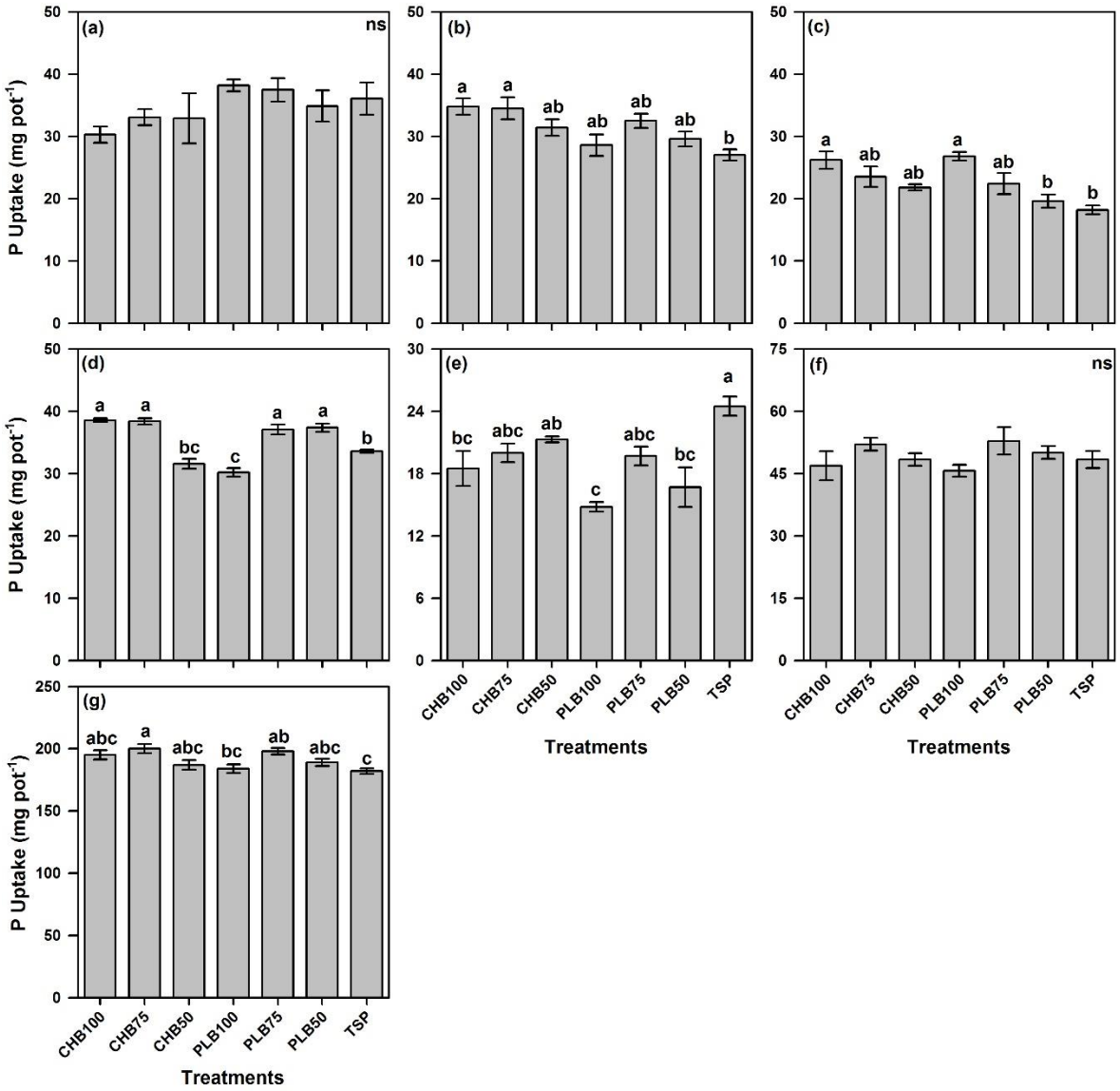

Fig. 4. P uptake by Mombasa grass in the first cropping cycle (a), second cycle (b), third cycle (c); maize plants (d); and by bean plants (e) and grains (f); and total P uptake by plants (g) under BBFs and TSP fertilization. [ns] Means of the treatments do not differ from each other by the Tukey test ($p > 0.05$). Mean followed by the same letters in the bars do not differ from each other by the Tukey test ($p < 0.05$); Error bars represent standard error (n = 4).

After aging into the soil for 217 d, the effect of BBF alone or in combination with TSP was more evidenced, where CHB100, CHB75, PLB75, and PLB50 promoted higher P uptake (from 9.4% to 12.9%) by maize plants (Fig. 4d). When common bean was cultivated, the effect of BBF was similar or lower than TSP, mainly when BBF was used alone. In general, the P

uptake by plants was higher than TSP (from 8% to 9%) when BBF was combined with 25% of TSP (CHB75 and PLB75) (Fig. 4g).

The lower P uptake by bean plants when BBFs were applied alone may be related to the lower availability of P in the soil (refer to the next section) and due to its higher requirement of P when compared to grass and maize. According to Martinez et al. (1999), critical levels of P in the plants of *Megathyrsus maximus*, maize and common beans are 0.8 - 1.1 g kg^{-1}, 2.5 - 3.5 g kg^{-1} and 4.0 - 7.0 g kg^{-1}, respectively.

When applied to sandy and loam soils a biochar fertilizer enriched with H_3PO_4 in post-pyrolysis process, presented similar shoot P uptake by sugarcane when compared to TSP, while in the clayey soil, the biochar fertilizer presented 30% higher shoot P uptake than TSP (Borges et al., 2020). BBF from wheat straw enriched with rock phosphate showed higher P uptake by rice plants when compared to chemical fertilization (Chew et al., 2020). Conversely, a BBF from poultry litter enriched with rock phosphate showed lower P uptake in maize when compared to TSP (Leite et al., 2020).

Coating of TSP with 15% biochar increased the maize P uptake by 10% in a clayey soil and showed no difference in a sandy soil (Pogorzelski et al., 2020). According to the authors, the coating protected P against fast soil sorption or precipitation with metals in the fertilizer granule. Lustosa Filho et al. (2020) showed that P uptake from TSP fertilization by grass plants reduces considerably over time, while BBF increases P uptake, being more efficient in the long-term due to P protection coordinated with a slower and steady release. Our results also showed a similar trend until maize cultivation, where the BBFs alone or combined with TSP promoted higher P uptake when compared with TSP fertilizer alone.

Calcium (Ca) and magnesium (Mg) uptake by plants is shown on Table S6. Calcium uptake was higher when TSP was used in the first planting (grass), due to TSP composition that presented high Ca concentration (100 g kg^{-1}), while CHB and PLB have 6.76 and 17.2 g kg^{-1},

respectively (Table 1). As for maize and common bean plants, Ca uptake was similar when fertilized with BBF or TSP. The Mg uptake was higher in plants fertilized with BBF, either alone or combined with TSP. An increase in Mg uptake by rice plants was also observed when BBF was applied (Chew et al., 2020). The higher P uptake by plants fertilized with BBF could be explained by synergistic effect with Mg (González-Ponce et al., 2009; Lustosa Filho et al., 2020, 2017; Niu et al., 2015). BBF application promotes an increase in Mg and P uptake by plants, presenting a strong positive correlation between P and Mg uptake, which reinforces evidences of synergism (Lustosa Filho et al., 2020, 2017). As the movement of phosphate ions to the sites through which it is taken up into root cells occurs by diffusion, which is a relatively slow process, results in the depletion of phosphate concentration in the solution around plant roots, mainly in P-deficient soils (Schachtman et al., 1998; Smith, 2002). Besides, phosphate from soil solution is in equilibrium with phosphate sorbed onto soil minerals and colloids, maintain low the concentrations of phosphate in soil solution (Schachtman et al., 1998; Smith, 2002). Thus, the BBF could be a strategy for improving P uptake reducing this depletion zone, by slow and steady releasing P, in order to increase the solution phosphate concentration immediately adjacent to the sites of phosphate uptake by plant roots.

3.5. Soil analysis: pH and available phosphorus

Soil pH and available P were measured before maize planting (317 d), before common bean planting (438 d), and after common bean harvest (520 d after P application), with results being presented in Fig. S4 and Fig. 5, respectively. Soil pH was not affected by BBF fertilization regardless of the cultivation, when compared to TSP (Fig. S4) that presented an average pH of 5.5 before maize planting, and average pH of 5.2 before common bean planting and after harvest. In short-term experiments with BBF an increase in soil pH have been observed when compared with TSP in maize cultivation (Lustosa Filho et al., 2019, 2017). It has also been

observed that biochar fertilizer increased the soil solution pH with a transient effect (< 40 d) for sugarcane cultivation (Borges et al., 2020).

Available P by Mehlich-1 was higher for TSP fertilization after all plantings (Fig. 5). After grass cultivation (Fig. 5a) the available P did not differ when CHB was used alone (CHB100) or in combination with TSP, presenting approximately 6.5 mg kg^{-1}, while PLB in combination with TSP showed a higher availability (6.9 and 7.6 mg kg^{-1}) when compared to PLB alone (5.3 mg kg^{-1}). After maize cultivation (Fig. 5b) the available P increase 53% when CHB was combined to TSP (ratio 1:1), but did not differ from PLB. After common bean cultivation (Fig. 5c) the available P increased about from 54% to 66%, when both BBFs were combined with TSP in ratio 1:1.

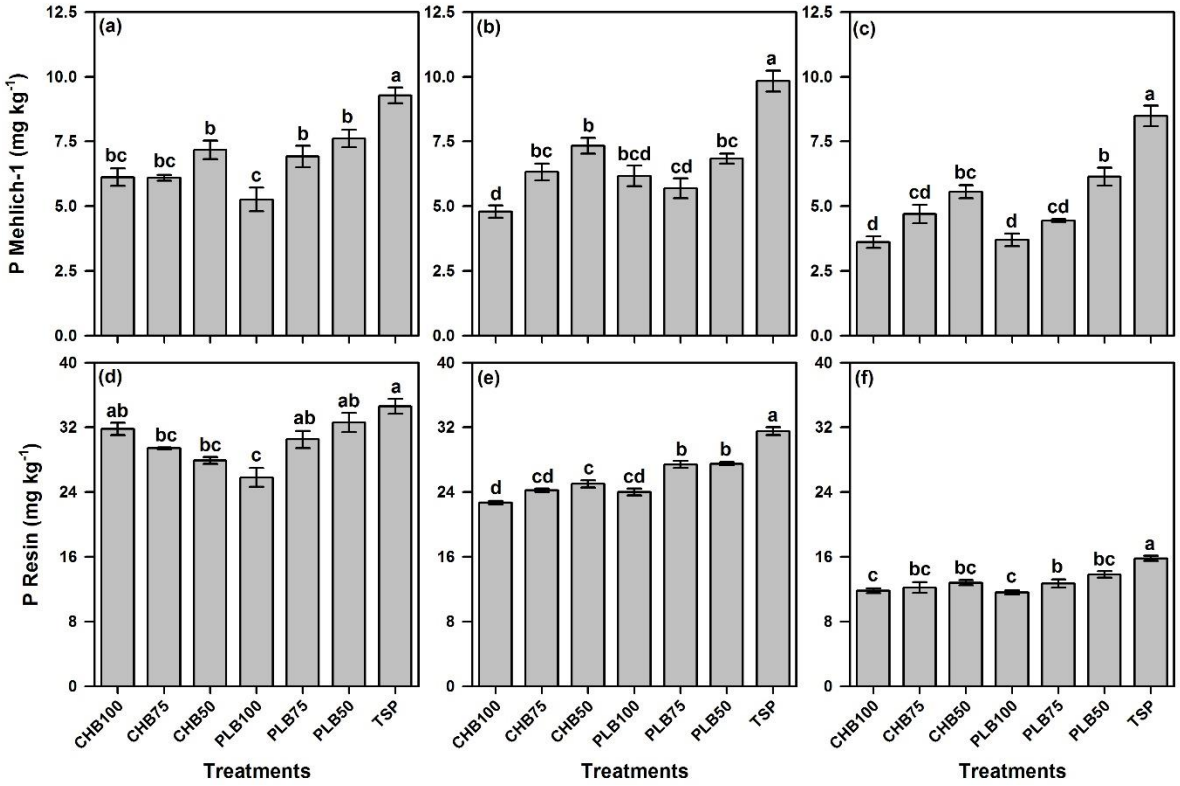

Fig. 5. P available in the soil by Mehlich-1 and Resin extractor after Mombasa grass (a and d), maize (b and e) and common bean (c and f) cultivation respectively, under BBFs and TSP fertilization. Mean followed by the same letters in the bars do not differ from each other by the Tukey test ($p < 0.05$); Error bars represent standard error (n = 4).

Available P by Mehlich-1 in the soil was considered adequate (8.0 – 12.0 mg kg^{-1} of soil) in all plantings using TSP as fertilizer, while BBFs alone or in combination with TSP in the first (Fig. 5a) and second planting (Fig. 5b) were considered medium (5.5 – 8.0 mg kg^{-1} of soil), except for CHB100, which presented a low level of available P (2.8 – 5.4 mg kg^{-1} of soil) (Venegas et al., 1999). In the third planting (Fig. 5c) when CHB50 and PLB50 [BBF:TSP (1:1)] were applied, the available P was considered medium, and the other treatments present low P availability (Venegas et al., 1999). The lower available P when CHB or PLB were used, probably occurred due to the gradual and constant P release (Fig. 2). No difference was observed in the available P in soil (Mehlich-1) when TSP associated with biochar were used to fertilize a clayey Oxisol for maize growth, except for biochar of wood sawdust (350 ºC) + TSP (Santos et al., 2019). These results were probably found because P was added to biochar in post-pyrolysis, and kept the TSP characteristics of fast P release, being prone to adsorption in soil.

For the resin P, when CHB alone and PLB were applied in combination with TSP there was no difference to TSP alone after the first cultivation (Fig. 5d), presenting 32.4 mg kg^{-1}. As for the second (Fig. 5e) and third cropping (Fig. 5f), available P for TSP fertilization was higher than BBFs from 12% to 28%, even when combined with TSP. The available resin P was considered medium (16 – 40 mg kg^{-1} of soil) in the first and second planting, and low in the third planting (7 – 15 mg kg^{-1} of soil) for all treatments (Raij., 2011).

An increase of available resin P in soil was observed when BBF produced using soluble (MAP, TSP and H_3PO_4) (Lustosa Filho et al., 2017) and insoluble (rock phosphate) (Leite et al., 2020) P sources were applied to the soil as fertilizer, however, results were lower than those with TSP fertilizer. This is likely due to P forming C−O−P or C−P bindings, which requires extra energy for breaking and releasing P rapidly to the soil in the first days (Zhao et al., 2016).

Application of biochar together with TSP fertilizers did not increase the P extracted by anion exchange membrane, when compared to TSP alone. However, when the P-loaded biochar

was applied, there was an increase in the P content extracted by the anion exchange membrane (Li et al., 2020). The combined use of organic matrix with P fertilizers is a strategy to decrease P adsorption in weathered soils, since organic ligands contribute to maintaining a negatively charged soil matrix and decrease the phosphate adsorption (Jiang et al., 2015; Lustosa Filho et al., 2017). Overall, Mehlich-1 P was lower than resin P, which is caused by a loss of extraction capacity in soils of high P buffering capacity (Novais et al., 2015), such as the one used in this study with high clay content (600 g kg^{-1}) (Table S1), while the resin is not as exhausted as Mehlich-1 due to an exchange extraction mechanism (Freitas et al., 2013).

3.6. Relative agronomic effectiveness

Relative agronomic effectiveness (RAE) of BBFs and TSP are shown on Fig. 6. In the first and second grass cropping cycles (Fig. 6a and b), the BBF presented RAE equal to or higher than TSP. In the first cropping cycle, PLB and PLB75 showed 8% and 13% higher RAE than TSP, respectively. In the second cropping cycle, CHB75 was 15% higher than TSP, and in the third grass cropping cycle (Fig. 6c), maize (Fig. 6d), and common bean (Fig. 6e) showed no difference for RAE among BBFs and TSP.

In the third Mombasa grass cropping cycle, the CHB100 and PLB100 presented the lowest RAE, which can be related to their low water soluble P (Table 1) and low P release rate (Fig. 2) when compared with TSP fertilizer (Lustosa Filho et al., 2020). BBFs presented a much lower P solubility in water and release rate than TSP (Table 1 and Fig. 2). Soil P release and availability by BBFs occurred quickly in the first hours followed by a slow and steady release over time, resulting in better grass growth in the first cycles, as well as higher RAE. Also, presence of Mg in the BBFs favored the Mg uptake by plants (Table S6), and consequently the higher accumulation of P, due to its synergistic effect, being a significant differential of the BBF in relation to TSP. Probably the P surplus released by BBFs was uptake in the first cycles,

limiting P access by plants in the third cycle and promoting lower dry mass production. In subsequent cultivates, RAE results were similar to TSP, probably due to the aging time, which allowed BBF to release more P to the soil.

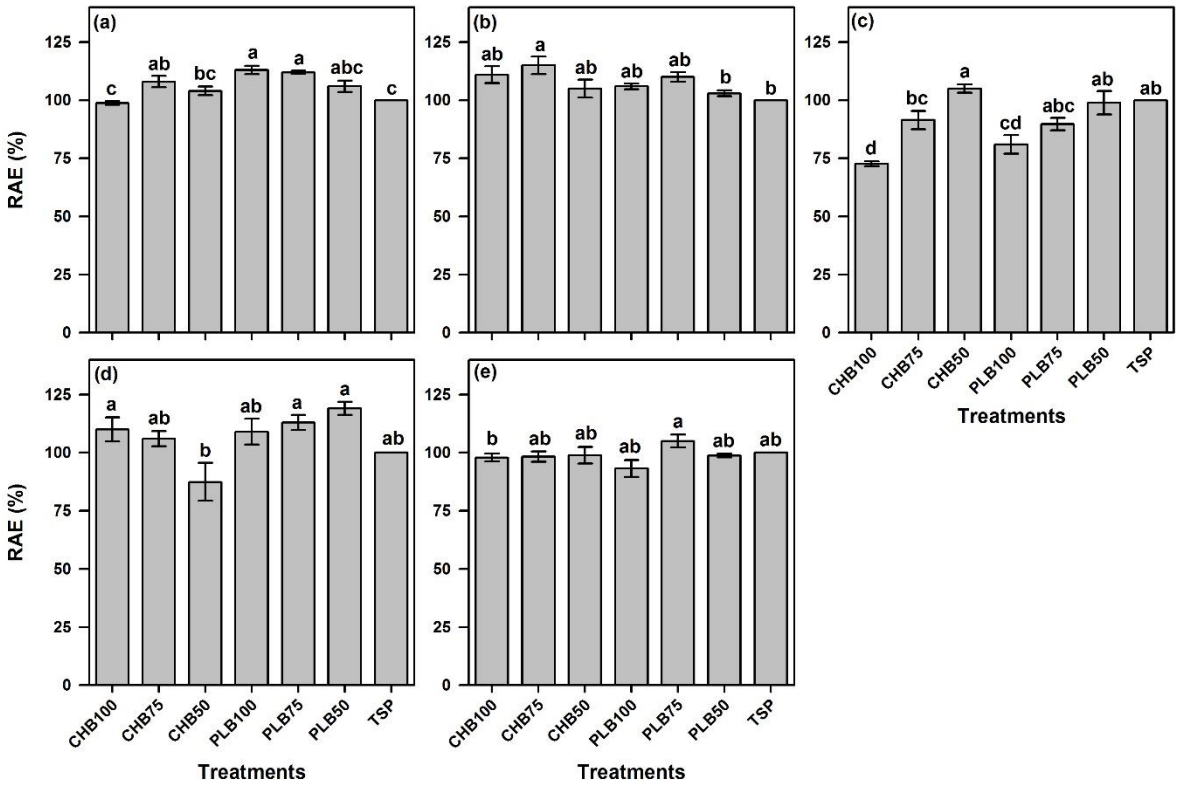

Fig. 6. Relative agronomic effectiveness (RAE) of the BBFs and TSP fertilizer to Mombasa grass in the first cropping cycle (a), second cycle (b), and third cycle (c), maize (d) and bean (e) production. Mean followed by the same letters in the bars do not differ from each other by the Tukey test ($p < 0.05$); Error bars represent standard error (n = 4).

In sandy and loam soils P use efficiency by sugarcane plants was similar for both TSP and biochar fertilizer, however, efficiency was 8% greater for biochar fertilizer than TSP in the clayey soil. Besides that, there was an increase in total P use efficiency of 15% when biochar fertilizer was applied in the clayey soil compared to TSP (Borges et al., 2020). BBFs presented higher relative agronomic effectiveness than TSP in 12% to 18% when applied at a dose of 300 mg kg^{-1} in an Oxisol, in powder form (Lustosa Filho et al., 2019). When applied in granule form, BBF had lower RAE than TSP as a result of the low P dissolution and diffusion from the BBF granule as compared with TSP (Lustosa Filho et al., 2019). The use of biochar associated

with TSP had equal or better relative agronomic effectiveness when compared to TSP alone, which is attributed to a P protection effect by the biochar, providing better P access to the plants (Santos et al., 2019).

Recently, Lustosa Filho et al. (2020) verified that BBF at 200 mg kg^{-1} rate after aging into the soil for 100 d presented similar RAE to TSP by Marandu grass yield after three harvests. These results were obtained after 220 days (100 days of aging and 120 days of cropping grass). Maybe after each harvest the effect of BBF on RAE could be more pronounced, as showed in the results in the first planting (Mombasa grass). Results of this study, and the studies cited above have shown positive responses to the use of BBF when compared with conventional phosphate fertilizers, which demonstrates the potential of biochar as a matrix to deliver P more efficiently than soluble sources.

3.7. Phosphorus fractionation

The soil P fractionation results measured after 520 d of P application into the soil using CHB, PLB and TSP fertilizer, and after three cultivations are shown in Table 3.

Table 3. Phosphorus content (mg kg^{-1}) [(mean ± standard error (n = 4)] in inorganic and organic fractions on the soil after P fertilization with BBFs and TSP.

Treat[a]	Inorganic P fractions				
	Resin	$NaHCO_3$	0.1 M[b] NaOH	HCl	0.5 M NaOH
CHB	9.88 ± 1.26 a[*]	16.4 ± 5.53 a	135 ± 12.2 b	26.6 ± 0.60 a	61.8 ± 9.09 a
PLB	8.00 ± 3.49 a	7.34 ± 3.96 b	148 ± 4.63 ab	25.9 ± 0.28 a	57.2 ± 9.49 a
TSP	10.3 ± 1.82 a	10.3 ± 1.25 ab	152 ± 1.84 a	23.1 ± 1.53 b	51.3 ± 18.1 a
	Organic P fractions				
	$NaHCO_3$	0.1 M NaOH	0.5 M NaOH	Residual P	
CHB	29.2 ± 5.96 b	145 ± 19.9 a	128 ± 11.7 a	1,935 ± 24.5 a	
PLB	39.0 ± 4.53 a	137 ± 10.2 a	118 ± 46.9 a	1,883 ± 25.2 b	
TSP	43.7 ± 0.70 a	123 ± 3.65 a	91.9 ± 17.1 a	1,867 ± 25.5 b	
	Labile P	Moderately labile P	Non-labile P	Total P[c]	
CHB	55.5 ± 1.53 b	306 ± 8.96 a	2,125 ± 26.5 a	2,460 ± 31.5 a	
PLB	54.3 ± 4.17 b	310 ± 12.9 a	2,058 ± 37.3 b	2,397 ± 54.0 ab	
TSP	64.3 ± 1.31 a	298 ± 5.15 a	2,010 ± 26.5 b	2,349 ± 29.4 b	

[*]Mean followed by the same letters in the columns do not differ from each other by the Tukey test ($p < 0.05$); [a]Treat: treatments; [b]M: mol L^{-1};[c]Sum of all inorganic and organic, and residual P fractions.

Inorganic fractions were similar for BBF and TSP for all extractors, except for HCl, which was higher for BBFs by 12%. The higher inorganic P content extracted by HCl was related to the more stable P forms in BBFs, such as pyrophosphates. As for the organic fractions, $NaHCO_3$ was 33.2% higher for TSP when compared with CHB. The inorganic fractions of BBF and TSP represented approximately 10% of total P and were similar among treatments. The organic fractions represent 12% and 11% of total P for CHB and PLB, respectively. CHB and PLB increased the soil P organic fractions in 14% and 12%, respectively when compared with TSP (Table 3).

Labile P represented 2.0–3.0% of the total P in the soil and was 14.6% higher for TSP in comparison to BBFs (Table 3). These values are typical for tropical soils, due to their capacity of immobilizing P added as fertilizers (Teles et al., 2017). Labile P was predominantly formed by organic fraction extract with $NaHCO_3$, which is a fraction very important to P availability to plants in tropical soils (Caione et al., 2015; Teles et al., 2017). The $NaHCO_3$ extracts labile inorganic P weakly adsorbed on the surface of crystalline compounds and labile organic P compounds with low persistence (Tiessen and Moir, 1993).

Moderately labile P was similar in all treatments (approximately 305 mg kg^{-1}), and was dominated by the NaOH-Pi fraction (135 to152 mg kg^{-1}) when compared with HCl-Pi (23.1 to 26.6 mg kg^{-1}), which is similar to data that was observed by others (Lustosa Filho et al., 2020; Rodrigues et al., 2016). This fraction represented inorganic P bound to oxides and silicate clay minerals with intermediate binding energy (Caione et al., 2015). The organic P fraction extracted with 0.1 mol L^{-1} NaOH is moderately labile organic P stabilized by Fe/Al oxides and hydroxides (Almeida et al., 2018; Hedley et al., 1982; Teles et al., 2017). In tropical soils, major proportions of P are found in fractions extracted with NaOH, which might be bound to Fe and Al (hydr)oxides, kaolinite and soil organic matter (Pavinato et al., 2009). Moderately labile fraction extracted with 0.1 mol L^{-1} NaOH might contribute to P availability for plant uptake in

the future (Caione et al., 2015; Pavinato et al., 2009), mainly in tropical soils, which act as a buffer to labile P forms in soil (Almeida et al., 2018; Olibone and Rosolem, 2010).

Addition of CHB to the soil increased the residual P, non-labile P, and total P in 3.6%, 5.7% and 4.7%, respectively, when compared with TSP fertilizer, while PLB did not differ from TSP. Residual P represents about 78 - 79% of the total P to BBFs and TSP fertilizers, while non-labile P represents 85 – 86% of total P. Highly weathered tropical soils have a tendency to accumulate P in non-labile forms (Rodrigues et al., 2016). Non-labile P fractions extracted with 0.5 mol L^{-1} NaOH represents recalcitrant inorganic P forms associated with Fe, Al and clay minerals, while non-labile forms of organic P are associated with fulvic and humic acids (Condron et al., 1985). Residual fraction represented organic and inorganic stable P forms (Caione et al., 2015; Pavinato et al., 2009), and supposedly does not contribute in the availability of P to plants (Rodrigues et al., 2016).

High non-labile P fraction was related to high clay content (600 g kg^{-1}) (Table S1), mainly formed by kaolinite, hematite, goethite and gibbsite, which are capable of strongly adsorbing P making it unavailable for plant uptake (Olibone and Rosolem, 2010; Pavinato et al., 2009; Teles et al., 2017). Phosphate fertilizer applications normally exceed the amount of P required by plants, because the soil acts as a strong sink for P, competing with plants for P in the soil solution (Teles et al., 2017). Therefore, an increase in total P stocks is important, since P extracted with $NaHCO_3$, NaOH, HCl and residual-P can be either bioavailable or transformed into available pools (Almeida et al., 2018).

PCA was conducted to determine variations among the BBFs and TSP, considering the fractions of P lability (labile P, moderately labile P and non-labile P) of soil after three plantings [Mombasa grass (Fig. S5), maize (Fig. S6), and common bean (Fig. S7)] as well as shoot dry matter yield and P uptake by plants (Fig. 7).

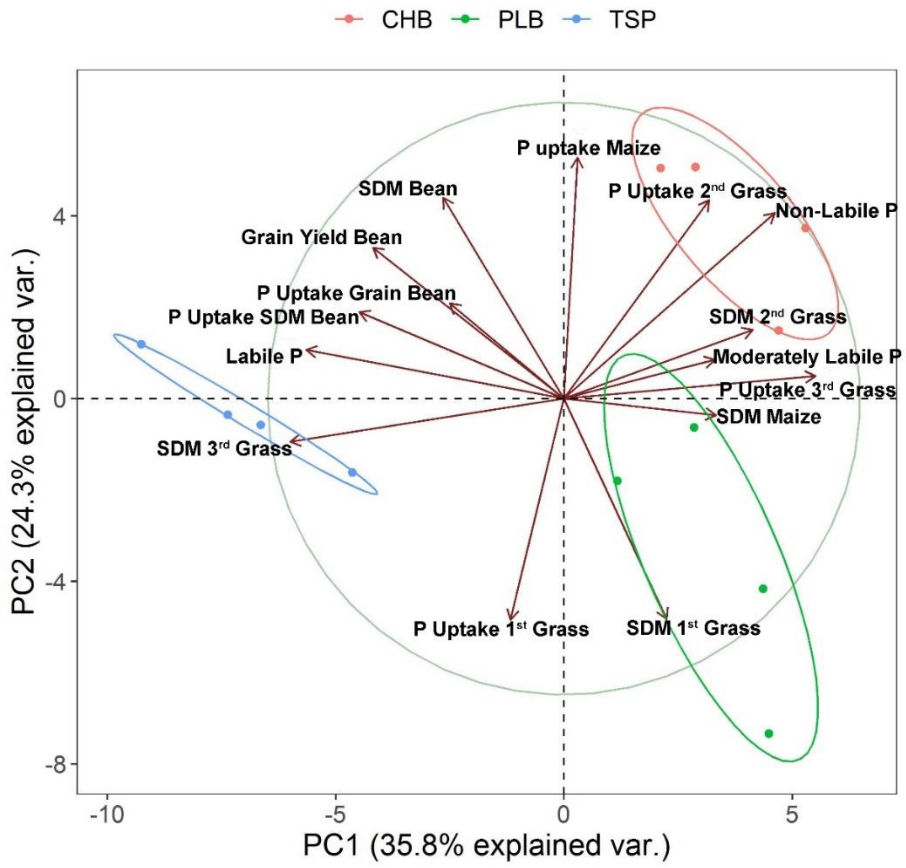

Fig. 7. Principal component analysis of BBFs and TSP effect in plant production, P uptake and P fractions in the soil. 1st Grass: first cropping cycle; 2nd Grass: second cropping cycle; 3rd Grass: third cropping cycle; SDM (shoot dry mass).

The two first principal components explained 60.1% of the total variation (PC1: 35.8% and PC2: 24.3%). Reducing from fifteen original variables to the two main components simplified the analysis without loss of information. PCA revealed that CHB was more associated to moderately labile P and non-labile P fractions, reinforcing the results of Table 3. TSP fertilizer was more related to grass shoot dry mass in the third cropping cycle and P uptake by grass in the first cropping cycle, while BBFs were related to all other variables measured in Mombasa grass, and also maize plants variables. P uptake by grass in the second and third cropping cycles, as well as maize plants, was related to CHB fertilizer, while shoot dry mass in the first grass cropping cycle was related to PLB. Labile P fraction was more related to TSP fertilizer, confirming the results presented in Table 3. Common bean cultivation did not relate

to fertilizers, likely due to the equivalent effect of BBFs and TSP caused by long-term application.

PCA enabled a combined evaluation of most of the studied variables and showed that BBFs fertilizers influenced the dynamics of P fractions in the soil, especially the non-labile and moderately labile fractions. Results obtained through the PCA plot reinforced the effect of BBF to increase the P reserve of soil, since the non-labile P and moderately labile P were better related to BBF application in the soil as fertilizer. Besides this, the BBFs were better related to P uptake by grass and maize plants, which can be indicative of an increase in the P use efficiency by plants. The principal component analysis was efficient in evaluating the effect of several BBF and TSP in the soil P fractions and grass production (Lustosa Filho et al., 2020). Besides, principal component analysis was efficient in grouping treatments of biochar and P application to evaluate the chemical P forms (Farrell et al., 2014).

4. Environment and agronomic implications

Phosphorus is the most limiting nutrient in highly weathered tropical soils and requires an adequate P supply to achieve high crop yields. Due to low efficiency of soluble P fertilizer sources, surplus application rates are required, which is costly and an environmental hazard due to losses that might trigger eutrophication of water resources. Incorporation of P in an organic matrix may be an effective strategy to increase P efficiency use by plants and decrease the adsorption of P in tropical soils since the organic matrix negatively charged can reduce the anions adsorption (Fig. 8). Employment of residues for fertilizer production, such as poultry litter and coffee husk, increase their agronomic value, and favor an adequate disposal of these residues.

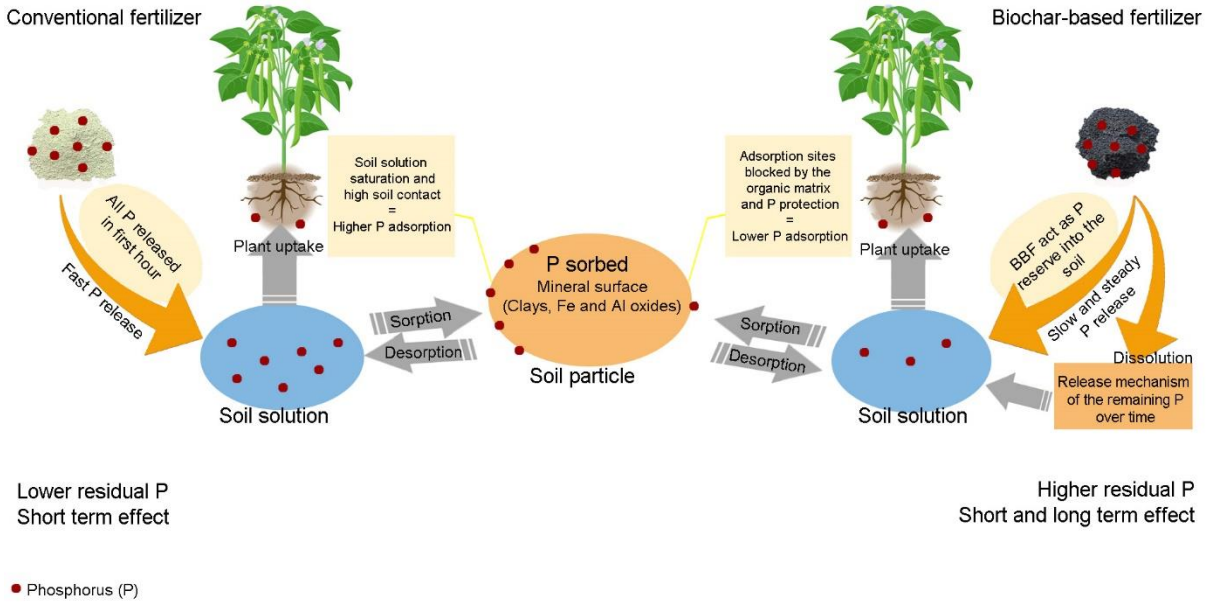

Fig. 8. Phosphorus dynamics in a soil-plant system fertilized with either conventional fertilizer (triple superphosphate – TSP) or biochar-based fertilizer (BBF).

Use of BBF as a P fertilizer was shown to sustain crop production in the short- and long-term runs similar to TSP and contribute to adding a stable carbon fraction to the soil. Increase in soil P reserve pool and high agronomic effectiveness, associated with a gradual and constant P release profile, make the BBFs an alternative to increase P efficiency use and favor the recycling of residues or byproducts of agriculture and industries that are produced in large quantities, which may cause environmental problems.

5. Conclusions

Despite the slow P release profile of BBF when compared with TSP, similar or higher crop yields were observed, either in the short- or long-term runs for the cultivations of different crops (grass, maize, and common bean). The Mg present in BBFs probably contributed to the synergistic effect with P, increasing the performance of BBFs as phosphate fertilizers. Either the BBF application alone or in combination with TSP is recommended and showed that BBF can replace partially or totally conventional fertilizer source. The effect of BBF in the short-term is due to its lower P release and protection against fast adsorption in the soil, which

ultimately reflected in equal or better plant growth and P uptake than soluble fertilizer. BBFs application increases the P reserves in the soil due to its recalcitrant forms, such as pyrophosphate. Further studies under field conditions should be carried out to confirm the results of this study.

Funding

This work was supported by the Coordination for the Improvement of Higher Education Personnel, Brazil (CAPES – PROEX 593-2018), and by the National Council for Scientific and Technological Development – CNPq, Brazil (Grant No 404076/2016-5). CNPq also provided a PhD scholarship to the first author (Grant No. 140976/2018-3) and a research scholarship to the corresponding author (Grant No. 308943/2018-0).

CRediT authorship contribution statement

Jefferson Santana da Silva Carneiro: Conceptualization, Methodology, Formal analysis, Investigation, Writing - original draft, Writing - review & editing. **Ivan Célio Andrade Ribeiro:** Conceptualization, Methodology, Formal analysis, Writing - review & editing. **Bárbara Olinda Nardis:** Methodology, Writing - review & editing. **Cristiane Francisca Barbosa:** Methodology, Writing - review & editing. **José Ferreira Lustosa Filho:** Conceptualization, Writing - review & editing. **Leônidas Carrijo Azevedo Melo:** Conceptualization, Resources, Validation, Writing - review & editing, Supervision, Project administration, Funding acquisition.

Declaration of competing interest

The authors declare that they have no known competing financial interests or personal relationships that could have appeared to influence the work reported in this paper.

Acknowledgments

The authors are grateful to Ms. Dagna Ariele da Costa Leite for providing valuable support during the conduction of this study.

Supplementary material

Chemical and textural properties of soil used in the plant study (Table S1); concentrations of nutrients used for plant growth (Table S2); kinetics models (Table S3); parameters of kinetic models (Table S4); phosphorus content in plants (Table S5); calcium and magnesium uptake by plants (Table S6); scanning electron microscopy images of BBFs and energy dispersive spectroscopy mappings for P, Ca and Mg (Fig. S1); height of grass and maize plants (Fig. S2); grain yield of common bean (Fig. S3); soil pH after cultivations (Fig. S4); visualization of the Mombasa grass plants growth (Fig. S5); visualization of the maize plants growth (Fig. S6) and visualization of the common bean plants growth (Fig. S7) can be found in the online version. Supplementary material to this article can be found online at doi: https://doi.org/10.1016/j.scitotenv.2020.143955.

References

Abdala, D.B., Northrup, P.A., Arai, Y., Sparks, D.L., 2015a. Surface loading effects on orthophosphate surface complexation at the goethite/water interface as examined by extended X-ray Absorption Fine Structure (EXAFS) spectroscopy. J. Colloid Interface Sci. 437, 297–303. https://doi.org/10.1016/j.jcis.2014.09.057

Abdala, D.B., Silva, I.R., Vergütz, L., Sparks, D.L., 2015b. Long-term manure application effects on phosphorus speciation, kinetics and distribution in highly weathered agricultural soils. Chemosphere 119, 504–514. https://doi.org/10.1016/j.chemosphere.2014.07.029

Akaike, H., 1974. A New Look at the Statistical Model Identification. IEEE Trans. Automat. Contr. 19, 716–723. https://doi.org/10.1109/TAC.1974.1100705

Almeida, D.S., Penn, C.J., Rosolem, C.A., 2018. Assessment of phosphorus availability in soil cultivated with ruzigrass. Geoderma 312, 64–73. https://doi.org/10.1016/j.geoderma.2017.10.003

Baligar, V.C., Bennett, O.L., 1986. Outlook on fertilizer use efficiency in the tropics. Fertil. Res. 10, 83–96. https://doi.org/10.1007/BF01073907

Baty, F., Ritz, C., Charles, S., Brutsche, M., Flandrois, J.-P., Delignette-Muller, M.-L., 2015. A toolbox for nonlinear regression in R: The package nlstools. J. Stat. Softw. 66, 1–21. https://doi.org/10.18637/jss.v066.i05

Borges, B.M.M.N., Strauss, M., Camelo, P.A., Sohi, S.P., Franco, H.C.J., 2020. Re-use of sugarcane residue as a novel biochar fertiliser - Increased phosphorus use efficiency and plant yield. J. Clean. Prod. 262, 121406. https://doi.org/10.1016/j.jclepro.2020.121406

Brasil, 2017. Manual de métodos analíticos oficiais para fertilizantes e corretivos. MAPA, Ministério da Agricultura Pecuária e Abastecimento/SDA, Secretaria de Defesa Agropecuária, Brasilia - DF.

Caione, G., Prado, R.M., Campos, C.N.S., Rodrigues, M., Pavinato, P.S., Agostinho, F.B., 2015. Phosphorus Fractionation in Soil Cultivated with Sugarcane Fertilized by Filter Cake and Phosphate Sources. Commun. Soil Sci. Plant Anal. 46, 2449–2459. https://doi.org/10.1080/00103624.2015.1081926

Carneiro, J.S.S., Lustosa Filho, J.F., Nardis, B.O., Ribeiro-Soares, J., Zinn, Y.L., Melo, L.C.A., 2018. Carbon Stability of Engineered Biochar-Based Phosphate Fertilizers. ACS Sustain. Chem. Eng. 6, 14203–14212. https://doi.org/10.1021/acssuschemeng.8b02841

Carneiro, J.S.S., Silva, P.S.S., Santos, A.C.M., Freitas, G.A., Silva, R.R., 2017. Resposta do

capim mombaça sob efeito de fontes e doses de fósforo na adubação de formação. J. bioenergy food Sci. 4, 12–25. https://doi.org/10.18067/jbfs.v4i1.117

Chew, J., Zhu, L., Nielsen, S., Graber, E., Mitchell, D.R.G., Horvat, J., Mohammed, M., Liu, M., van Zwieten, L., Donne, S., Munroe, P., Taherymoosavi, S., Pace, B., Rawal, A., Hook, J., Marjo, C., Thomas, D.S., Pan, G., Li, L., Bian, R., McBeath, A., Bird, M., Thomas, T., Husson, O., Solaiman, Z., Joseph, S., Fan, X., 2020. Biochar-based fertilizer: Supercharging root membrane potential and biomass yield of rice. Sci. Total Environ. 713, 136431. https://doi.org/10.1016/j.scitotenv.2019.136431

Condron, L.M., Goh, K.M., Newman, R.H., 1985. Nature and distribution of soil phosphorus as revealed by a sequential extraction method followed by 31P nuclear magnetic resonance analysis. J. Soil Sci. 36, 199–207. https://doi.org/10.1111/j.1365-2389.1985.tb00324.x

Cross, A.F., Schlesinger, W.H., 1995. A literature review and evaluation of the Hedley fractionation : Applications to the biogeochemical cycle of soil phosphorus in natural ecosystems. Geoderma 64, 197–214. https://doi.org/10.1016/0016-7061(94)00023-4

Degryse, F., Baird, R., Silva, R.C., McLaughlin, M.J., 2017. Dissolution rate and agronomic effectiveness of struvite fertilizers – effect of soil pH, granulation and base excess. Plant Soil 410, 139–152. https://doi.org/10.1007/s11104-016-2990-2

Domingues, R.R., Trugilho, P.F., Silva, C.A., Melo, I.C.N.A., Melo, L.C.A., Magriotis, Z.M., Sánchez-Monedero, M.A., 2017. Properties of biochar derived from wood and high-nutrient biomasses with the aim of agronomic and environmental benefits. PLoS One 12, 1–19. https://doi.org/10.1371/journal.pone.0176884

Enders, A., Lehmann, J., 2012. Comparison of Wet-Digestion and Dry-Ashing Methods for Total Elemental Analysis of Biochar. Commun. Soil Sci. Plant Anal. 43, 1042–1052. https://doi.org/10.1080/00103624.2012.656167

Everaert, M., Warrinnier, R., Baken, S., Gustafsson, J.P., De Vos, D., Smolders, E., 2016. Phosphate-Exchanged Mg-Al Layered Double Hydroxides: A New Slow Release Phosphate Fertilizer. ACS Sustain. Chem. Eng. 4, 4280–4287. https://doi.org/10.1021/acssuschemeng.6b00778

Farrell, M., Macdonald, L.M., Butler, G., Chirino-Valle, I., Condron, L.M., 2014. Biochar and fertiliser applications influence phosphorus fractionation and wheat yield. Biol. Fertil. Soils 50, 169–178. https://doi.org/10.1007/s00374-013-0845-z

Freitas, I.F., Novais, R.F., Villani, E.M.A., Novais, S.V., 2013. Phosphorus extracted by ion exchange resins and mehlich-1 from oxisols (latosols) treated with different phosphorus rates and sources for varied soil-source contact periods. Rev. Bras. Ciência do Solo 37, 667–677. https://doi.org/10.1590/s0100-06832013000300013

González-Ponce, R., López-de-Sá, E.G., Plaza, C., 2009. Lettuce response to phosphorus fertilization with struvite recovered from municipal wastewater. HortScience 44, 426–430.

Hedley, M.J., Stewart, J.W.B., Chauhan, B.S., 1982. Changes in inorganic and organic soil phosphorus fractions induced by cultivation practices and by laboratory incubations. Soil Sci. Soc. Am. J. 46, 970–976. https://doi.org/10.2136/sssaj1982.03615995004600050017x

Jiang, J., Yuan, M., Xu, R., Bish, D.L., 2015. Mobilization of phosphate in variable-charge soils amended with biochars derived from crop straws. Soil Tillage Res. 146, 139–147. https://doi.org/10.1016/j.still.2014.10.009

Joseph, S., Graber, E.R., Chia, C., Munroe, P., Donne, S., Thomas, T., Nielsen, S., Marjo, C., Rutlidge, H., Pan, G., Li, L., Taylor, P., Rawal, a, Hook, J., 2013. Shifting paradigms: development of high-efficiency biochar fertilizers based on nano-structures and soluble components. Carbon Manag. 4, 323–343. https://doi.org/10.4155/cmt.13.23

Khan, M.R., Rizvi, T.F., 2017. Application of Nanofertilizer and Nanopesticides for Improvements in Crop Production and Protection, in: Ghorbanpour, M., Manika, K., Varma, A. (Eds.), Nanoscience and Plant–Soil Systems, Soil Biology. Springer International Publishing, pp. 405–427. https://doi.org/10.1007/978-3-319-46835-8_15

Kingdom, F.A.A., Prins, N., 2016. Model Comparisons, in: Kingdom, F.A.A., Prins, N. (Eds.), Psychophysics: A Pratical Introduction. Academic press, United States of America, pp. 247–307. https://doi.org/10.1016/b978-0-12-407156-8.00009-8

Lehmann, J., Joseph, S. (Eds.), 2015. Biochar for Environmental Management: Science, Technology and Implementation, 2nd ed. Routledge: Taylor and Francis group, London and New York.

Leite, A.A., Cardoso, A.A.S., Leite, R.A., Oliveira-Longatti, S.M., Lustosa Filho, J.F., Moreira, F.M.S., Melo, L.C.A., 2020. Selected bacterial strains enhance phosphorus availability from biochar-based rock phosphate fertilizer. Ann. Microbiol. 70, 1–13. https://doi.org/10.1186/s13213-020-01550-3

Lenth, R., Singman, H., Love, J., Buerkner, P., Herve, M., 2019. Package ‘emmeans’: Estimated Marginal Means, aka Least-Squares Means. CRAN R Proj.

Li, H., Li, Y., Xu, Y., Lu, X., 2020. Biochar phosphorus fertilizer effects on soil phosphorus availability. Chemosphere 244, 125471. https://doi.org/10.1016/j.chemosphere.2019.125471

Lopes, A.S., Guilherme, L.R.G., 2016. A career perspective on soil management in the Cerrado region of Brazil. Adv. Agron. 137, 1–72. https://doi.org/10.1016/bs.agron.2015.12.004

Lopes, A.S., Guilherme, L.R.G., Ramos, S.J., 2012. The saga of the agricultural development of the brazilian cerrado. Int. Potash Institute, Res. Find. 32, 29–56.

Lustosa Filho, J.F., Barbosa, C.F., Carneiro, J.S.S., Melo, L.C.A., 2019. Diffusion and

phosphorus solubility of biochar-based fertilizer: Visualization, chemical assessment and availability to plants. Soil Tillage Res. 194, 104298. https://doi.org/10.1016/j.still.2019.104298

Lustosa Filho, J.F., Carneiro, J.S.S., Barbosa, C.F., Lima, K.P., Leite, A.A., Melo, L.C.A., 2020. Aging of biochar-based fertilizers in soil: Effects on phosphorus pools and availability to Urochloa brizantha grass. Sci. Total Environ. 709, 136028. https://doi.org/10.1016/j.scitotenv.2019.136028

Lustosa Filho, J.F., Penido, E.S., Castro, P.P., Silva, C.A., Melo, L.C.A., 2017. Co-Pyrolysis of Poultry Litter and Phosphate and Magnesium Generates Alternative Slow-Release Fertilizer Suitable for Tropical Soils. ACS Sustain. Chem. Eng. 5, 9043–9052. https://doi.org/10.1021/acssuschemeng.7b01935

Malavolta, E., 1980. Elementos de nutrição mineral das plantas. Agronômica Ceres, São Paulo.

Malavolta, E., Vitti, G.C., Oliveira, S.A., 1997. Avaliação do estado nutricional das plantas - Princípios e aplicações, 2nd ed. Associação Brasileira para Pesquisa da Potassa e do Fósforo, Piracicaba, SP.

Martinez, H.E.P., Carvalho, J.G., Souza, R.B., 1999. Diagnose Foliar, in: Ribeiro, A.C., Guimarães, P.T.G., Venegas, V.H.A. (Eds.), Recomendações Para o Uso de Corretivos e Fertilizantes Em Minas Gerais - 5° Aproximação. Comissão de Fertilidade do solo do estado de Minas Gerais- CFSEMG, Viçosa, MG, Brazil, pp. 142–168.

Murphy, J., Riley, J.P., 1962. A modified single solution method for the determination of phosphate in natural waters. Anal. Chim. Acta 27, 31–36. https://doi.org/10.1016/S0003-2670(00)88444-5

Nardis, B.O., Carneiro, J.S.S., Souza, I.M.G., Barros, R.G., Melo, L.C.A., 2020. Phosphorus recovery using magnesium-enriched biochar and its potential use as fertilizer. Arch.

Agron. Soil Sci. https://doi.org/10.1080/03650340.2020.1771699

Niu, Y., Jin, G., Li, X., Tang, C., Zhang, Y., Liang, Y., Yu, J., 2015. Phosphorus and magnesium interactively modulate the elongation and directional growth of primary roots in Arabidopsis thaliana (L.) Heynh. J. Exp. Bot. 66, 3841–3854. https://doi.org/10.1093/jxb/erv181

Novais, R.F., Neves, J.C.L., Barros, N.F., 1991. Ensaio em ambiente controlado, in: Oliveira, A.J., Garrido, W.E., Araújo, J.D., Lourenço, S. (Eds.), Métodos de Pesquisa Em Fertilidade Do Solo. Embrapa-SEA, Brasília, pp. 189–253.

Novais, R.F., Smyth, T.J., 1999. Fósforo em solo e planta em condições tropicais. Univesidade Federal de Viçosa, Viçosa, MG, Brazil.

Novais, S.V., Mattiello, E.M., Vergutz, L., Melo, L.C.A., Freitas, Í.F., Novais, R.F., 2015. Desgaste dos extratores mehlich-1 e fosfato monocálcico como variável do P-remanescente e sua relação com os níveis críticos de fósforo e de enxofre nos solos. Rev. Bras. Cienc. do Solo 39, 1079–1087. https://doi.org/10.1590/01000683rbcs20140551

Olibone, D., Rosolem, C.A., 2010. Phosphate fertilization and phosphorus forms in an Oxisol under no-till. Sci. Agric. 67, 465–471. https://doi.org/10.1590/s0103-90162010000400014

Pavinato, P.S., Merlin, A., Rosolem, C.A., 2009. Phosphorus fractions in Brazilian Cerrado soils as affected by tillage. Soil Tillage Res. 105, 149–155. https://doi.org/10.1016/j.still.2009.07.001

Peng, Y., Sun, Y., Sun, R., Zhou, Y., Tsang, D.C.W., Chen, Q., 2019. Optimizing the synthesis of Fe/Al (Hydr)oxides-Biochars to maximize phosphate removal via response surface model. J. Clean. Prod. 237, 117770. https://doi.org/10.1016/j.jclepro.2019.117770

Penido, E.S., Melo, L.C.A., Guilherme, L.R.G., Bianchi, M.L., 2019. Cadmium binding mechanisms and adsorption capacity by novel phosphorus/magnesium-engineered biochars. Sci. Total Environ. 671, 1134–1143. https://doi.org/10.1016/j.scitotenv.2019.03.437

Pogorzelski, D., Lustosa Filho, J.F., Matias, P.C., Santos, W.O., Vergütz, L., Melo, L.C.A., 2020. Biochar as composite of phosphate fertilizer: Characterization and agronomic effectiveness. Sci. Total Environ. 743, 140604. https://doi.org/10.1016/j.scitotenv.2020.140604

R Core Team, 2019. R: A language and environment for statistical computing. R Found. Stat. Comput.

Raij., B. Van, 2011. Fertilidade do solo e manejo de nutrientes. International Plant Nutrition Institute, Instituto Agronômico de Campinas, Piracicaba, SP, Brazil.

Raij, B. van, Quaggio, J.A., Silva, N.M., 1986. Extraction of phosphorus, potassium, calcium, and magnesium from soils by an ion-exchange resin procedure. Commun. Soil Sci. Plant Anal. 17, 547–566. https://doi.org/10.1080/00103628609367733

Rivaie, A.A., Loganathan, P., Graham, J.D., Tillman, R.W., Payn, T.W., 2008. Effect of phosphate rock and triple superphosphate on soil phosphorus fractions and their plant-availability and downward movement in two volcanic ash soils under Pinus radiata plantations in New Zealand. Nutr. Cycl. Agroecosystems 82, 75–88. https://doi.org/10.1007/s10705-008-9170-6

Rodrigues, M., Pavinato, P.S., Withers, P.J.A., Teles, A.P.B., Herrera, W.F.B., 2016. Legacy phosphorus and no tillage agriculture in tropical oxisols of the Brazilian savanna. Sci. Total Environ. 542, 1050–1061. https://doi.org/10.1016/j.scitotenv.2015.08.118

Sá, J.M., Jantalia, C.P., Teixeira, P.C., Polidoro, J.C., Benites, V. de M., Araújo, A.P., 2017. Agronomic and P recovery efficiency of organomineral phosphate fertilizer from

poultry litter in sandy and clayey soils. Pesqui. Agropecu. Bras. 52, 786–793. https://doi.org/10.1590/S0100-204X2017000900011

Sahin, O., Taskin, M.B., Kaya, E.C., Atakol, O., Emir, E., Inal, A., Gunes, A., 2017. Effect of acid modification of biochar on nutrient availability and maize growth in a calcareous soil. Soil Use Manag. 33, 447–456. https://doi.org/10.1111/sum.12360

Sanchez, P.A., Uehara, G., 1980. Management Considerations for Acid Soils with High Phosphorus Fixation Capacity, in: Kamprath, F.E., Sample, E.C., Kamprath, E.J. (Eds.), The Role of Phosphorus in Agriculture. American Society of Agronomy, Inc. Crop Science Society of America, Inc. Soil Science Society of America Inc., pp. 471–514. https://doi.org/10.2134/1980.roleofphosphorus.c18

Santos, S.R., Lustosa Filho, J.F., Vergütz, L., Melo, L.C.A., 2019. Biochar association with phosphate fertilizer and its influence on phosphorus use efficiency by maize. Cienc. e Agrotecnologia 43. https://doi.org/10.1590/1413-7054201943025718

Schachtman, D.P., Reid, R.J., Ayling, S.M., 1998. Phosphorus Uptake by Plants: From Soil to Cell. Plant Physiol. 116, 447–453. https://doi.org/10.1104/pp.116.2.447

Scholz, R.W., Ulrich, A.E., Eilittä, M., Roy, A., 2013. Sustainable use of phosphorus: A finite resource. Sci. Total Environ. 461–462, 799–803. https://doi.org/10.1016/j.scitotenv.2013.05.043

Shariatmadari, H., Shirvani, M., Jafari, A., 2006. Phosphorus release kinetics and availability in calcareous soils of selected arid and semiarid toposequences. Geoderma 132, 261–272. https://doi.org/10.1016/j.geoderma.2005.05.011

Silva, F.C., 2009. Manual de análises químicas de solos, plantas e fertilizantes, 2nd ed. Empresa Brasileira de Pesquisa Agropecuária, Embrapa Solos, Brasília, DF.

Smith, F.W., 2002. The phosphate uptake mechanism. Plant Soil 245, 105–114. https://doi.org/10.1023/A:1020660023284

Solanki, P., Bhargava, A., Chhipa, H., Jain, N., Panwar, J., 2015. Nano-fertilizers and Their Smart Delivery System, in: Rai, M., Ribeiro, C., Mattoso, L., Duran, N. (Eds.), Nanotechnologies in Food and Agriculture. Springer International Publishing, pp. 81–101. https://doi.org/10.1007/978-3-319-14024-7_4

Teles, A.P.B., Rodrigues, M., Bejarano Herrera, W.F., Soltangheisi, A., Sartor, L.R., Withers, P.J.A., Pavinato, P.S., 2017. Do cover crops change the lability of phosphorus in a clayey subtropical soil under different phosphate fertilizers? Soil Use Manag. 33, 34–44. https://doi.org/10.1111/sum.12327

Tiessen, H., Moir, J.O., 1993. Characterization of available P by sequential extraction, in: Carter, M.R. (Ed.), Soil Sampling and Methods of Analysis Canadian Society of Soil Science. Lewis Publications, Boca Raton, pp. 75–86.

Venegas, V.H.A., Novais, R.F., Barros, N.F., Cantarutti, R.B., Lopes, A.S., 1999. Interpretação dos resultados das análises de solo, in: Ribeiro, A.C., Guimarães, P.T.G., Venegas, V.H.A. (Eds.), Recomendações Para o Uso de Corretivos e Fertilizantes Em Minas Gerais, 5ª Aproximação. Comissão de Fertilidade do Solo do Estado de Minas Gerais – CFSEMG, Viçosa, MG, Brazil, pp. 25–36.

Vu, V.Q., 2011. ggbiplot: A ggplot2 based biplot. R package version 0.55. Retrieved from http://github.com/vqv/ggbiplot.

Withers, P.J.A., Rodrigues, M., Soltangheisi, A., Carvalho, T.S., Guilherme, L.R.G., Benites, V.D.M., Gatiboni, L.C., Sousa, D.M.G., Nunes, R.D.S., Rosolem, C.A., Andreote, F.D., Oliveira, A. De, Coutinho, E.L.M., Pavinato, P.S., 2018. Transitions to sustainable management of phosphorus in Brazilian agriculture. Sci. Rep. 8, 1–13. https://doi.org/10.1038/s41598-018-20887-z

Yang, F., Zhang, S., Sun, Y., Tsang, D.C.W., Cheng, K., Ok, Y.S., 2019. Assembling biochar with various layered double hydroxides for enhancement of phosphorus

recovery. J. Hazard. Mater. 365, 665–673. https://doi.org/10.1016/j.jhazmat.2018.11.047

Yao, C., Joseph, S., Li, L., Pan, G., Lin, Y., Munroe, P., Pace, B., Taherymoosavi, S., Van zwieten, L., Thomas, T., Nielsen, S., Ye, J., Donne, S., 2015. Developing More Effective Enhanced Biochar Fertilisers for Improvement of Pepper Yield and Quality. Pedosphere 25, 703–712. https://doi.org/10.1016/S1002-0160(15)30051-5

Zhang, T., He, X., Deng, Y., Tsang, D.C.W., Jiang, R., Becker, G.C., Kruse, A., 2020. Phosphorus recovered from digestate by hydrothermal processes with struvite crystallization and its potential as a fertilizer. Sci. Total Environ. https://doi.org/10.1016/j.scitotenv.2019.134240

Zhao, L., Cao, X., Zheng, W., Kan, Y., 2014. Phosphorus-assisted biomass thermal conversion: Reducing carbon loss and improving biochar stability. PLoS One 9, 1–15. https://doi.org/10.1371/journal.pone.0115373

Zhao, L., Cao, X., Zheng, W., Scott, J.W., Sharma, B.K., Chen, X., 2016. Copyrolysis of Biomass with Phosphate Fertilizers to Improve Biochar Carbon Retention, Slow Nutrient Release, and Stabilize Heavy Metals in Soil. ACS Sustain. Chem. Eng. 4, 1630–1636. https://doi.org/10.1021/acssuschemeng.5b01570

APPENDIX A

Supplementary material

Long-term effect of biochar-based fertilizers application in tropical soil: agronomic efficiency and phosphorus availability

Jefferson Santana da Silva Carneiro [a], *Ivan Célio Andrade Ribeiro* [a], *Bárbara Olinda Nardis* [a], *Cristiane Francisca Barbosa* [a], *José Ferreira Lustosa Filho* [b], *Leônidas Carrijo Azevedo Melo* [a, *]

[a] Federal University of Lavras, Soil Science Department, Lavras, 37200-900, Minas Gerais, Brazil.

[b] Federal University of Viçosa, Department of Soils, Viçosa, 36570-900, Minas Gerais, Brazil.

*Corresponding author

Leônidas Carrijo Azevedo Melo,

E-mail: leonidas.melo@ufla.br

This supplementary material can be found online at doi:

https://doi.org/10.1016/j.scitotenv.2020.143955

Soil characterization and pots fertilization

Table S1 – Chemical and textural properties[a] of soil used in plant study.

pH H_2O	4.60
K (mg kg^{-1})	19.4
P (mg kg^{-1})	0.77
Ca^{2+} ($cmol_c$ kg^{-1})	0.12
Mg^{2+} ($cmol_c$ kg^{-1})	0.10
Al^{3+} ($cmol_c$ kg^{-1})	0.65
H+Al ($cmol_c$ kg^{-1})	6.97
SB ($cmol_c$ kg^{-1})	0.27
t ($cmol_c$ kg^{-1})	0.92
T ($cmol_c$ kg^{-1})	7.24
V (%)	3.73
m (%)	70.7
O.M. (dag kg^{-1})	2.28
P-Rem (mg kg^{-1})	10.9
Zn (mg kg^{-1})	0.94
Fe (mg kg^{-1})	78.7
Mn (mg kg^{-1})	8.75
Cu (mg kg^{-1})	1.83
B (mg kg^{-1})	0.01
S (mg kg^{-1})	11.2
Clay (g kg^{-1})	600
Silt (g kg^{-1})	160
Sand (g kg^{-1})	240

[a]Ca^{2+}, Mg^{2+} and Al^{3+}: KCl extractor (1mol L^{-1}); P, K, Fe, Zn, Mn, and Cu: Mehlich-1 extractor; H+Al: SMP extractor; B: Hot water extractor; S: monocalcium phosphate in acetic acid extractor; O.M.: organic matter by $Na_2Cr_2O_7$ 4 mol L^{-1} + H_2SO_4 10 mol L^{-1} oxidation; SB: sum of exchangeable bases; P-rem: remaining phosphorus; T: cation exchange capacity at pH 7; t: effective cation exchange capacity; V: base saturation index; and m%: aluminum saturation index.

Table S2 – Concentrations of nutrients used for plants growth.

Nutrients[a] mg kg^{-1} of soil	Mombasa grass[e]	Maize	Bean
N	150[c]	150[c]	300[d]
P[b]	240	-	-
K	150[c]	150[c]	200[d]
S	40.0	40.0	40.0
Cu	1.50	1.50	1.50
Mn	3.50	3.50	3.50
Fe	3.00	3.00	3.00
B	0.80	0.80	0.80
Mo	0.10	0.10	0.10
Zn	5.00	5.00	5.00

[a]According to Novais et al. (1991) and Malavolta (1980); [b]P fertilization was made only in the first planting using BBF or TSP according to the treatments; [c]It was carried out in three applications: planting, 15 and at 25 days for grass, and at 30 days for maize plants; [d] It was carried out in three applications: planting, and V2, V4 and R5 stages; [e]After each forage harvest, 150 mg kg^{-1} of N and 100 mg kg^{-1} of K were applied after cutting, and at 15 and 25 days after cutting.

Kinetics models of P release

Table S3 - Equations tested to describe P release kinetic data of BBFs and TSP.

Kinetics equations	Parameters	Reference
First order:	k_1, first order rate constant	Simonin (2016)
$Q_t = Q_e\,[1 - exp(-k_1\,t)]$	(h^{-1})	
Second order:	k_2, second order rate constant	Simonin (2016)
$Q_t = Q_e\,[(k_2\,t)/(1+k_2\,t)]$	[(g P kg^{-1})$^{-1}$]	
Power function:	a, initial P desorption rate	Shariatmadari et al. (2006)
$Q_t = a\,t^b$	(g P kg^{-1} h^{-1})^b	
	b, desorption rate coefficient	
	[(g P kg^{-1})$^{-1}$]	
Elovich:	α, initial P desorption	Lustosa Filho et al. (2017)
$Q_t = \alpha - \beta \ln(t)$	(g P kg^{-1} h^{-1})	
	β, P desorption constant	
	[(g P kg^{-1})$^{-1}$]	
Parabolic diffusion:	R, diffusion rate constant	Shariatmadari et al. (2006)
$Q_t = Q_e + R\,t^{0.5}$	[(g P kg^{-1})$^{-0.5}$]	

where Q_t (g P kg^{-1}) is the cumulative P release at t time; Q_e (g P kg^{-1}) is the amount of P release at equilibrium or maximum P released.

These mathematical models were tested and mathematically adjusted to a P kinetics data set, and the quality of the fit was observed based on its standard error of the estimative (SE) (Equation 1) (Shariatmadari et al., 2006) and the better model was chosen based on Akaike information criterion (AIC) (Equation 2) (Akaike, 1974; Kingdom and Prins, 2016).

$$SE = \left[\left(Q_t - Q_t'\right)^2/(N - 2)\right]^{1/2} \qquad \text{Equation 1}$$

where Q_t and Q'_t are the measured and predicted amounts of released P at time *t*, respectively, and *N* is the number of measurements.

$$AIC = -2LL(\theta|y,M_i) + 2K_i \quad \text{Equation 2}$$

where $LL(\theta|y,M_i)$ is the log-likelihood for model M_i using maximum likelihood estimates for its parameters θ, based on the observed data *y*, and K_i is the number of free parameters in model M_i.

Table S4– Parameters and standard error of estimative (SE) of the examined models for P release kinetics of BBFs and TSP.

Models	Parameters[a]	Fertilizers		
		TSP	CHB	PLB
First Order	Q_e (g P kg^{-1})	197.7	81.80	42.12
	k_1 (h^{-1})	9.916	0.070	0.178
	SE	7.607	7.113	8.265
	AIC	79.65	78.17	81.47
Second Order	Q_e (g P kg^{-1})	200.0	91.60	45.12
	k_2 [(g P $kg^{-1})^{-1}$]	32.42	0.089	0.275
	SE	5.605	4.658	6.498
	AIC	72.93	68.86	76.18
Power Function	a (g P kg^{-1} $h^{-1})^b$	188.0	20.44	16.57
	b [(g P $kg^{-1})^{-1}$]	0.018	0.293	0.217
	SE	3.067	7.391	1.191
	AIC	59.67	79.01	38.84
Elovich	α (g P kg^{-1} h^{-1})	189.0	17.04	16.52
	β [(g P $kg^{-1})^{-1}$]	-3.559	-13.31	-5.998
	SE	3.002	6.881	2.926
	AIC	59.20	77.44	58.63
Parabolic Difusion	Q_e (g P kg^{-1})	188.9	16.12	15.70
	R (g P $kg^{-1})^{-0.5}$	1.393	6.031	2.797
	SE	5.733	11.83	3.986
	AIC	73.43	89.37	65.43

[a]k_1 is the first order rate constant; k_2 is the second order rate constant; a is the initial P desorption rate; β is the P desorption constant; R is the diffusion rate constant; Q_e is the amount of P release at equilibrium or maximum P released; SE is the standard error of estimative and AIC is the Akaike Information Criterion.

Phosphorus content in plants

Table S5 – Phosphorus content (g kg^{-1}) [mean ± standard error (n = 4)] in plants.

	Mombasa grass[a]			Maize[a]	Bean	
Treatments	1st cycle[b]	2nd cycle	3rd cycle		SDM	Grain
CHB100	1.53 ± 0.09 a	1.44 ± 0.02 a	2.28 ± 0.05 a	1.28 ± 0.11 a	1.03 ± 0.03 ab	2.83 ± 0.21 a
CHB75	1.52 ± 0.04 a	1.38 ± 0.05 ab	1.55 ± 0.06 c	1.38 ± 0.04 a	1.04 ± 0.05 ab	2.86 ± 0.16 a
CHB50	1.78 ± 0.04 a	1.37 ± 0.03 ab	1.26 ± 0.04 d	1.45 ± 0.11 a	0.99 ± 0.06 ab	2.87 ± 0.12 a
PLB100	1.69 ± 0.02 a	1.24 ± 0.06 b	2.01 ± 0.07 b	1.10 ± 0.06 a	0.80 ± 0.01 b	2.63 ± 0.09 a
PLB75	1.67 ± 0.09 a	1.34 ± 0.03 ab	1.51 ± 0.07 c	1.24 ± 0.08 a	1.23 ± 0.08 a	2.68 ± 0.19 a
PLB50	1.79 ± 0.06 a	1.33 ± 0.04 ab	1.20 ± 0.01 d	1.27 ± 0.07 a	0.80 ± 0.09 b	2.87 ± 0.13 a
TSP	1.79 ± 0.08 a	1.25 ± 0.03 b	1.10 ± 0.03 d	1.45 ± 0.14 a	1.23 ± 0.05 a	2.84 ± 0.09 a

*Mean followed by the same letters in the columns do not differ from each other by the Tukey test ($p < 0.05$); [a]Determined in shoot dry mass (SDM); [b]cropping cycle.

Calcium and magnesium uptake by plants

Table S6 – Calcium (Ca) and magnesium (Mg) [(mean ± standard error (n = 4)] uptake by plants.

	Mombasa grass[a]			Maize[a]	Bean	
Treatments	1st cycle[b]	2nd cycle	3rd cycle		SDM	Grain
	Calcium (Ca) (mg pot^{-1})					
CHB100	60.8±5.50 d[*]	65.5±3.78 bc	38.3±1.51 e	56.3±1.79 ab	410±9.15 ab	33.9±2.06 ab
CHB75	79.3±2.48 bc	71.0±4.09 abc	55.0±2.96 c	52.3±1.70 ab	403±12.2 ab	30.5±1.38 b
CHB50	90.1±2.81 b	79.3±1.40 ab	65.0±1.74 b	52.7±0.93 ab	465±17.3 a	36.9±1.55 ab
PLB100	72.3±6.50 cd	57.9±2.75 c	44.2±0.63 de	49.7±1.98 b	386±23.9 b	37.7±1.76 ab
PLB75	89.7±2.31 bc	72.5±2.85 ab	50.6±1.93 cd	55.5±1.60 ab	415±17.4 ab	34.8±1.45 ab
PLB50	94.7±2.77 ab	71.7±3.45 abc	63.7±0.98 b	52.6±0.81 ab	400±19.4 ab	35.5±2.78 ab
TSP	109±2.12 a	80.6±2.06 a	79.6±2.16 a	58.2±1.59 a	450±11.7 ab	42.4±2.26 a
Treatments	Magnesium (Mg) (mg pot^{-1})					
CHB100	106±5.25 cd	86.5±2.00 ab	33.1±0.90 c	58.8±2.97 ab	74.5±2.45 ab	35.3±1.15 a
CHB75	124±2.47 b	91.9±4.32 a	40.9±1.40 ab	47.5±1.87 bc	49.2±1.84 c	32.5±0.80 a
CHB50	122±3.91 bc	75.7±2.64 b	35.8±1.23 c	34.3±2.39 d	38.9±2.41 cd	26.9±0.44 b
PLB100	137±4.05 ab	93.4±3.77 a	43.8±1.03 a	62.1±4.33 a	81.6±3.79 a	34.5±2.00 a
PLB75	142±2.64 a	94.2±3.80 a	43.7±1.08 a	53.0±2.21 abc	67.4±3.16 b	35.4±1.67 a
PLB50	134±2.84 ab	75.7±0.71 b	34.7±1.15 bc	44.2±1.71 cd	37.5±1.07 d	30.4±0.97 ab
TSP	105±0.86 d	53.4±2.50 c	18.8±0.60 d	32.3±2.10 d	14.9±1.46 e	20.7±0.58 c

[*]Mean followed by the same letters in the columns do not differ from each other by the Tukey test ($p < 0.05$); [a]Ca and Mg uptake by shoot dry mass (SDM); [b]cropping cycle.

Scanning electron microscopy (SEM) and energy dispersive spectroscopy (EDS)

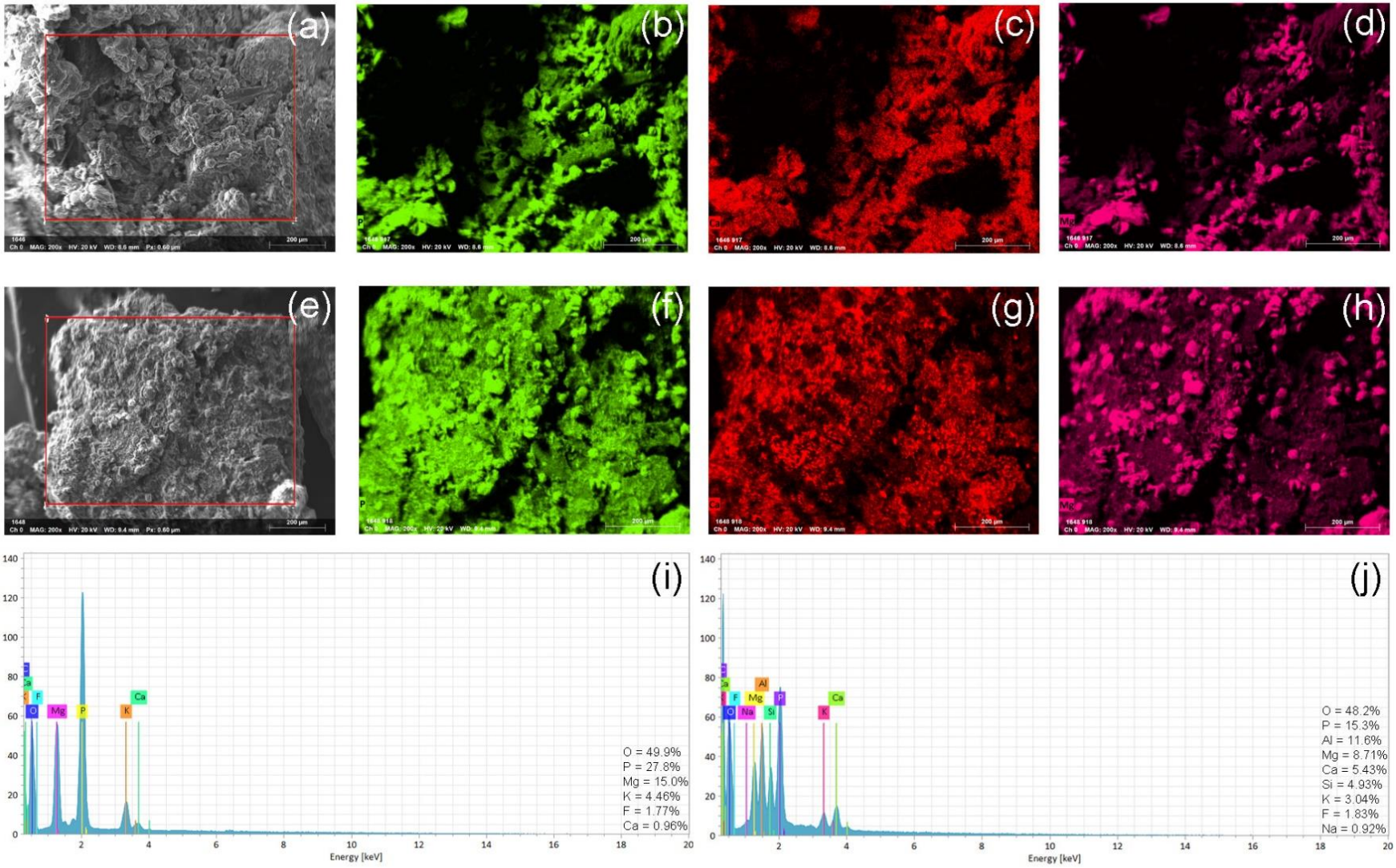

Figure S1 - SEM images of BBFs (a and b), SEM-EDS mapping for P (b and f), Ca (c and g) and Mg (d and h), and SEM-EDX spectrum (i and j) respectively to CHB and PLB.

Plant height

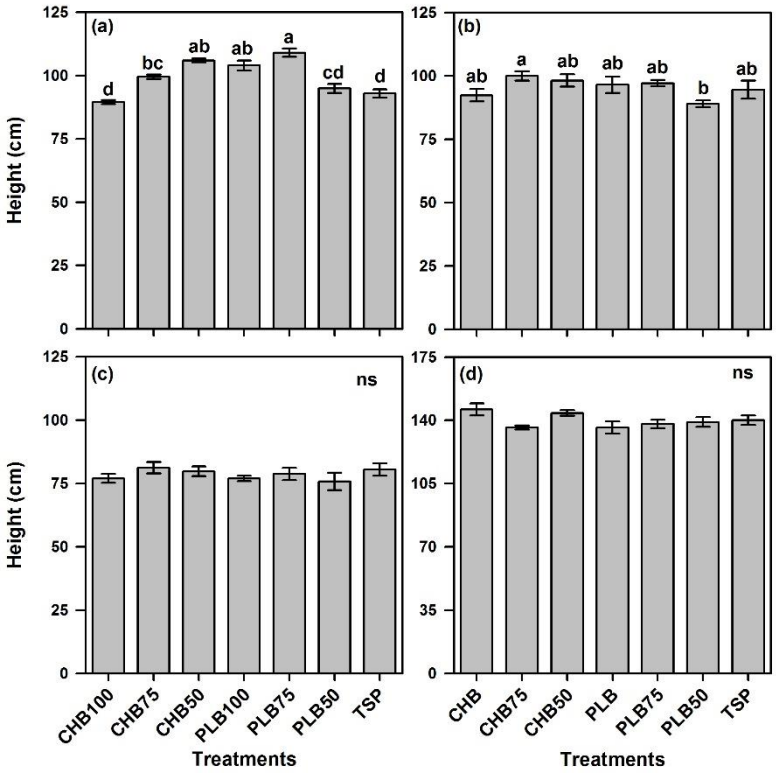

Figure S2 – Height of Mombasa grass in the first cropping cycle (a), second cycle (b), and third cycle (c) and maize plants (d) under BBFs and TSP fertilization. [ns] Means of the treatments do not differ from each other by the Tukey test ($p > 0.05$). Mean followed by the same letters in the bars do not differ from each other by the Tukey test ($p < 0.05$); Error bars represent standard error (n = 4).

Grain yield of common bean plants

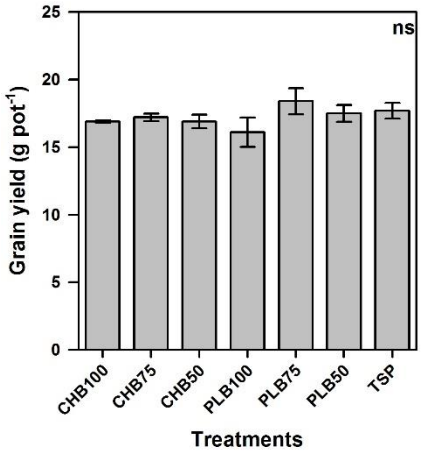

Figure S3 –Grain yield of bean plants under BBFs and TSP fertilization. [ns] Means of the treatments do not differ from each other by the Tukey test ($p > 0.05$); Error bars represent standard error (n = 4).

Soil pH

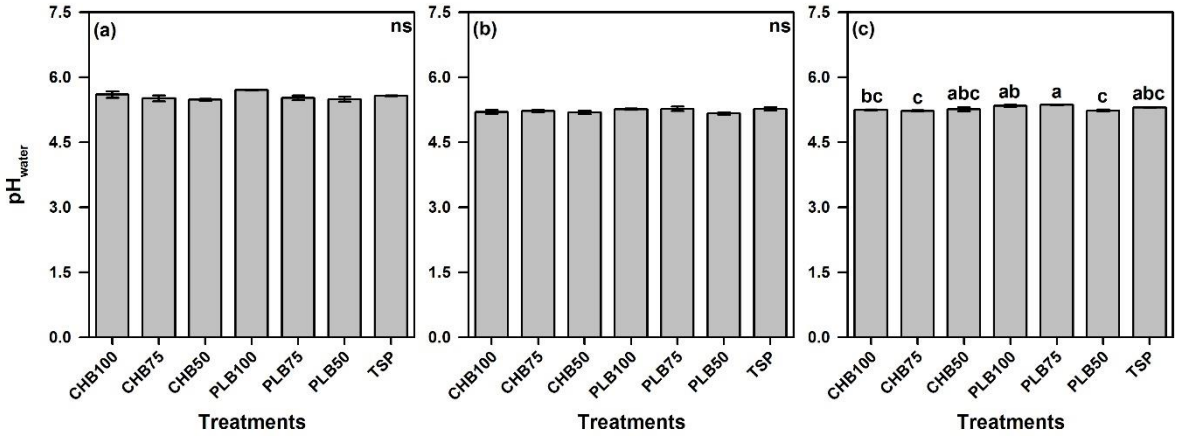

Figure S4 – Soil pH after each cultivation under BBFs and TSP fertilization. Mombasa grass (a), maize (b) and common bean (c). ^{ns} Means of the treatments do not differ from each other by the Tukey test ($p > 0.05$). Mean followed by the same letters in the bars do not differ from each other by the Tukey test ($p < 0.05$); Error bars represent standard error (n = 4).

Plants grown in the first, second and third cultivation

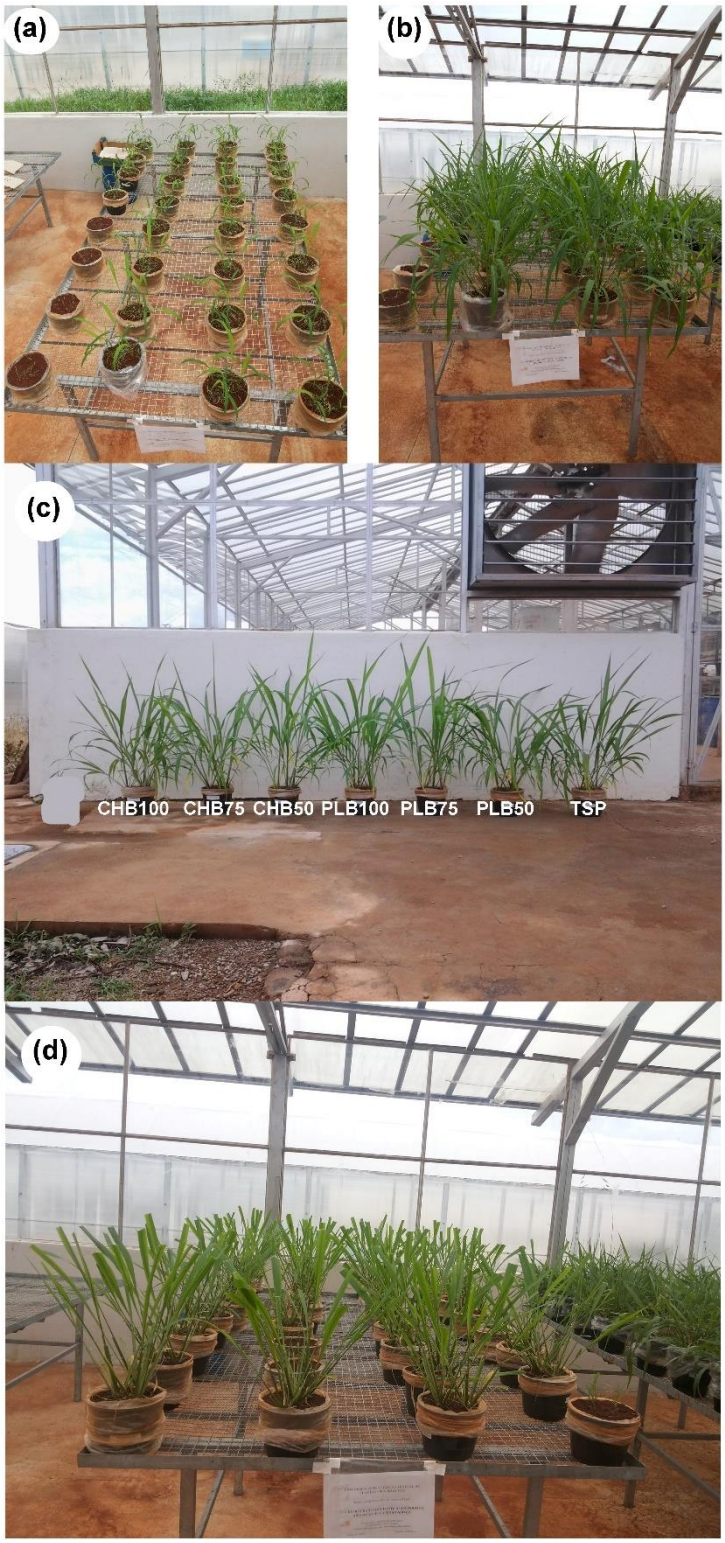

Figure S5 – Mombasa grass plants grown under BBFs and TSP fertilization at 15 days after emergency (a), 30 days after emergency (b), at first harvest (40 days) (c) and at 4 days after the first harvest (d).

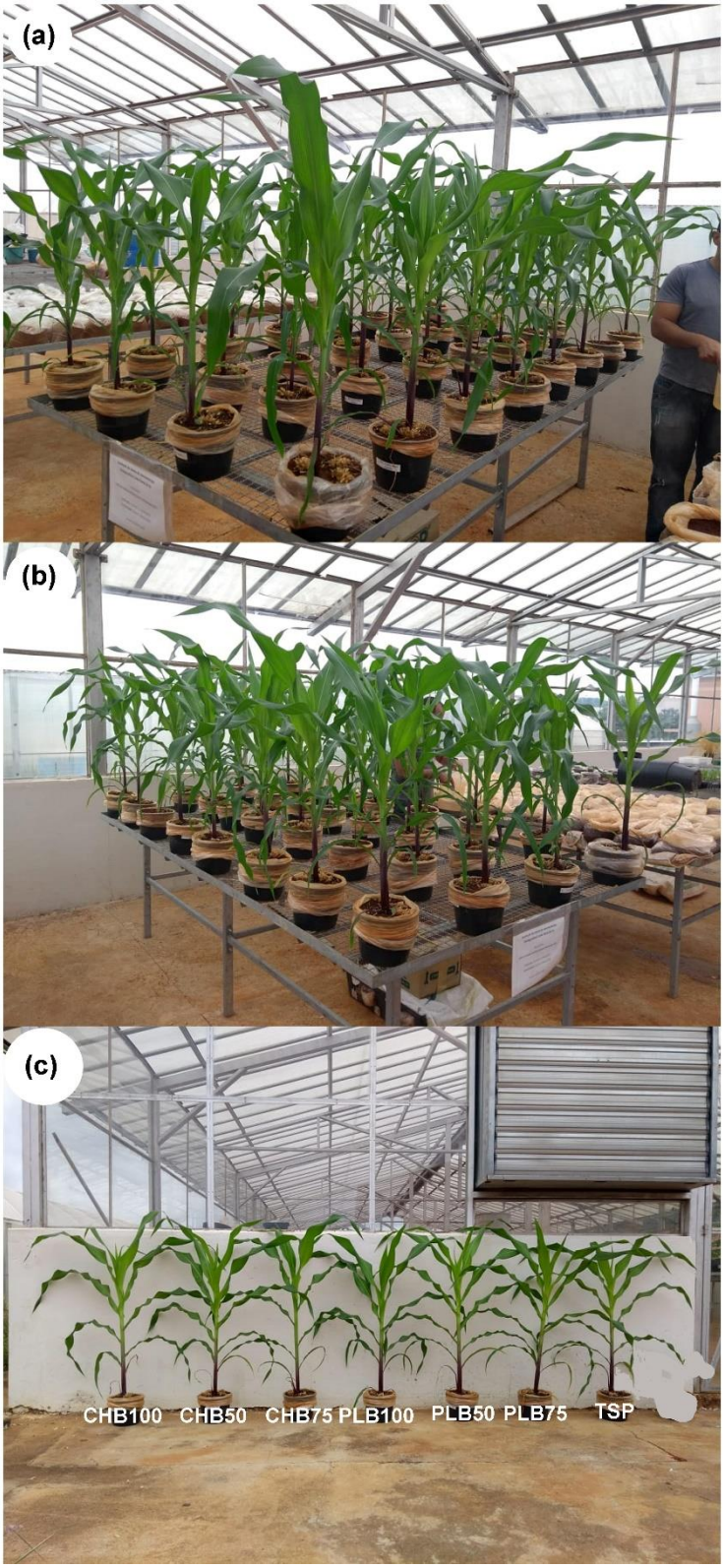

Figure S6 – Maize plants grown under BBFs and TSP fertilization at 30 days after emergency (a), 35 days after emergency (b) and at harvest (c) (45 days).

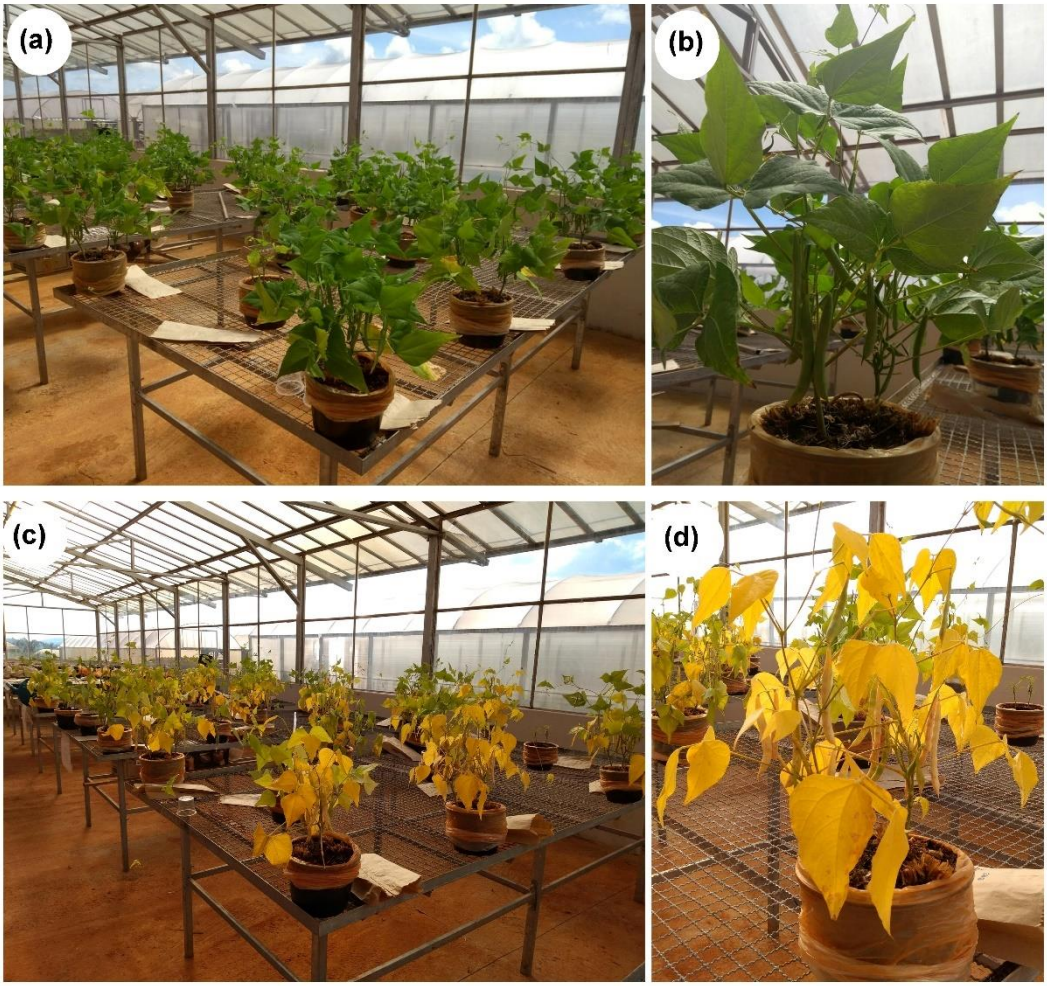

Figure S7 – Common bean plants grown under BBFs and TSP fertilization at 35 days after emergency (a and b) and 55 days after emergency (c and d).

References

Akaike, H., 1974. A New Look at the Statistical Model Identification. IEEE Trans. Automat. Contr. 19, 716–723. https://doi.org/10.1109/TAC.1974.1100705

Kingdom, F.A.A., Prins, N., 2016. Model Comparisons, in: Kingdom, F.A.A., Prins, N. (Eds.), Psychophysics: A Pratical Introduction. Academic press, United States of America, pp. 247–307. https://doi.org/10.1016/b978-0-12-407156-8.00009-8

Lustosa Filho, J.F., Penido, E.S., Castro, P.P., Silva, C.A., Melo, L.C.A., 2017. Co-Pyrolysis of Poultry Litter and Phosphate and Magnesium Generates Alternative Slow-Release Fertilizer Suitable for Tropical Soils. ACS Sustain. Chem. Eng. 5, 9043–9052. https://doi.org/10.1021/acssuschemeng.7b01935

Malavolta, E., 1980. Elementos de nutrição mineral das plantas. Agronômica Ceres, São Paulo.

Novais, R.F., Neves, J.C.L., Barros, N.F., 1991. Ensaio em ambiente controlado, in: Oliveira, A.J., Garrido, W.E., Araújo, J.D., Lourenço, S. (Eds.), Métodos de Pesquisa Em Fertilidade Do Solo. Embrapa-SEA, Brasília, pp. 189–253.

Shariatmadari, H., Shirvani, M., Jafari, A., 2006. Phosphorus release kinetics and availability in calcareous soils of selected arid and semiarid toposequences. Geoderma 132, 261–272. https://doi.org/10.1016/j.geoderma.2005.05.011

Simonin, J.P., 2016. On the comparison of pseudo-first order and pseudo-second order rate laws in the modeling of adsorption kinetics. Chem. Eng. J. 300, 254–263. https://doi.org/10.1016/j.cej.2016.04.079

THIRD PART

ARTICLE 2

Biochar and graphene oxide composite matrix producing micronutrient fertilizer: a new approach towards the improvement of effectiveness in tropical soil

(Article under review in the *Journal of Cleaner Production*)

Biochar and graphene oxide composite matrix producing micronutrient fertilizer: a new approach towards the improvement of effectiveness in tropical soil

Jefferson Santana da Silva Carneiro[a], Dagna Ariele da Costa Leite[b], Gustavo Mesquita de Castro[a], José Romão Franca[c], Lívia Botelho[a], Jenaina Ribeiro Soares[c], Juliano Elvis de Oliveira[d], Leônidas Carrijo Azevedo Melo[a*]

[a] Federal University of Lavras, School of Agricultural Sciences, Soil Science Department, Lavras, 37200-900, Minas Gerais, Brazil.

[b] Federal University of Tocantins, Gurupi campus, Gurupi, 77402-970, Tocantins, Brazil.

[c] Federal University of Lavras, Institute of Natural Sciences, Physics Department, Lavras, 37200-900, Minas Gerais, Brazil.

[d] Federal University of Lavras, School of Engineering, Engineering Department, Lavras, 37200-900, Minas Gerais, Brazil.

*Corresponding author

Leônidas Carrijo Azevedo Melo

E-mail: leonidas.melo@ufla.br

Highlights

- Graphene oxide and poultry litter biochar (PLB-GO) composite as a novel adsorbent.

- PLB-GO increased Cu and Zn adsorption capacity.

- Cu and Zn adsorbed on PLB-GO have very low water solubility.

- Cu and Zn-loaded PLB-GO showed enhanced fertilizer efficiency in highly weathered soil.

Graphical abstract

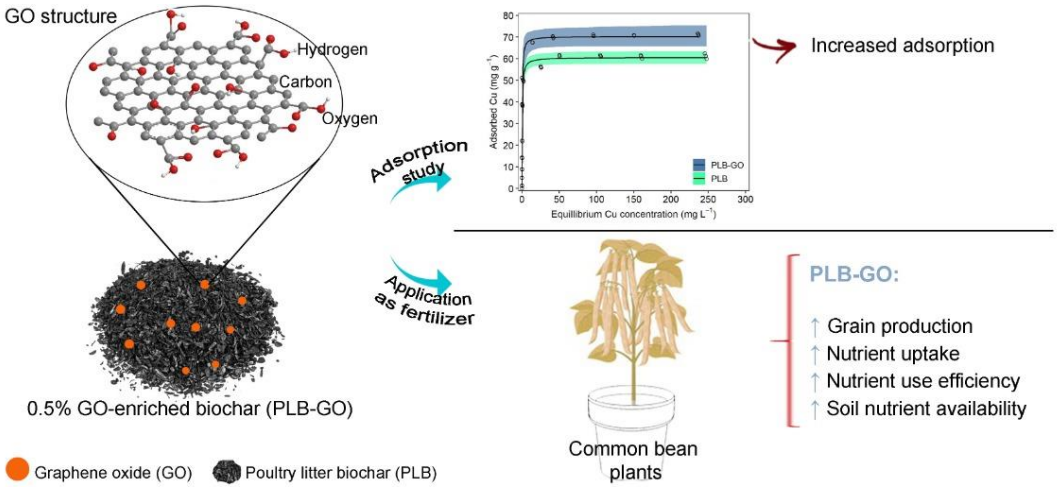

Abstract

Highly weathered soils have low micronutrient availability and very low efficiency for most soluble fertilizers used to overcome this issue. In this article the effect of poultry litter biochar-graphene oxide composite (PLB-GO) as a novel adsorbent for copper (Cu) and zinc (Zn) was evaluated, as well as fertilizing effects on plant growth, nutrient use efficiency and soil fertility. In order to do so, poultry litter biochar (PLB) and PLB-GO were produced, characterized and evaluated by isotherm adsorption and kinetics to evaluate their Cu and Zn sorption and desorption properties. Cu and Zn loaded to PLB and PLB-GO as biochar-based fertilizers (BBF) were researched. PLB-GO showed higher adsorption capacity for Cu (16.2%) and Zn (17.7%) than pristine PLB and in both cases < 0.5% of the sorbed metal content was released in water. Plant effects on growth, nutrient uptake and nutrient use efficiency were, in general, as shown in the following order both for Cu and Zn: PLB-GO ≥ PLB ≥ Sulfates. PLB increased Cu availability while PLB-GO increased Zn availability after cultivation, even after increasing nutrient uptake and being little soluble in water. Addition of small amounts (≤ 0.5%) of GO in biochar has potential to increase its properties to retain micronutrients and enhance fertilizer use effectiveness in highly weathered soils.

Keywords: metal adsorption, biochar-based fertilizers, tropical soil, nutrient use efficiency.

1 Introduction

In highly weathered soils, the natural content and availability of some micronutrients (e.g. Cu and Zn) is very low, which limits the development of economically important crops due to their essential role for plant growth and development (Casagrande et al., 2008; Lavres Junior et al., 2012; Watts-Williams et al., 2020). Micronutrient deficiency not only affects plant growth but is also critical for human health (Kabiri et al., 2017) and may delay growth and cognitive development, impair immune functions, increase risk for cardiovascular and metabolic diseases

or even lead to anemia and other clinical conditions (Delfini et al., 2020; Feitosa et al., 2018). For these reasons, micronutrient fertilizers have been applied in order to increase yield and food biofortification (Delfini et al., 2020; Kabiri et al., 2017; Watts-Williams et al., 2020).

Micronutrient fertilizers used in agriculture are generally highly water-soluble and have fast release, which causes considerable loss due to adsorption and low residual fertilization effect (An et al., 2021; Kabiri et al., 2017; Watts-Williams et al., 2020). When these fertilizers are added into soils, a series of reactions occur with the soil components, including adsorption to clays and precipitation of insoluble compounds, which dramatically reduce their efficacy (Andelkovic et al., 2018; Kabiri et al., 2017; Natarelli et al., 2021).

Development of more adequate fertilizers is needed in order to overcome low effectiveness and meet future demands for food with higher nutritional quality (An et al., 2021; Watts-Williams et al., 2020). One alternative is the employment of slow-release fertilizers, which might increase plant uptake through the sustained release of nutrients and the maintenance of their availability in the long-term (Gwenzi et al., 2018). However, only a handful of slow-release micronutrient fertilizers are commercially available and their high costs are their major drawback (Kabiri et al., 2017; Sashidhar et al., 2020).

Currently, carbonaceous materials such as biochar and graphene oxide have emerged as candidates to produce slow-release fertilizers. Biochar is a stable and carbon-rich byproduct synthesized by pyrolysis/carbonization of plant- or animal-based feedstock under limited oxygen conditions and is low-cost, environmentally friendly and a renewable material (Huang et al., 2017; Lehmann and Joseph, 2015; Zhang et al., 2018). Furthermore, it is a porous substance with multiple functional groups which might be a very effective sorbent and can be a suitable material for efficient nutrient retention and delivery (Ghaffar and Younis, 2014; Gwenzi et al., 2018; Liu et al., 2016).

Graphene oxide (GO) is a water-dispersible material produced through the chemical oxidation of graphite that presents a high density of oxygen functional groups, surface area, hydrophilicity and good biocompatibility (Ma et al., 2021; Marcano et al., 2018, 2010; Wang et al., 2013; Zhang et al., 2018). Due to its high surface area and unique 2-d structure, this material provides an ideal platform for nutrient loading, with the potential of being employed in the manufacture of slow-release fertilizers (Andelkovic et al., 2018; Ghaffar and Younis, 2014).

Papers have shown promising results regarding the use of enriched biochar called biochar-based fertilizers (BBF) as carriers of nutrients (e.g. N, P, and K) with slow-release characteristics (An et al., 2020; Carneiro et al., 2021; Chen et al., 2017; Gwenzi et al., 2018; Lustosa Filho et al., 2017). Graphene oxide has also been employed as a carrier for nutrients, such as P (Andelkovic et al., 2018), Cu and Zn (Kabiri et al., 2017; Watts-Williams et al., 2020) and as an improver of the physical/chemical properties and the nutrient release rate of conventional fertilizers (Kabiri et al., 2018; Yuan et al., 2018; Zhang et al., 2014).

Although biochar has capabilities of an excellent adsorbent, its sorption capacity can be low when produced directly from feedstock without pretreatment (Shang et al., 2016). In contrast, graphene oxide possesses high sorption abilities (Kabiri et al., 2017; Wang et al., 2013; White et al., 2018); however, its use in large scale is restricted due to high costs (Huang et al., 2017). Therefore, for this article, enriched biochar was synthesized by taking advantage of the combination of both graphene oxide and biochar properties.

Combining biochar with graphene oxide is a promising strategy when it comes to the improvement of their physicochemical properties, while still maintaining low-costs (Ghaffar and Younis, 2014; Huang et al., 2017; Liu et al., 2016; Zhang et al., 2018). Graphene oxide enriched biochar has been used to adsorb cadmium, lead (Liu et al., 2016; Zhang et al., 2018), chromium (IV) (Shang et al., 2016) and organic chemicals, such as atrazine (Zhang et al., 2018),

imidacloprid (Ma et al., 2021) and sulfamethazine (Huang et al., 2017). However, to current knowledge, there hasn't been any articles so far concerning graphene oxide enriched biochar for Cu and Zn adsorption, as well as its reusability as biochar-based fertilizers.

This article hypothesized that graphene oxide enriched biochar increases Cu and Zn adsorption when compared to pristine biochar, as well as increasing its effectiveness as BBFs when applied to soil for plant growth. The objectives of this article were (i) to evaluate the effects of PLB and PLB-GO on the sorption of Cu and Zn; and (ii) to evaluate their effectiveness as fertilizers in plant growth, nutrition, and soil fertility.

2 Materials and Methods

2.1 Preparation of materials

2.1.1 Graphene oxide

Graphene oxide was prepared according to Hummers' improved method as described in Marcano et al. (2010) and Marcano et al. (2018). In short, a 9:1 mixture of concentrated H_2SO_4/H_3PO_4 acids was added to a mixture of graphite flakes and $KMnO_4$. The reaction was heated to 50 °C and stirred for 12 h, then cooled to room temperature and poured onto deionized water in ice form with 30% H_2O_2.

The mixture was sieved through a metal U.S. Standard testing sieve (300 μm) and then centrifuged at 4000 rpm for 4 h, and then the supernatant was decanted away. The remaining solid material was washed in succession with deionized water, 30% HCl and ethanol. The material remaining after the multiple-washing process was coagulated and the suspension was filtered using a membrane with 0.45 μm pore size. Solid accumulated on the filter was vacuum-dried overnight at room temperature, obtaining graphene oxide (GO) (more details are given in the supplementary material).

2.1.2 Pristine biochar and graphene oxide enriched biochar (PLB-GO)

Pristine biochar (PLB) and graphene oxide enriched-biochar (PLB-GO) were produced from poultry litter collected from farms near Lavras - Minas Gerais (MG), Brazil. The poultry litter was air-dried at room temperature and ground so that it could pass through a 1.00 mm sieve, then it was pyrolyzed at 600 °C for 1 h (Zhang et al., 2012) in an adapted muffle furnace.

PLB-GO was produced under the same pyrolysis conditions, but first the poultry litter was impregnated with graphene oxide according to Liu et al. (2016) with some modifications. A suspension was prepared by adding 0.75 g of graphene oxide into 700 mL of deionized water, which was stirred for 1 h using a magnetic stirrer. About 150 g of poultry litter were fully dipped and coated with the graphene oxide suspension for 2 h, and then the mixture was oven-dried at 70 °C until it reached a constant weight. Both PLB and PLB-GO were ground and passed through a 500 µm sieve with the objective of homogenizing particle size for further characterization and experimentation.

2.2 Adsorption isotherms and kinetics research

Batch adsorption experiments were conducted individually for Zn and Cu in triplicates, which solutions being prepared by dissolving zinc sulfate ($ZnSO_4 \cdot 7H_2O$, 99%) and copper sulfate ($CuSO_4 \cdot 5H_2O$, 98%). All solutions and dilutions were prepared in milli-Q® ultrapure water.

Adsorption isotherms were obtained by mixing 0.05 g of PLB or PLB-GO with 50 mL of varying concentrations (0, 5, 10, 15, 20, 30, 45, 60, 90, 120, 170, 220, and 300 mg L^{-1}) of Zn or Cu solutions. Initial pHs of the solutions were approximately 4.8 and 5.2 for Zn and Cu, respectively. These pH values are natural pH of the solutions and within the range where Cu and Zn are available predominantly in their cationic forms (Kabiri et al., 2017; Sitko et al., 2013). The suspension was then shaken on a mechanical shaker at 120 rpm at room temperature

(25 °C) for 24 h. Kinetic adsorption research was carried out by mixing 0.05 g of adsorbent and 50 mL of Cu or Zn solution (at 80 mg L^{-1}) in polypropylene centrifuge tubes. The mixture was shaken on a mechanical shaker at 120 rpm and sampled at 0.02, 0.05, 0.08, 0.12, 0.17, 0.5, 1, 2, 4, 8, 12, 24, 48, and 72 h.

Suspensions obtained in both adsorption isotherms and kinetics experiments were immediately filtered through 0.45 µm Millipore® filters and Zn and Cu concentrations in the filtrates were measured via inductively coupled plasma optical emission spectrometry - ICP-OES (Spectro, Model Blue, Germany).

Copper and Zn adsorption capacities (Q_e) by the adsorbents were calculated through mass balance using Eq.1:

$$Q_e \text{ (mg g}^{-1}) = \frac{(C_i - C_e)\, V}{m} \qquad \text{Eq. (1)}$$

In which C_i and C_e are the initial solution concentration and the concentration at equilibrium (mg L^{-1}), respectively. V is the volume of the solution (L) and m is the adsorbent mass used (g).

Data was adjusted to several non-linear models in order to simulate sorption kinetics and isotherm parameters. Models used are described in the supplementary materials.

2.3 Cu and Zn loading on PLB and PLB-GO for testing as biochar-based fertilizers

$CuSO_4 \cdot 5H_2O$ and $ZnSO_4 \cdot 7H_2O$ salts were used as Cu and Zn sources. A portion of 150 g of PLB or PLB-GO was added into 2 L bottles containing 1.5 L of a solution with 90 mg L^{-1} of Cu (initial pH ~4.8) or 100 mg $L^{-1}$of Zn (initial pH ~5.2) and shaken on a mechanical shaker at 120 rpm for 24 h, then immediately filtered through 0.45 µm Millipore® filters. Concentrations of Zn and Cu in the filtrates were determined by ICP-OES in order to estimate the amount of Cu and Zn loaded on the biochar. Filters with solids were oven-dried at 60 °C for 72 h, after

which time solids were then collected and stored for characterization and use as fertilizers in the plant research.

Fertilizer materials were named: PLB-Cu - poultry litter biochar loaded with Cu; PLB-Zn - poultry litter biochar loaded with Zn; PLB-GO-Cu - graphene oxide enriched poultry litter biochar loaded with Cu; and PLB-GO-Zn - graphene oxide enriched poultry litter loaded with Zn.

2.4 Cu and Zn release from biochar-based fertilizers

Kinetics of Cu and Zn releases from BBFs and conventional micronutrient fertilizers ($CuSO_4$ and $ZnSO_4$) were performed according to Carneiro et al. (2021), with a few modifications. In summary, 0.15 g of the sample was mixed with 30 mL of deionized water (pH of approximately 6.4) in 50 mL centrifuge tubes and shaken in a reciprocating shaker at 120 rpm for up to 48 h at 25 °C. Samples were collected at 0.08, 0.17,0.50, 1, 2, 4, 8, 12, 24, and 48 h. Triplicate tubes were taken out at each sampling time and the solids in suspension were rapidly separated from the liquid phase by being sieved through 0.45 µm Millipore® filters, whose Cu and Zn concentrations in solutions were determined by using ICP-OES. Kinetics of Cu and Zn releases were identified as "changes in concentration" over time, while the release of Cu or Zn data as a function of sampling time was fitted using the models presented in Table S3.

2.5 Characterization of Biochars and BBFs

Samples of biochar and biochar-based fertilizers before and after Cu and Zn adsorption were characterized. Electrical conductivity (EC) and pH were measured in duplicate according to Singh et al. (2017). Ash contents were evaluated via standard method ASTM D1762-84 (American Society for Testing and Materials, 2007). Carbon (C) contents in the samples were determined using an Elemental Analyzer (Elementar, model Vario TOC cube, Germany).

Fourier transform infrared (FTIR) spectroscopy was recorded using a Digilab Excalibur spectrometer with a spectral range in-between 4000 − 400 cm^{-1} with 32 scans and 4 cm^{-1} resolutions.

Microscopic features and morphology of each material were characterized using scanning electron microscopy (Tescan Vega 3) with a secondary electron detector and tungsten filament, after coating the samples with gold in a metallizer, model Desk V (Denton Vacuum). EDX mapping was done with energy-dispersive X-ray spectroscopy (Brunker - Quantax EDX).

X-ray diffraction (XRD) analysis was also employed in order to identify any crystallographic structures in the samples by using an XRD instrument model Empyrean (PANalytical) with CoKα (1.78901 Å) radiation in-between the range of 5 - 80° (2θ), operated at 40 kV and 20 mA, with Fe filter for Kβ suppression. XRD data was used to determine the crystallite size (L) of the samples as described in the supplementary material, according to Bishnoi et al. (2017).

Specific surface area (SSA) and pore volumes (PV) were determined through N_2 adsorption/desorption analysis at 77 K using an accelerated surface area and porosimetry system (ASAP) (Micromeritics, model ASAP 2420). Total nutrient contents were determined according to Enders et al. (2017). To achieve these results, 0.20 g of biochar or BBF sample were ashed in a muffle furnace for 8 h at 500 °C, then nitric acid was added and the samples were digested at 120 °C with the addition of H_2O_2 in the final digestion step in order to oxidize all organic carbon. Finally, the digested material was dissolved in 20 mL of 5% (v/v) HCl solution using sonication. Contents of the tubes were filtered in membranes (0.45 μm) and the elements were quantified by ICP-OES (Model Blue, Germany). Data of selected properties of biochar and BBFs was presented in Table 1 and Table S6, respectively.

Table 1 –Total nutrient content[a] (g kg^{-1}) and properties of poultry litter biochar (PLB) and graphene oxide enriched poultry litter biochar (PLB-GO).

Biochar	Phosphorus (P)	Potassium (K)	Calcium (Ca)	Magnesium (Mg)	Sulphur (S)
PLB	57.7±0.33	54.4±0.24	263±2.39	11.3±0.14	8.14±0.09
PLB-GO	57.2±0.24	52.5±0.51	269±0.31	11.4±0.06	8.00±0.00
	Copper (Cu)	Zinc (Zn)	Manganese (Mn)	Iron (Fe)	pH[b] (1:2.5)
PLB	0.10±0.00	0.93±0.00	0.96±0.03	6.04±0.18	11.0±0.00
PLB-GO	0.10±0.00	0.89±0.01	0.94±0.02	5.62±0.03	11.1±0.01
	EC[b] (mS cm^{-1})	Yield[b] (%)	Ash[b] (%)	C content[b] (%)	*L* (nm)
PLB	7.78±0.11	50.4±1.42	60.8±0.26	20.5±0.73	85.4
PLB-GO	8.84±0.01	54.5±3.35	61.5±0.08	21.3±0.34	79.6
	SSA (m^2 g^{-1})	PV (cm^3 g^{-1})			
PLB	19.9	0.057			
PLB-GO	16.9	0.054			

[a]Mean ± SE (n = 3); [b] Mean ± SE (n = 2); *L* = average crystallite size; SSA = specific surface area; PV = Pore volume; EC = Electric conductivity; C = carbon; Yield = $\left(\frac{\text{Dry weight of biochar (g)}}{\text{Dry weight of biomass (g)}}\right)$ x 100.

Copper and Zn solubility of BBFs was assessed in water, citric acid, and neutral ammonium citrate + water, according to the methodology described in Brasil (2017).

2.6 Plant Growth-Pot Experiment

2.6.1 Soil sample and preparation

Soil samples were collected from the subsoil layer (30-100 cm) of an Oxisol in Itumirim city, Minas Gerais - MG, Brazil (952 m altitude, 21°17′13.66″ S and 44°47′46.38″ W). A representative soil sample was air-dried and then passed through a 2 mm sieve for chemical and physical soil characterization (Raij et al., 2001). This soil was chosen due to its representativeness of important cultivation areas in Brazil and worldwide, as well as due to its low Cu and Zn availability (0.50 and 0.15 mg kg^{-1}, respectively) (Table S4). The subsurface layer was chosen in order to reduce the influence of organic soil matter mineralization on the

supply of Cu and Zn and to evaluate the role of BBF treatments on the interactions between Cu and Zn with the mineral soil phase.

Five kg of air-dried and sieved (4 mm) soil was placed into clean and sterilized plastic bags and mixed with $CaCO_3$ + $MgCO_3$ at a Ca/Mg molar ratio of 3:1, with the intention of increasing the soil's base saturation to 70%. Soil was wetted to 80% of its field capacity (based on previous tests) and incubated for 30 days with its humidity corrected weekly. Thereafter, the soil was air-dried, homogenized and fertilized with the following nutrients: N, P, K, S, Cu, Zn, Mn, Fe, B, and Mo, which were applied at the rates of 300, 300, 200, 40, 1.50, 5.00, 4.00, 2.00, 0.80, and 0.15 mg kg^{-1} of soil, respectively, to ensure a proper fertility condition for optimum plant growth in pots (Malavolta, 1980; Novais et al., 1991). Soil and fertilizers were thoroughly mixed before sowing. Total N and K were split into four applications, including planting, 15, 30, and 45 days after planting.

2.6.2 Experimental design and plant growth

Experimental design was completely randomized with 4 replicates. Treatments were prepared as follows: Cu applied via PLB-Cu; Zn applied via PLB-Zn; Cu applied via PLB-GO-Cu; Zn applied via PLB-GO-Zn; Cu applied via $CuSO_4$; Zn applied via $ZnSO_4$; Control (without Cu application); and Control (without Zn application).

Six seeds of common bean (*Phaseolus vulgaris* L. cv. BRSMG UAI) were sowed into each pot containing prepped soil and after 10 days only three plants where left, which were grown during 80 days, until grain production. Zn and Cu applied via BBF were based on the adsorbed contents as described previously and using conventional micronutrient fertilizers ($ZnSO_4$ and $CuSO_4$) at 5.0 and 1.5 mg $kg^{-1}$of Zn and Cu, respectively.

2.6.3 Plant and soil analysis

During the experimental period, senescent leaves of common beans were collected in a paper bag until plant maturity, when the grains were harvested. Afterwards, leaves were mixed with shoots and pods in order to determine shoot dry mass (SDM) and grain mass, separately. SDM and grains were oven-dried at 65 °C until weight stabilization (approximately 72 h), weighed and ground for chemical analysis.

All plant and grain samples were digested using a nitric-perchloric acid mixture (Malavolta et al., 1997) and Cu and Zn contents were measured in the extract by using ICP-OES. These values were used to calculate nutrient uptake in each pot by both shoot dry mass and grains, taking into account their biomass production. A soil sample was collected after the experiment from each pot in order to determine the pH in water and soil-available Cu and Zn using a Mehlich-1 solution, as described by Silva (2009).

2.6.4 Micronutrient use efficiency

Cu and Zn use efficiency was calculated according to Hertzberger et al. (2021) for the apparent fertilizer nutrient uptake (AFNU) and apparent nutrient use efficiency (ANUE). AFNU was calculated as the difference in Zn or Cu uptake from fertilized treatments and the Zn or Cu uptake from control (without Zn or Cu application) (Eq. 2).

$$AFNU\ (mg\ pot^{-1}) = NF - NUF \qquad \text{Eq. (2)}$$

Where NF is total nutrient uptake by plants from fertilized treatments (with Cu or Zn application) and NUF is total nutrient uptake by plants from unfertilized treatments (without Zn or Cu application).

Apparent nutrient use efficiency (ANUE) was calculated by dividing AFNU per total nutrient fertilizer application per pot, which was 25 mg of Zn and 7.5 mg of Cu (Eq. 3).

$$\text{ANUE (\%)} = \left(\frac{\text{AFNU}}{\text{mg of Cu or Zn applied pot}^{-1}}\right) * 100 \qquad \text{Eq. (3)}$$

In which AFNU is the apparent fertilizer nutrient uptake (mg pot^{-1}).

2.7 Statistical analysis

All data for pot experiments was presented as mean values and standard error of the mean of four replicates. After checking the assumptions (normality and homoscedasticity), data was subjected to variance analysis (one-way ANOVA, $p< 0.05$) and when significant difference ($p< 0.05$) was observed, the means were compared through the Tukey test ($p< 0.05$) using the *emmeans* package (Lenth et al., 2019). Isotherm and kinetics data for Cu and Zn adsorption by biochars and kinetic data for Cu and Zn release by fertilizers were fitted to non-linear models using the *nlstools* package (Baty et al., 2015). The quality of the model fitting was based on its standard error of the estimative (SE) (Shariatmadari et al., 2006) and the most appropriate model was chosen based on the Akaike information criterion (AIC) (Akaike, 1974; Kingdom and Prins, 2016). Pearson correlation between the pot experiment variables was performed using the *corrplot* package (Wei and Simko, 2021). All analyzes were performed by using R software version 3.6.1 (R Core Team, 2019).

3 Results and discussion

3.1 Isotherms adsorption research

The data for copper and Zn adsorption isotherms, as well as the fitting to models are shown in Figure 1. The data fit more appropriately to Langmuir and Langmuir-Freundlich (SIPS) models, presenting lower SE and lower AIC values than the Freundlich model (Table 2). The copper adsorption (Figure 1a) fit was similar for the Langmuir and the Langmuir-Freundlich models, whilst regarding Zn (Figure 1b), it better fit the Langmuir-Freundlich model.

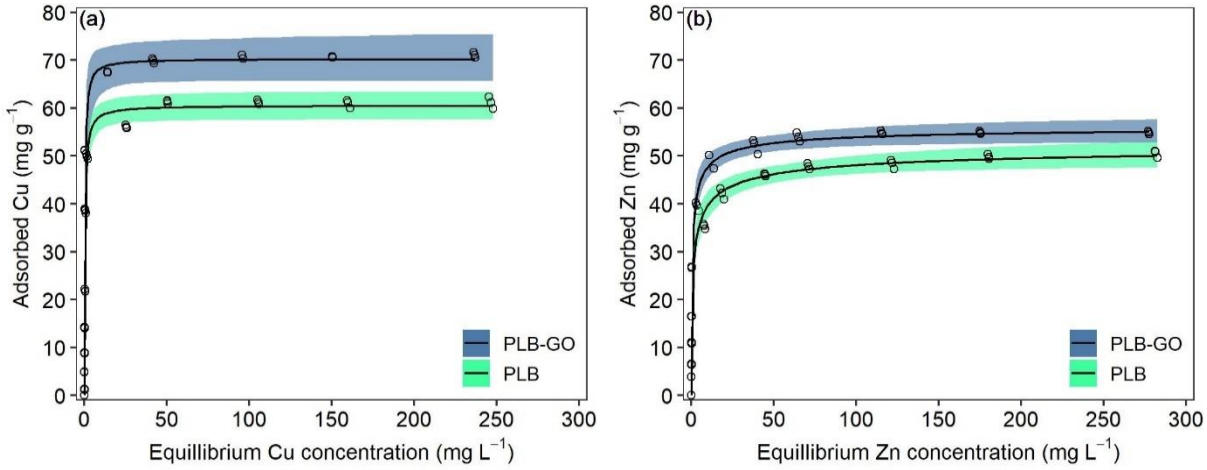

Figure 1 – Copper (a) and zinc (b) adsorption isotherms in samples of poultry litter biochar (PLB) and graphene oxide enriched poultry litter biochar (PLB-GO). Notes: points are experimental data; color shading indicates 95% confidence interval and lines are predicted data according to best-fitting model.

Maximum Cu adsorption capacities (q_m) for PLB and PLB-GO were 60.6 and 70.3 mg g^{-1}, respectively, as estimated by the Langmuir model (Table 2). The maximum Zn adsorption capacities for PLB and PLB-GO were 48.0 and 56.5 mg g^{-1}, respectively, as estimated by the SIPS model. A comparison between Cu and Zn adsorption capacities obtained in this research with other biochars obtained from diverse feedstock and pyrolysis conditions is shown in Table S5 (Supplementary material). Overall, Cu and Zn adsorption obtained in this research was higher than several other biochars and used the lowest adsorbent dose (1.0 g L^{-1}), which shows a good performance for the developed materials. PLB-GO increased Cu and Zn adsorption by 16.2% and 17.7%, respectively, when compared to PLB. Thus, a relatively small amount (≤ 0.5%) of graphene oxide was able to modify biochar properties related to adsorption capacity. PLB-GO presented a lower average of crystallite size (L) (Table 1), which indicates the occurrence of amorphous carbon in its surface (Carneiro et al., 2018). Amorphous carbon favors a higher oxygen surface functionality, which probably explains the high adsorption of Cu and Zn by this biochar (Carrier et al., 2017).

Table 2 – Langmuir, Freundlich, and SIPS (Langmuir-Freundlich) parameters for isotherm models of Cu and Zn sorption by poultry litter biochar (PLB), and graphene oxide enriched poultry litter biochar (PLB-GO).

Models and parameters	Copper		Zinc	
	PLB	PLB-GO	PLB	PLB-GO
Langmuir				
q_m	60.6	70.3	46.4	52.1
K_L	2.61	3.25	2.91	4.71
SE	5.66	9.15	4.52	4.60
AIC	250	287	232	234
Freundlich				
K_f	28.4	33.1	22.0	26.2
n	6.10	6.10	6.00	6.40
$1/n$	0.164	0.164	0.167	0.156
SE	10.6	12.9	5.73	7.11
AIC	296	314	251	268
SIPS				
q_m	60.5	70.3	48.0	56.5
n_s	1.01	1.02	0.381	0.581
K_s	2.65	3.40	0.59	1.43
SE	5.66	9.15	3.92	4.00
AIC	252	289	223	225

q_m: is the maximum adsorption capacity of the adsorbate (mg g^{-1}); K_L: is the Langmuir equilibrium constant (L mg^{-1}); K_f: is the Freundlich equilibrium constant; n: is the Freundlich nonlinearity constant; K_s and n_s: are the SIPS constants; SE: Standard errors of estimates of the models and AIC: Akaike information criterion.

The Langmuir model indicates a predominance of monolayer adsorption and homogeneous distributions of adsorption sites (Vikrant et al., 2018), whilst the SIPS model indicates a mix of homogeneous and heterogeneous adsorption systems (Wang and Guo, 2020). For the SIPS model, when Cu or Zn concentrations are low, it becomes the Freundlich model, while at high concentrations, it becomes the Langmuir model (Ayawei et al., 2017; Wang and Guo, 2020a).Thus, it appears that monolayer adsorption and a homogeneous or heterogeneous site distribution for Cu and Zn adsorption on the biochars probably occurred, since data better fit these two models (Shen et al., 2017).

Despite the adsorption not presenting an adequate fit to the Freundlich model (higher AIC and SE values), parameters obtained by the model can still provide information regarding

adsorption sites and adsorption feasibility (Saadi et al., 2015; Tran et al., 2017). The high *n* value (≥ 6.00) observed indicates that biochars present great heterogeneity of adsorption sites on their surface (Nardis et al., 2020). Moreover, results indicate that Cu and Zn adsorption was favorable in both biochars, once that 1/*n* was less than one and closer to zero (Penido et al., 2019; Saadi et al., 2015), which also shows that the adsorbent surface is more heterogeneous (Saadi et al., 2015).

3.2 Kinetics adsorption study

In Figure 2, it is shown that Cu and Zn adsorption increased with contact time and that the process can be divided into two stages: 1) fast adsorption (< 4 h), and 2) slow adsorption (> 4 h), nearly reaching equilibrium after 24 h (Figure 2a and b).

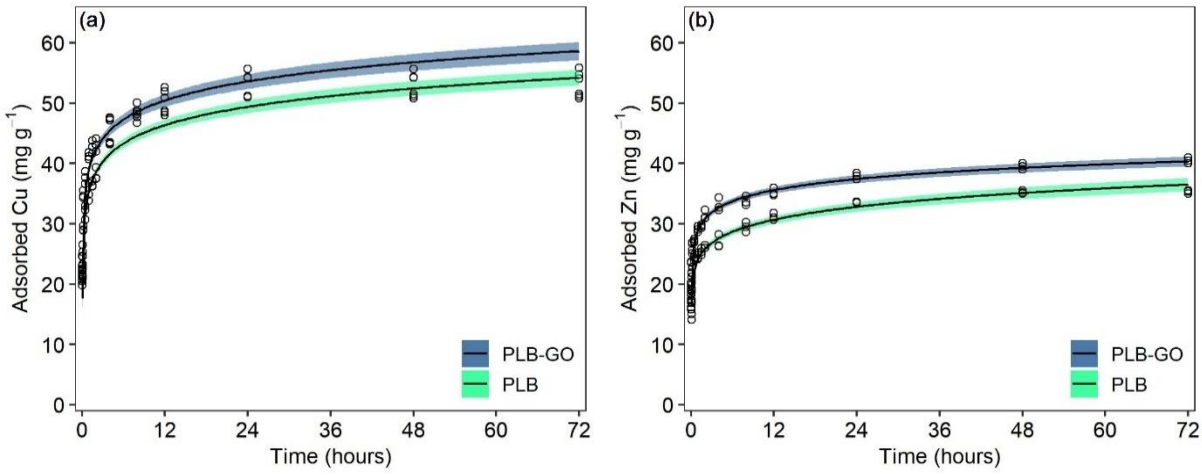

Figure 2 – Copper (a) and zinc (b) adsorption kinetics in samples of poultry litter biochar (PLB) and graphene oxide enriched poultry litter biochar (PLB-GO). Notes: points are experimental data; color shading indicates 95% confidence interval and lines are data predicted by the best-fitting model.

Similar to the isotherm research, PLB-GO presented higher Cu and Zn adsorption (Table 3) than PLB. Cu and Zn adsorbed by PLB and PLB-GO in the first 4 h was equivalent to 95.5-95.7% and 93.8-96.4%, respectively, of the equilibrium adsorption amount. A fast initial adsorption is due to abundant unoccupied active sites (Ma et al., 2021) and the lower Cu and Zn adsorption by PLB may be due to their higher crystallite size (*L*), which indicates lower

amorphous carbon, consequently presenting decreased oxygen surface functionality (Figure 2 and Table 1) (Carneiro et al., 2018; Carrier et al., 2017).

Table 3 – Pseudo First-order, Pseudo Second-order and Intraparticle diffusion parameter kinetics models for sorption of copper and zinc by poultry litter biochar (PLB) and graphene oxide enriched poultry litter biochar (PLB-GO).

Models and parameters	Copper (Cu^{2+})		Zinc (Zn^{2+})	
	PLB	PLB-GO	PLB	PLB-GO
Pseudo First-order				
Q_e	43.4	47.6	28.9	33.1
K_1	8.44	8.85	12.2	15.0
SE	7.56	6.82	5.26	5.57
AIC	314	305	281	286
Pseudo Second-order				
Q_e	45.4	49.5	29.6	33.9
K_2	11.6	23.0	22.4	28.4
SE	6.07	5.35	4.42	4.42
AIC	294	283	265	265
Intraparticle diffusion				
K_p	0.485	0.487	0.289	0.307
C	28.1	31.7	20.4	24.3
R_i	0.531	0.502	0.483	0.453
SE	6.29	7.21	3.22	3.41
AIC	297	309	237	242

Q_e is the maximum adsorption capacity of the adsorbate (mg g^{-1}); K_1: first order rate constant (h^{-1}); K_2: second order rate constant [(mg $g^{-1})^{-1}$]; K_p, C and R_i are intraparticle diffusion rate constant (mg(g $min^{1/2})^{-1}$), the constant for any experiment (mgg^{-1}) and the initial adsorption factor, respectively; SE: Standard error of the estimate for the models and AIC: Akaike information criterion.

Pseudo first-order, pseudo second-order and intraparticle diffusion models were used to simulate adsorption kinetics and the adsorption parameters are presented in Table 3. The pseudo second-order model presented the best fit (Lower SE and AIC) for Cu and Zn adsorption data, which suggests that the adsorbent is abundant in active sites, therefore, adsorption kinetics are dominated by adsorption onto active sites (Wang and Guo, 2020b). Moreover, it indicates that the adsorption process depended more on the number of active sites and the rate-limiting step may be chemical adsorption through the sharing or exchange of electrons (Penido et al., 2019).

The intraparticle diffusion model showed the best fit for Zn adsorption data by PLB and PLB-GO, according to lower AIC and SE values (Table 3). According to the initial factor (R_i) (Table S2) for intraparticle diffusion model, Cu adsorption has an intermediate initial adsorption ($0.9 > R_i > 0.5$) and Zn adsorption has a strong initial adsorption ($0.5 > R_i > 0.1$) (Pholosi et al., 2020; Wu et al., 2009). PLB presents higher R_i values and lower C values when compared to PLB-GO adsorption (Table 3), which indicates a contribution of wider pore size for PLB-GO, such as mesopores (Wu et al., 2009). This result confirms the decreased SSA (Table 1) observed for PLB-GO, since micropores contribute more to the increase in SSA than mesopores do (Leng et al., 2021).

Porous adsorbents tend to present different steps associated with the transportation process during adsorption (Tran et al., 2017). In Figure 2, one can observe three stages of adsorption: the first from 0 to 2 h, the second from 4 to 8 h and the third from 12 to 72 h, for both elements (Cu and Zn) and adsorbents (PLB and PLB-GO). The first stage represents a liquid film transfer, where the adsorbate is transported from the bulk of the solution to the external surface of the adsorbent (i.e., external surface adsorption or instantaneous adsorption); the second stage is dominated by intraparticle diffusion, where the adsorbate from the external surface moves into the internal pores of the adsorbent; and finally the third stage indicates adsorption equilibrium, in which the solute moves slowly from larger pores to micropores, causing a slow adsorption rate (Ma et al., 2021; Wu et al., 2009). In most cases, adsorption kinetics may be controlled by film diffusion and intraparticle diffusion, simultaneously (Qiu et al., 2009).

3.3 Characterization of pristine and Cu and Zn-loaded biochar

3.3.1 FTIR analysis

There was no difference in functional groups of PLB and PLB-GO before and after loading with Cu and Zn (Figure 3). The band between 1500-1400 cm^{-1} was assigned to symmetric vibration chains (–COO–) (Sarfaraz et al., 2020), presence of carbonyl or carbonates (CO_3^{2-}) (Bekiaris et al., 2016; Zhao et al., 2015) and C=C or/and saturated C−H bending vibration (Taherymoosavi et al., 2017).

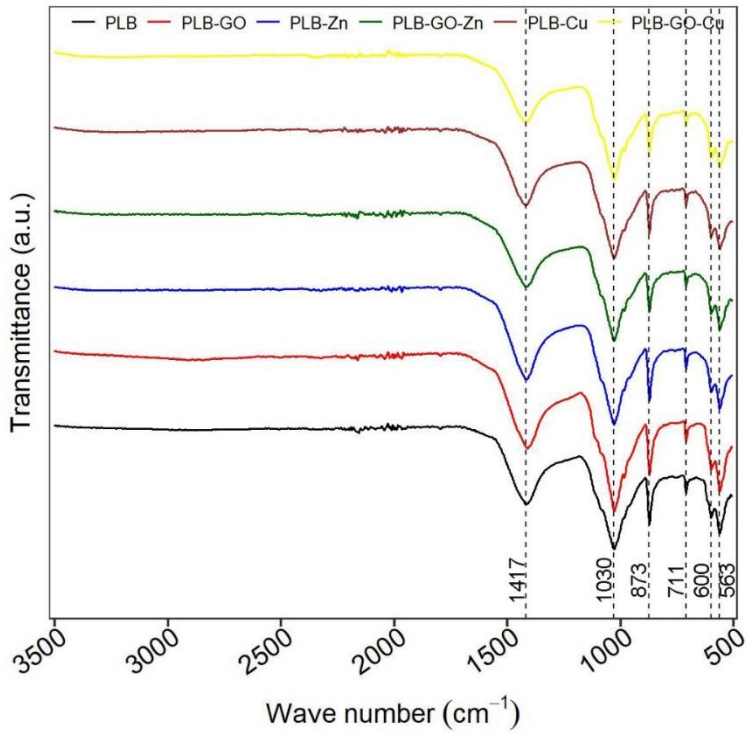

Figure 3 – FTIR spectra (3500 – 500 cm^{-1}) of poultry litter biochar (PLB), graphene oxide enriched poultry litter biochar (PLB-GO) and biochar-based micronutrient fertilizers (PLB-Zn, PLB-GO-Zn, PLB-Cu, and PLB-GO-Cu).

Bands between 1050-1020 cm^{-1} were assigned to CH_2 chains (Sarfaraz et al., 2020), C−O of epoxy and C−O−C of alkoxy groups (Mannan et al., 2018), C−O−C symmetric stretching in aliphatic groups and acid derivatives (Janu et al., 2021). The C−O and/or C=O stretching vibrations of polysaccharide, polysaccharide-like substances, alcohols and acids (Bekiaris et al., 2016, 2015; Carneiro et al., 2018; Li et al., 2018) and stretching vibrations of conjugated

C–C bonds of aromatic rings were also assigned to these bands between 1050-1020 cm^{-1}.The region between 1050 and 1020 cm^{-1} also represented the Si–O–Si stretching vibration (Cuixia et al., 2020). Bands at 873 cm^{-1} and close regions were assigned to C−H chains (aromatic C−H out of deformation plane) (Sarfaraz et al., 2020) and to P−O−P stretching (Bekiaris et al., 2016; Lustosa Filho et al., 2017). The band at 711 cm^{-1} was attributed to –C=C groups (aromatics rings) (Sarfaraz et al., 2020) and wagging vibrations of C−H bonds in aromatic and heteroaromatic compounds (Bavariani et al., 2019). Bands between 600 and 500 cm^{-1} were attributed to P−O or P=O stretching (Bekiaris et al., 2016; Lustosa Filho et al., 2017) and the presence of inorganic metals (Sarfaraz et al., 2020).

3.3.2 XRD analysis

XRD patterns for PLB, PLB-GO and their Cu or Zn-loaded counterparts showed peaks of calcite-like compounds ($CaCO_3$) and quartz (SiO_2) in all samples (Figure 4). There was no difference between the diffractograms of both pristine metal-loaded biochars, except for Cu-loaded biochar, in which the formation of hoganite-like compounds [$Cu(CH_3COO)_2 \cdot H_2O$] occurred (Figure 4).

The absence of crystalline Zn mineral peaks in the diffractograms and the presence of a Cu compound bound to C, H and O (hoganite) are indicators that there was no significant precipitation during the adsorption process. This reinforces that chemisorption of Cu and Zn to surface functional groups or physical adsorption took place on the material's surface. Copper ions tend to bind in a syn conformation with oxygen-containing functional groups, whereas Zn^{2+} ions are more likely to bind in a direct conformation by sharing two oxygen atoms of the same carboxylic group (Kabiri et al., 2017).

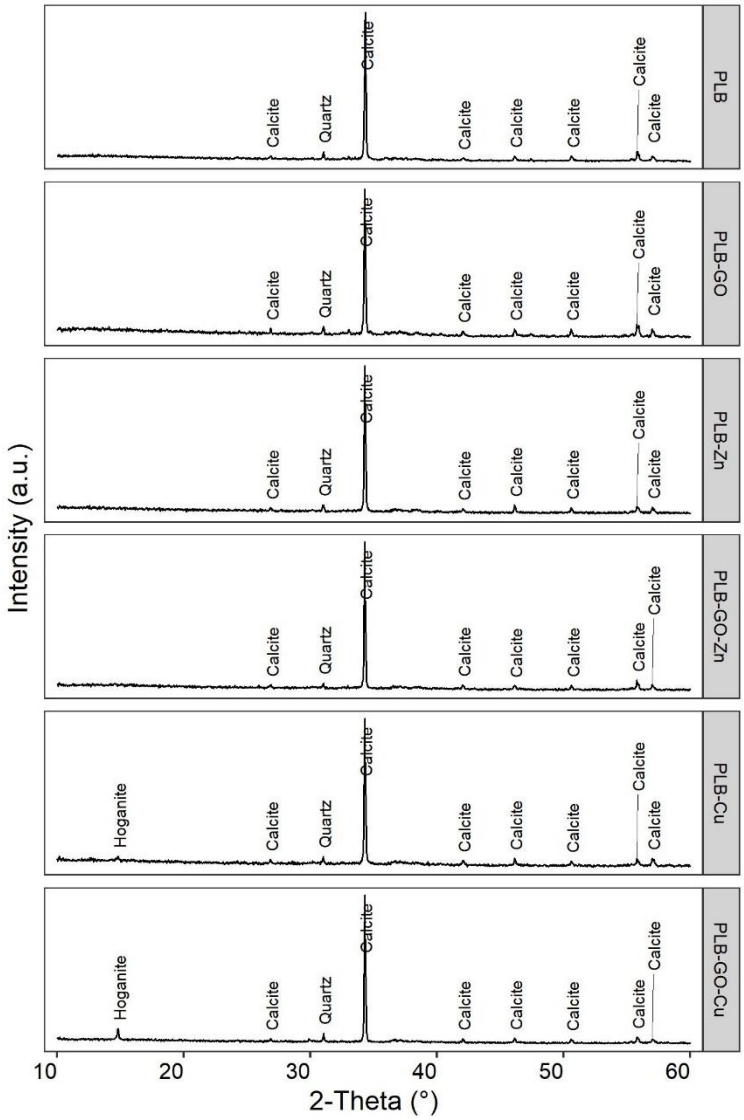

Figure 4 – Diffractograms of poultry litter biochar (PLB), graphene oxide enriched poultry litter biochar (PLB-GO) and biochar-based micronutrient fertilizers (PLB-Zn, PLB-GO-Zn, PLB-Cu and PLB-GO-Cu). Notes: Calcite ($CaCO_3$), Quartz (SiO_2) and Hoganite [$Cu(CH_3COO)_2{\cdot}H_2O$].

Carbonates (CO_3^{2-}) were also identified through FTIR analysis and Ca achieved the main peak observed by SEM-EDX spectrum (discussed in the next section). The presence of $CaCO_3$ and other crystalline minerals in biochar has been confirmed by others (Domingues et al., 2017; Lustosa Filho et al., 2017; Nardis et al., 2020). The presence of quartz is probably due to the presence of sand in the feedstock, which was also observed through FTIR spectra as O−Si−O groups and characteristic peaks of Si by SEM-EDX. The presence of Si determined via SEM-EDX and quartz in XRD are highly correlated in biochar samples (Clemente et al., 2018).

3.3.3 SEM-EDS analysis

SEM images of PLB, PLB-GO and BBFs (PLB-Zn, PLB-Cu, PLB-GO-Zn, and PLB-GO-Cu) are shown in Figure 5. PLB (Figures 5a) and PLB-GO (Figures 5b) showed similar particle sizes and surface morphology, except for PLB-GO, which presented a rougher surface than PLB did. It was not possible to observe precipitates on the BBFs' surfaces (Figures 5b, 5c, 5d, and 5e), which indicates that Cu and Zn sorption has occurred (chemical or physical).

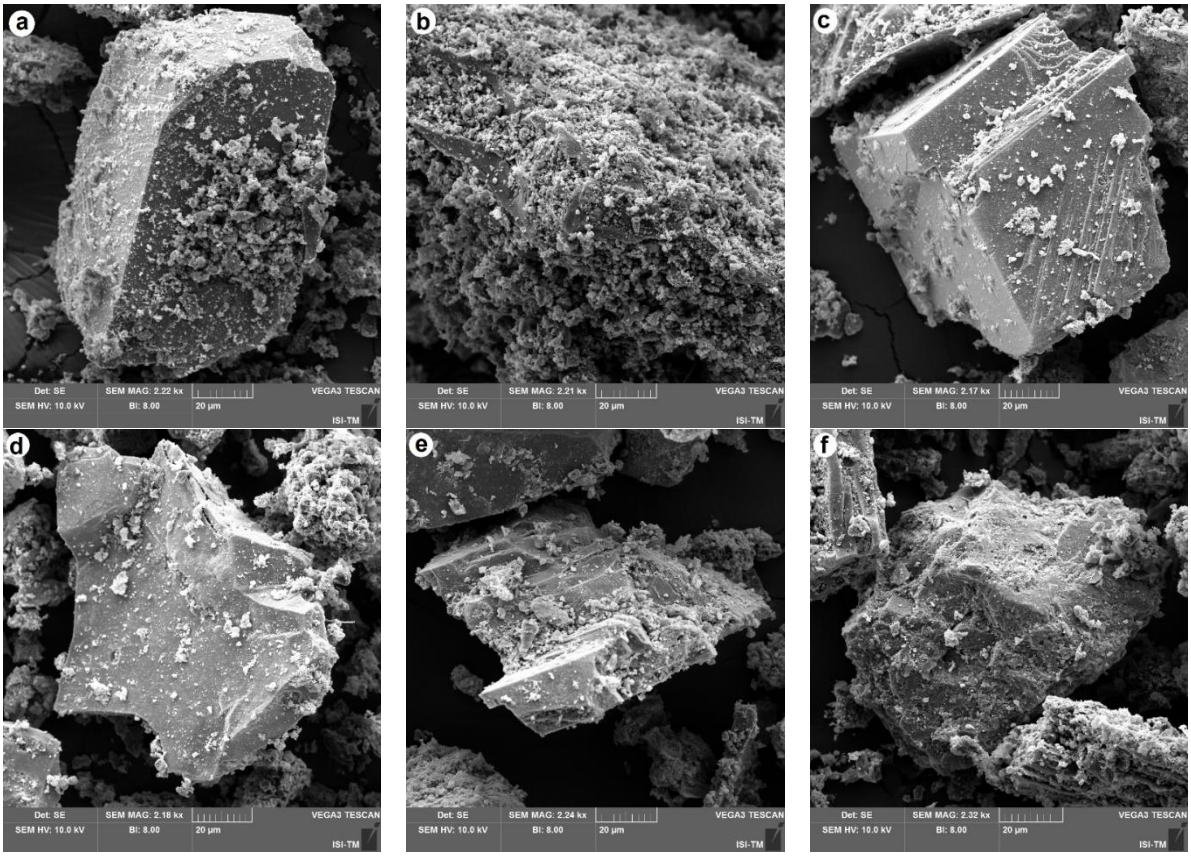

Figure 5 – SEM images of PLB (a), PLB-GO (b), PLB-Zn (c), PLB-GO-Zn (d), PLB-Cu (e), and PLB-GO-Cu (f).

EDS mapping with distribution of the main elements on both biochars' and BBFs' surfaces is shown in Figures S1 to S6. There was a homogenous distribution of Ca, K, P, and O on the surface of all materials. Zinc and Cu were only observed in BBFs (metal-loaded biochars). Main peaks observed in EDS for Ca, P, K and O in the materials are in accordance with their total concentrations (Table 1 and Table S6).

The relatively high level of O in the biochars and BBFs is associated with functional groups (as observed by FTIR analysis), while high P content (Table 1 and Table S6) in the materials originates from P-rich diets and bedding material from poultry litter (Bolan et al., 2010). High Ca values were observed through total nutrient determination (Table 1 and Table S6), a high peak in SEM-EDX and calcite ($CaCO_3$) in XRD analysis, the latter being used in poultry diets, which ends up accumulating in the poultry litter (Domingues et al., 2017; Nardis et al., 2020).

3.4 BBF Cu and Zn release

Total nutrient contents of BBFs are shown in Table S6. BBFs presented very low Cu and Zn solubility in water (Figure 6), as opposed to Cu and Zn sulfate salts (Figure S7), according to the methodology used to determine fertilizer solubility (Brasil, 2017). However, Cu and Zn solubility in 2% citric acid and neutral ammonium citrate + water in the BBFs was > 95% of the total content (Table S6), which indicates great potential for their employment as micronutrient fertilizers (Nardis et al., 2020).

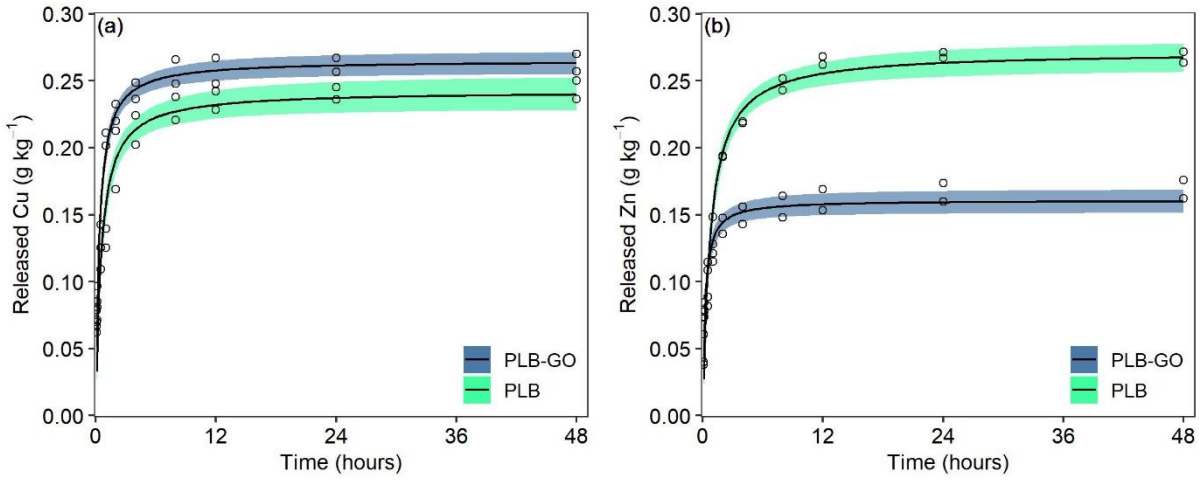

Figure 6 – Kinetics of copper (a) and zinc (b) release in water from biochar-based micronutrient fertilizers. Notes: points are experimental data; color shading indicates 95% confidence interval and lines are predicted data according to the best adjusted model.

The kinetic research showed that quick Cu and Zn releases from BBFs occurred during the first 2 h, followed by stability until 48 h (maximum period evaluated). PLB-GO-Cu showed a slightly higher release than PLB-Cu (Figure 6a), whilst for Zn, it was opposite; PLB-Zn released more Zn than PLB-GO-Zn (Figure 6b).The fast initial nutrient release from BBFs is likely due to physiosorbed metal salts or metal ions loosely adhered to the adsorbent surface (Kabiri et al., 2017).

Table 4 – Parameter of several kinetics models for copper and zinc release by biochar-based micronutrient fertilizers and conventional fertilizers.

Models and parameters[a]	Copper			Zinc		
	PLB	PLB-GO	$CuSO_4$	PLB	PLB-GO	$ZnSO_4$
Pseudo First-order						
Q_e	0.230	0.252	262	0.254	0.154	298
K_1	1.14	1.84	20.6	0.879	2.51	40.9
SE	0.025	0.020	10.1	0.023	0.021	2.02
AIC	-86.2	-96.7	153	-89.6	-93.4	88.9
Pseudo Second-order						
Q_e	0.242	0.265	266	0.272	0.161	298
K_2	1.88	2.90	53.3	1.33	4.41	313
SE	0.019	0.013	4.78	0.015	0.015	0.764
AIC	-98.3	-112	123	-108	-108	49.9
Power function						
a	0.142	0.170	250	0.143	0.112	296
b	0.175	0.150	0.026	0.202	0.133	0.005
SE	0.028	0.035	0.700	0.031	0.015	1.79
AIC	-83.1	-73.7	147	-78.2	-107	83.9
Simple Elovich						
a	0.146	0.172	250	0.148	0.114	296
β	-0.032	-0.033	-6.75	-0.040	-0.018	-1.52
SE	0.020	0.026	8.40	0.018	0.012	1.76
AIC	-96.0	-84.9	146	-99.2	-116	83.6
Parabolic diffusion						
Q_e	0.110	0.140	245	0.104	0.095	294
R	0.026	0.025	4.73	0.033	0.015	1.11
SE	0.042	0.051	13.0	0.048	0.024	2.78
AIC	-66.3	-58.7	163	-60.8	-88.5	102

[a] k_1 is the first order rate constant (h^{-1}); k_2 is the second order rate constant [(mg g^{-1})$^{-1}$]; a is the initial Cu or Zn desorption rate (mg g^{-1} h^{-1}); β is the Cu or Zn desorption constant [(mg g^{-1})$^{-1}$]; R is the diffusion rate constant [(mg g^{-1})$^{-0.5}$]; Q_e is the amount of Cu or Zn release at equilibrium or maximum Cu or Zn released (g kg^{-1}); SE is the standard error of estimate and AIC is the Akaike Information Criterion.

$CuSO_4$ released 95% (250 g kg^{-1}) of the total Cu in the first hour, as estimated through the Power function and Simple Elovich models, while BBFs released only 0.32% (0.14 g kg^{-1}) and 0.40% (0.17 g kg^{-1}) of total Cu in PLB-Cu and PLB-GO-Cu, respectively (Table S6). $ZnSO_4$ released 99% (296 g kg^{-1}) of Zn in the first hour, while BBFs released only 0.22% (0.11 g kg^{-1}) and 0.33% (0.14 g kg^{-1}) of total Zn in PLB-GO-Zn and PLB-Zn, respectively (Table S6).

Kinetics of Cu and Zn released from all fertilizers were better fitted to the Pseudo second-order (Lower SE and AIC values), except for PLB-GO-Zn, which was better fitted to the Simple Elovich model (Table 4). Maximum Cu released estimated through the Pseudo second-order model was 0.24, 0.27, and 266 g kg^{-1} for PLB-Cu, PLB-GO-Cu, and $CuSO_4$, respectively; maximum Zn release was 0.27, 0.16, and 298 g kg^{-1} for PLB-Zn, PLB-GO-Zn and $ZnSO_4$, respectively. Low BBF nutrient release is probably due to the predominance of the chemisorptions of cations to biochars, which has a high binding energy, as observed by isotherms and adsorption kinetics research. Chemisorption has a higher binding energy than those physically retained or adhered to the surface of biochars (Kabiri et al., 2017).

Cu and Zn release was lower than previously observed by others using only graphene oxide to adsorb these micronutrients and employ them as fertilizers (Kabiri et al., 2017). The relatively slow release of Cu and Zn from PLB and PLB-GO might be due to the higher binding energy for biochar than that for graphene oxide. Fast release of Cu and Zn from conventional micronutrient fertilizers ensures Cu and Zn supply to plants, although the fraction which is not absorbed by plants is rapidly adsorbed into Fe, Mn, and Al oxides in the clay fraction (Casagrande et al., 2008; Mouta et al., 2008; Natarelli et al., 2021; Silveira and Alleoni, 2003). Slow and steady release profile of Cu and Zn by BBFs may result in increased plant use efficiency due to the lower interaction with soil components (Kabiri et al., 2017; Natarelli et al., 2021), thus, this must be tested in a plant experiment.

3.5 Pot experiment

3.5.1 Plant growth and production

Responses from common bean plants to Cu and Zn fertilization using both BBFs and conventional fertilizers are shown in Figures 7 and Figure S8. There was no difference in plant height for Cu (48.6 cm) or Zn (48.8 cm) supplied via BBF, which were similar to or higher than conventional fertilizers. For the Cu fertilization using PLB-Cu and PLB-GO-Cu, plant height was 11.6% higher than for the $CuSO_4$ fertilizer (Figure S8a), whilst for the Zn fertilization using PLB-Zn, plant height was 14.7% higher than for the $ZnSO_4$ fertilizer (Figure S8b). The control treatment without Cu fertilizer did not differ from all others, with a plant height of 46.1 cm, while the control treatment without Zn fertilizer presented lower plant height (36.1 cm) when compared to others treatments. Figures S11 to Figures S18 in the supplementary material show the development of common bean plants at 30, 50, 60, and 80 days after emergency.

The shoot dry mass (SDM) of common bean was not affected by Cu fertilization (Figure 7a), with an average value of 59.2 g pot^{-1}, whilst for Zn fertilization there was no difference among fertilizers (average of 63.5 g pot^{-1}), although they were 52.5% higher than the control treatment without Zn (Figure 7b). For Cu, a higher grain mass production was observed for PLB-GO-Cu (52.0 g pot^{-1}), which produced 8.96% to 17.0% more than other treatments (Figure 7c), whilst for Zn there was no difference between BBFs (average of 49.5 g pot^{-1}) for grain mass, but they were 11.4% higher than $ZnSO_4$ fertilizer and 285% higher than the control without Zn (Figure 7d). Total dry mass for Cu fertilization was not affected by the treatments (Figure S8c) (average of 107.9 g pot^{-1}). Conversely, for Zn fertilization, higher total dry mass was observed for BBF treatments (114.6 g pot^{-1}), being 10.8% and 110.4% higher than the $ZnSO_4$ fertilizer and the control, respectively (Figure S8d).

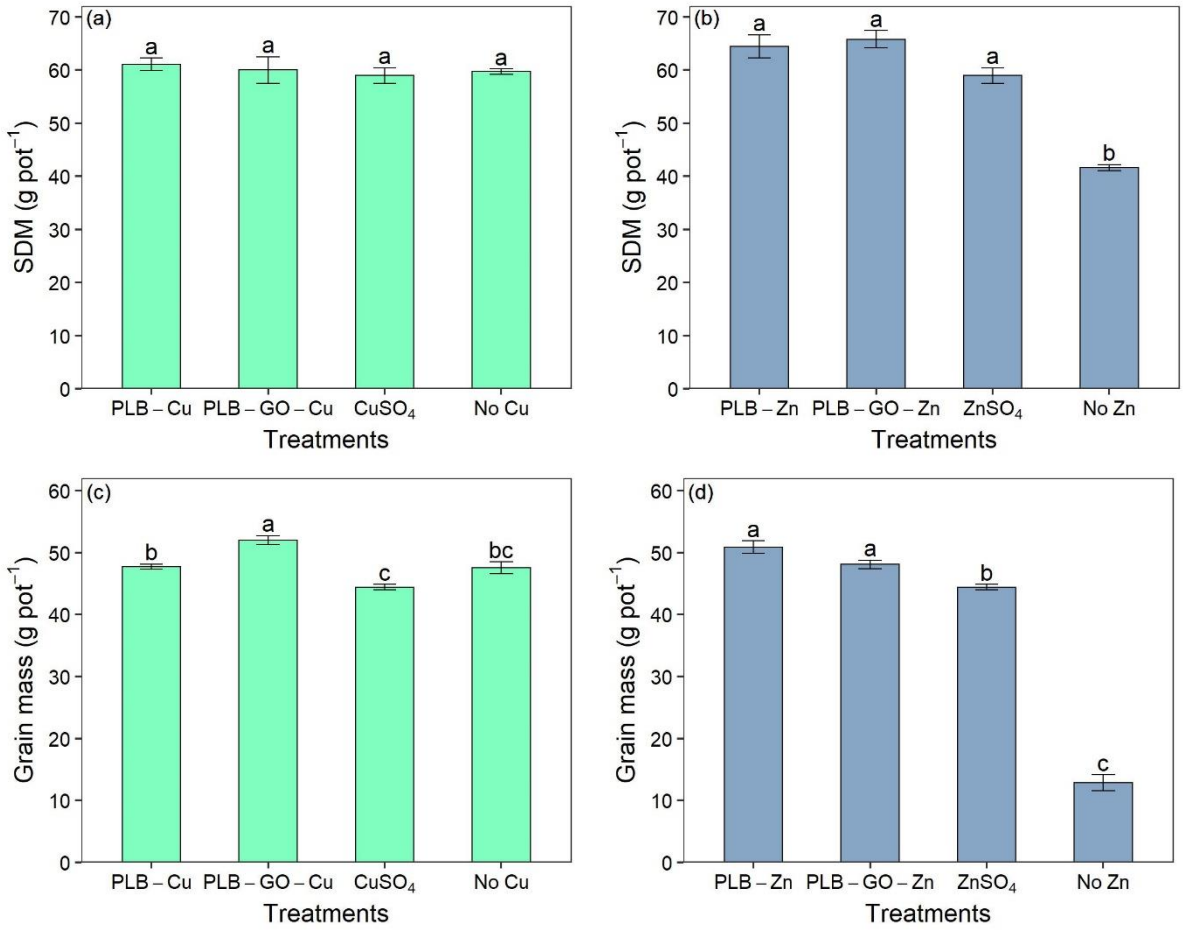

Figure 7 – Shoot dry mass (a and b) and grain mass (c and d) of common bean plants for copper and zinc fertilization, respectively, using BBFs, and conventional fertilizers. Means followed by the same letters in the bars do not differ from each other according to the Tukey test ($p< 0.05$); Error bars represent standard error of the mean (n = 4).

Kabiri et al. (2017) evaluated the effect of fertilizers produced from graphene oxide containing micronutrients (Cu and Zn) as fertilizers and verified that these materials have the potential to increase the production of wheat in a calcarosol when compared to both with and without fertilizer applications. However, these authors found a significant effect only for the Zn application, since there was no response for Cu fertilization. Watts-Williams et al. (2020) also observed positive results for shoot dry mass, pod dry mass and grain mass of *Medicago truncatula* and *Hordeum vulgare* when graphene oxide loaded with Zn was used as a fertilizer. Nevertheless, in their results there were no significant differences to the conventional fertilizer ($ZnSO_4$), except for grain dry mass of *Hordeum vulgare*, which was higher than for $ZnSO_4$.

According to these authors, Zn ions can be protected by graphene oxide and present less interaction with soil components, thus being more available for plant uptake.

3.5.2 Copper and zinc uptake

BBFs promoted higher Cu and Zn uptake by shoot dry mass of common bean plants (Figures 8a and b). For Cu fertilization, the highest Cu uptake was observed for PLB-GO-Cu (1.28 mg pot^{-1}), followed by PLB-Cu (1.04 mg pot^{-1}), whilst Cu uptake in the $CuSO_4$ fertilizer treatment and control without Cu was 0.91 mg pot^{-1}, not differing from each other (Figure 8a).

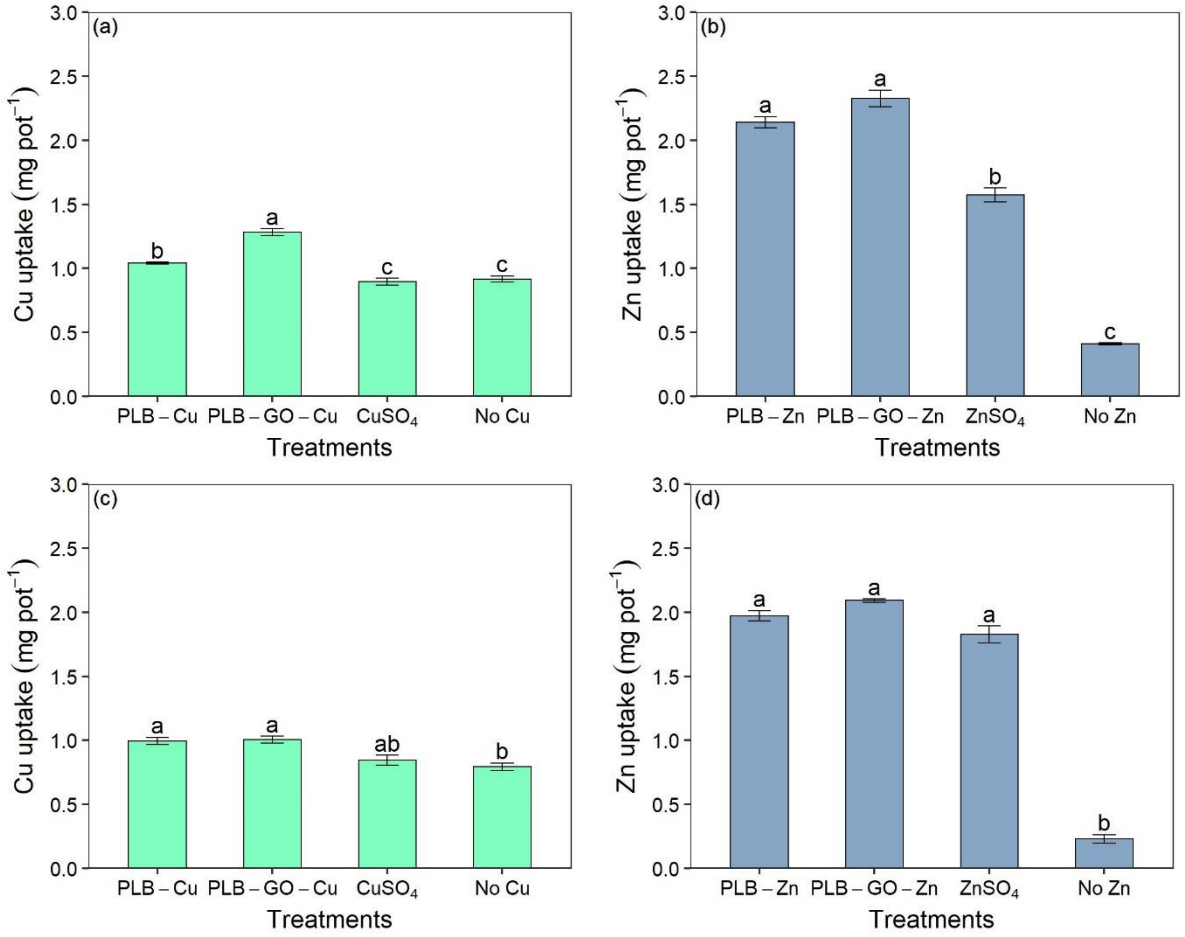

Figure 8 – Copper and zinc uptake by shoot dry mass (a and b) and grains (c and d) of common bean plants for copper and zinc fertilization, respectively, using BBFs and conventional fertilizers. Means followed by the same letters in the bars do not differ from each other according to the Tukey test (p< 0.05); Error bars represent standard error of the mean (n = 4).

For Zn, when common bean plants were fertilized with BBF, Zn uptake showed an average of 2.23 mg pot^{-1}, being 41.7% and 443% higher than $ZnSO_4$ and the control without Zn, respectively (Figure 8b). In the article by Kabiri et al. (2017) there was an increase in Zn uptake by wheat plants treated with Zn-loaded graphene oxide when compared to conventional fertilizers, whilst for Cu, there was no difference, which was attributed to the lack of wheat response to Cu under the researched conditions. Similar results were observed by Watts-Williams et al. (2020) using Zn-loaded graphene oxide as a fertilizer in powder form, where the authors verified an increase in Zn uptake when compared to the control (without Zn fertilization) in plants of *Medicago truncatula* and *Hordeum vulgare*.

Copper and Zn uptake in grains was not affected by different fertilizers throughout this research, with approximately 0.95 mg pot^{-1} of Cu and 1.96 mg pot^{-1} of Zn and no differences between BBFs and conventional fertilizers (Figures 8c and 8d). BBFs promoted an increase in Cu and Zn uptake in grains by 26.1% and 781%, respectively, when compared to controls without fertilization, whilst the $CuSO_4$ fertilizer (0.84 mg pot^{-1}) did not differ from the control (0.79 mg pot^{-1}) and the $ZnSO_4$ fertilizer increased Zn uptake in grains by 691% when compared to the control. Such increase in Zn uptake has also been observed in grains of *Hordeum vulgare* treated with Zn-loaded graphene oxide applied as a fertilizer when compared to the control, although no difference was observed for conventional fertilizers ($ZnSO_4$) (Watts-Williams et al., 2020).

In general, BBF increased total Cu and Zn uptake (sum of uptake by SDM and grains) by common bean plants with 2.29 mg pot^{-1} for PLB-GO-Cu, 2.03 mg pot^{-1} for PLB-Cu fertilizer, 1.74 mg pot^{-1} for $CuSO_4$ and 1.71 mg pot^{-1} for the control, with no difference between $CuSO_4$ and the control (Figure S9a). PLB-GO-Zn (4.42 mg pot^{-1}) and PLB-Zn (4.12 mg pot^{-1}) presented the highest total Zn uptake, being approximately 25.5 and 565% higher than the $ZnSO_4$ fertilizer and the control, respectively (Figure S9b). Higher nutrient uptake by common

bean plants treated with BBF was likely due to the gradual release, which caused lower interaction with soil components, keeping these micronutrients in available forms and facilitating plant uptake (Kabiri et al., 2017; Natarelli et al., 2021).

Copper and Zn contents in bean grains range from 7.8-17.6 mg kg^{-1} and 26.5-46.9 mg kg^{-1}, respectively (Delfini et al., 2020), with an average export of 9.9 (9.9 mg kg^{-1}) and 31.6 (31.6 mg kg^{-1}) g per ton of grains, respectively (Abreu et al., 2007). In this current research, Cu and Zn content in grains were higher than the values proposed by Abreu et al. (2007), except for the control (Table S7).

Critical levels of Cu and Zn in common bean plants are in the range of 5-15 mg kg^{-1} and 35-100 mg kg^{-1}, respectively, at the beginning of flowering (Malavolta, 2006), with a decrease during the grain production stage due to the redistribution to grains (Watts-Williams et al., 2020). Even so, we observed Zn contents in leaves within adequate levels (> 35 mg kg^{-1}) in BBFs, while for $ZnSO_4$, the content was lower than the critical range (Table S7).

There were no Cu and Zn deficiency symptoms in the fertilized plants (Figure 19Sa and Figure 19Sb), as well as for Cu deficiency in the control (Figure 19Sc and Figure 19Sd). However, plants showed visual and increasing symptoms of Zn deficiency in the control (Figures S15 to S17, and Figures 19Se to 19Sg), which was approximately 3.5 times lower than the minimum adequate level (35 mg kg^{-1}) (Malavolta, 2006), whilst Cu contents were always above critical level (15 mg kg^{-1}) even for the control, which explains the absence of visual symptoms for Cu deficiency.

In general, the effect of Zn deficiency is more evident in plant height due to Zn's role in the synthesis of auxin, which stimulates the development and elongation of young plant parts (Brown et al., 1993; Henriques et al., 2012). This effect of lower plant height was clearly observed in the control without Zn fertilization (Figure S18b). In addition, characteristic

symptoms of Zn deficiency were also observed, such as chlorosis evolving to necrosis in the leaves (Figures 21Se to Figure 21Sg) (Leal and Prado, 2008).

3.5.3 Soil pH and copper and zinc soil availability

Soil pH was not affected by Cu fertilization (Figure S10a), with a mean pH value of 5.38. For Zn, there was a slight increase in pH for BBF (5.46) when compared to the $ZnSO_4$ fertilizer (5.40), which, although significant ($p < 0.05$), has no effect on nutrient availability due to being a minor variation. In other research employing BBFs as fertilizers, minor or no effects on soil pH at longer growth periods were also observed (Borges et al., 2020; Carneiro et al., 2021),which might be due to a buffer effect caused by biochar during nutrient dissolution in BBF.

PLB-Cu caused an increase in soil available Cu (1.85 mg kg^{-1}), while PLB-GO-Cu showed the same level (1.58 mg kg^{-1}), alike $CuSO_4$ (1.52 mg kg^{-1}); all were higher than the control (0.56 mg kg^{-1}) (Figure 9a). For Zn, PLB-GO-Zn showed the highest level of soil available Zn (4.97 mg kg^{-1}), followed by PLB-Zn (4.37 mg kg^{-1}) and $ZnSO_4$ (3.90 mg kg^{-1}), all being at much higher Zn levels than the control (0.15 mg kg^{-1}) (Figure 9b).

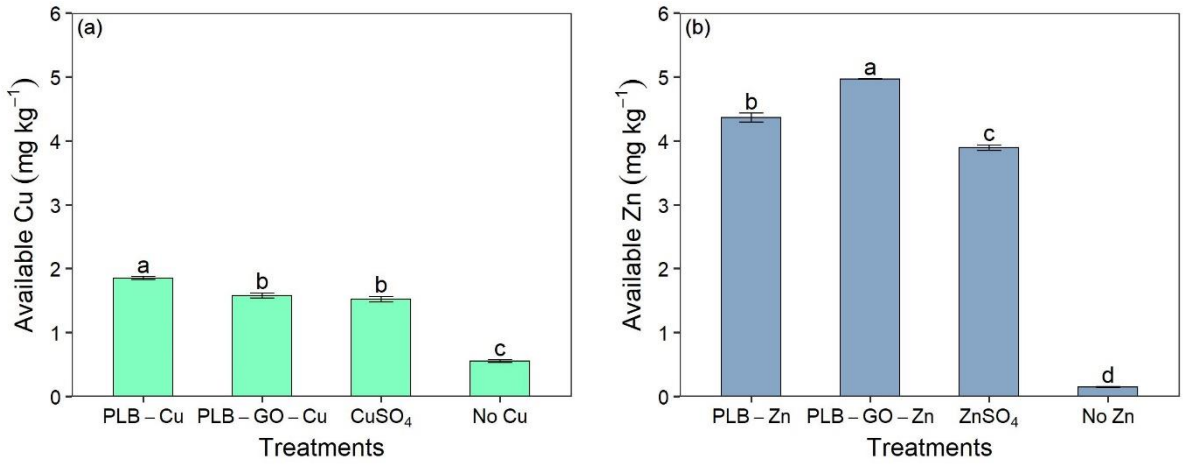

Figure 9 – Copper (a) and zinc (b) available in the soil through Mehlich-1 extractor after common bean plants grown under copper and zinc fertilization using BBFs and conventional fertilizers. Means followed by the same letters in the bars do not differ from each other via the Tukey test ($p< 0.05$); Error bars represent standard error of the mean (n = 4).

A greater soil availability of Cu for PLB-Cu and of Zn for PLB-GO-Zn may be related to the lower release rate these nutrients have in water (section 3.4), which might prevent these nutrients from being adsorbed in soil components. Higher Zn availability in soil for PLB-GO-Zn may also be related to the high stability of Zn complexation with graphene oxide, similar to chelated-Zn fertilizer, which leads to better performance when compared to $ZnSO_4$ (Kabiri et al., 2017; Watts-Williams et al., 2020). It should be highlighted that Mehlich-1 available Cu > 1.8 mg kg^{-1} and available Zn > 2.2 mg kg^{-1}in soil is considered high (Venegas et al., 1999).

3.5.4 Nutrient use efficiency

Copper and Zn use efficiency by common bean plants was evaluated by the apparent fertilizer nutrient uptake (AFNU) and apparent nutrient use efficiency (ANUE) (Hertzberger et al., 2021) are shown in Figure 10. BBFs increased the AFNU (Figure 10a and Figure 10b) and ANUE (Figure 10c and Figure 10d) by common bean plants. The AFNU for Cu was 0.58, 0.32, and 0.03 mg pot^{-1} for PLB-GO-Cu, PLB-Cu, and $CuSO_4$, respectively (Figure 10a), whilst for Zn it was 3.78, 3.47, and 2.76 mg pot^{-1} for PLB-GO-Zn, PLB-Zn, and $ZnSO_4$, respectively (Figure 10b). Both with Cu and Zn, the AFNU was higher for PLB-GO.

The ANUE showed a behavior similar to AFNU, in which BBF containing graphene oxide presented higher efficiency than other fertilizers (Figure 10c and Figure 10d). ANUE for PLB-GO-Cu (7.7%) was 3.4% and 7.3% higher than for PLB-Cu and $CuSO_4$ fertilizer, respectively. For Zn, the ANUE for PLB-GO-Zn (15.1%) was 1.2% and 4.1% higher than PLB-Zn and $ZnSO_4$ fertilizer, respectively. Common bean plants were more responsive to Zn fertilization than to Cu fertilization, presenting higher AFNU and ANUE values. The greater or the farthest from zero the AFNU and ANUE, the greater the crop's responsiveness to fertilization (Hertzberger et al., 2021).

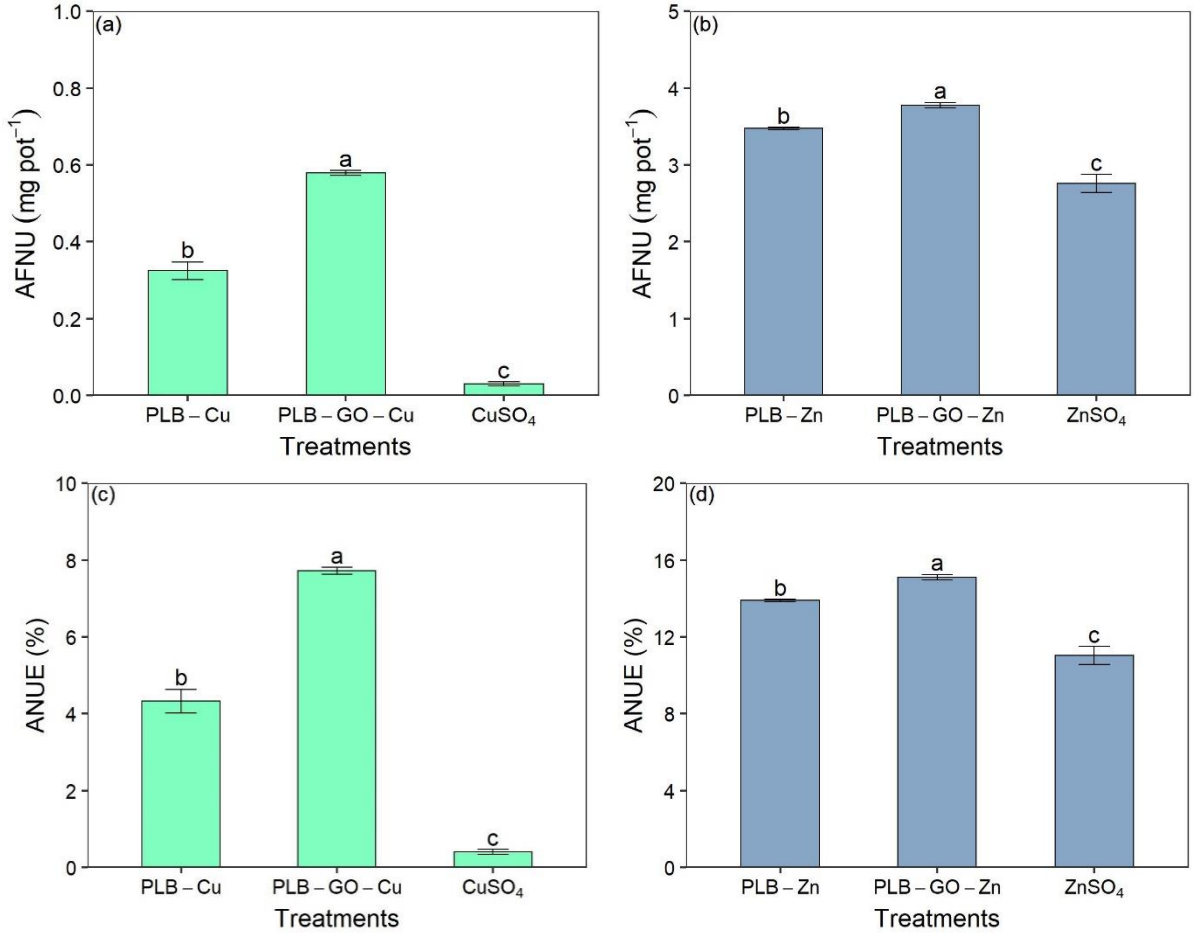

Figure 10 – Apparent fertilizer nutrient uptake (AFNU) (a and b) and apparent nutrient use efficiency (ANUE) (c and d) by common bean plants under copper and zinc fertilization, respectively, using BBFs and conventional fertilizers. Means followed by the same letters in the bars do not differ from each other through the Tukey test ($p < 0.05$); Error bars represent standard error of the mean (n = 4).

Higher nutrient use efficiency reflects a higher fertilizer efficacy in soil and can be explained by higher Cu and Zn availability, which leads to increased Cu and Zn total uptake by plants (Figure 11). Correlation coefficients for Cu experiments were lower than for Zn experiments. Nutrient use efficiency parameters for Cu fertilizers were highly correlated ($r \geq 0.93$) to grain mass, SDM Cu uptake and total Cu uptake, but had low correlation with available Cu in soil (Figure 11a). Furthermore, SDM presented low correlation with Cu uptake and soil Cu availability (Figure 11a). In contrast, nutrient use efficiency parameters for Zn fertilizers were highly correlated to all Zn uptake variables and to available Zn in soil (Figure 11b). There was also a great correlation with production variables (SDM, grain mass and total DM, $r \geq$

0.68), which explained the higher responsiveness common bean plants had towards Zn fertilization.

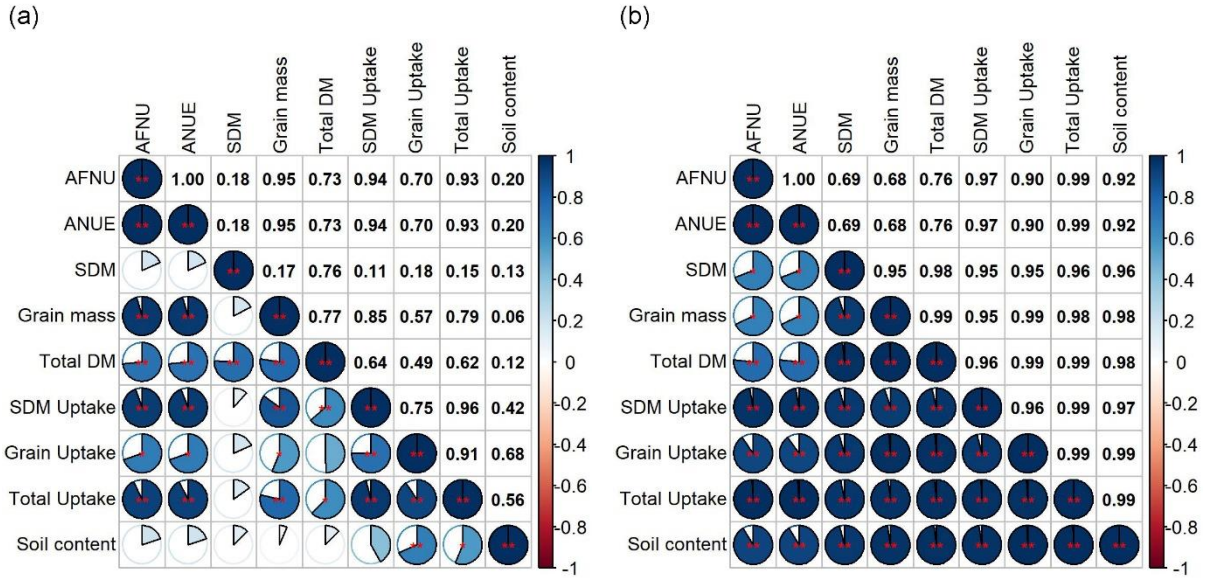

Figure 11 – Correlation diagrams and Pearson correlation coefficients between productive and nutritional parameters of common bean plants and soil nutrient availability due to copper (a) or zinc (b) fertilization using different fertilizers. Notes: ** significant at the 1% level ($p < 0.01$); and * significant at the 5% level ($p < 0.05$).

4 Environmental and Agronomic Implications

Copper and Zn are two limiting nutrients in highly weathered soils and require an adequate supply to achieve high crop yields, mainly in grain crops. Furthermore, fertilization is necessary to enrich the edible parts of plants and produce biofortified food important to human health. Due to the low effectiveness of soluble micronutrient fertilizer sources, alternatives which aim to overcome this issue are required, such as the incorporation of Cu and Zn in an organic matrix like biochar and/or graphene oxide as a strategy to effectively increase their plant use efficiency, primarily through decreasing the Cu and Zn interaction with soil components, slower release rates and higher plant availability. The employment of organic residues for biochar production, such as poultry litter, increases their fertilizer and agronomic value and provides adequate disposal, reducing their potential environmental pollution. An association of biochar with graphene oxide at low doses (≤ 0.5%) was tested for the first time

in this research, which aimed for it to act as a micronutrient (Cu and Zn) carrier and showed a slow-release profile that sustained crop production similarly or better than conventional fertilizers and caused an increase in Cu and Zn enrichment in common bean grains grown in an Oxisol, yet showed higher nutrient availability in the soil after cultivation. Thus, these characteristics make the association of biochar with minor levels of graphene oxide a possible alternative to help producing BBF of enhanced efficiency, especially for supplying micronutrients in highly weathered soils in intensive crop production systems.

5 Conclusions and future research

Graphene oxide enriched biochar was produced and evaluated for Cu and Zn adsorption and also for further use as a nutrient carrier (named biochar-based fertilizer – BBF) with which to supply these micronutrients to plants in an Oxisol. Copper and Zn adsorbed to PLB and PLB-GO present low solubility in water. BBF-loaded with Cu and Zn increases common bean production and micronutrient uptake, especially Zn, even more so than conventional soluble fertilizer. Higher micronutrient employment efficiency was attributed to the protection of the adsorption reactions that cationic metals had with soil components due to the functional organic matrix that caused their slow-release and favored plant uptake and nutrient availability after cultivation. Despite promising results, more in depth understanding of the micronutrient interactions in the rhizosphere is needed in order to design efficient and cost-effective novel fertilizers with a matrix carrier. Other approaches, such as coating/encapsulating should also be researched, testes and comprehended in more details. Finally, research on the residual effect of fertilization in the medium- to long-term as well as research under field conditions must be carried out prior to large scale recommendation.

Funding

This paper was supported by the Coordination for the Improvement of Higher Education Personnel, Brazil (CAPES – PROEX 593-2018),the Foundation for Research Support of Minas Gerais (Fapemig - Grants N° APQ-01865-17, APQ-01922-21, No. RED-00185-16, No. RED-00282-16), the L'Oréal – UNESCO - Academia Brasileira de Ciências, Prêmio Para Mulheres na Ciência (Prize for Women in Science; Brazil, 2017) and by the National Council for Scientific and Technological Development – CNPq, Brazil (Grants No 404076/2016-5, 433027/2018-5). CNPq also provided a PhD scholarship to the first author (Grant No. 140976/2018-3) and research scholarships to the corresponding author (LCAM) (Grant No. 308943/2018-0) and to JRS (Grant No. 312865/2020-1).

Authorship Contribution Statement

Jefferson Santana da Silva Carneiro: Conceptualized the project, carried out the experiments, developed the methodology, analyzed data and wrote the original draft and editing; **Dagna Ariele da Costa Leite:** Carried out the experiments, developed the methodology, contributed in writing, and reviewing; **Gustavo Mesquita de Castro:** Carried out the experiments, developed the methodology, contributed in writing, reviewing and editing the original draft; **José Romão Franca:** Carried out the experiments, developed the methodology, contributed in writing, and reviewing; **Lívia Botelho:** Carried out the experiments, developed the methodology, contributed in writing, and reviewing; **Jenaina Ribeiro Soares:** Supervised the project work, writing, and reviewing; **Juliano Elvis de Oliveira:** Supervised the project work, writing and reviewing; **Leônidas Carrijo Azevedo Melo:** Conceptualized the project plan, coordinated the project work, revised the work and reviewed the draft and contributed in writing and reviewing. Equally, all authors contributed for the final manuscript.

Declaration of competing interest

The authors declare that they have no known competing financial interests or personal relationships that could have appeared to influence the work reported in this paper.

Acknowledgments

The authors are grateful to Dr. Bárbara O. Nardis, Msc. Ivan C. A. Ribeiro, Dr. Evanise S. Penido and Msc. Robson C. Leite for providing valuable support during this research. The authors are also grateful towards Dr. Antonio R. Fernandes and Dr. Adriano R. Lucheta, director of SENAI Institute of Innovation in Mineral Technologies for providing conditions to make XRD and SEM analysis in their laboratories. We also thank the Nacional de Grafite company for providing the graphite flakes used for this paper.

Supplementary material

Description of graphene oxide preparation; Description of isotherms and kinetics models (Table S1 to Table S3); Chemical and textural properties of soil used in the plant research (Table S4); Comparison of Copper and Zinc sorption by different biochars (Table S5); SEM-EDS mapping and SEM-EDX spectrum (Figure S1 to Figure S8); Total nutrient content, solubility and BBF properties (Table S6); Kinetics of Cu and Zn release by conventional fertilizers (Figure S7); Plant height and total dry mass of common bean plants (Figure S8); Total copper and zinc uptake by common bean plants (Figure S9); Copper and zinc content in shoot dry mas and grains of common bean plants (Table S7); Soil pH (Figure S10); Plant growth and development (Figure S11 to Figure S18); and plants with and without fertilization and deficiency symptoms (Figure S19) can be found in the online version. Supplementary material to this article can be found online at doi: xxx.

References

Abreu, C.A. de, Lopes, A.S., Santos, G.C.G. dos, 2007. Micronutrientes, in: Novais, R.., Alvarez V, V.H., Barros, N.F., Cantarutti, R.B., Neves, J.C.L. (Eds.), Fertilidade Do Solo. Viçosa - Minas Gerias, pp. 645–724.

Akaike, H., 1974. A New Look at the Statistical Model Identification. IEEE Trans. Automat. Contr. 19, 716–723. https://doi.org/10.1109/TAC.1974.1100705

American Society for Testing and Materials, 2007. Standard test method for chemical analysis of wood charcoal - designation: D 1762 – 84 (2007). Annu. B. ASTM Stand. 1–2. https://doi.org/10.1520/D1762-84R07

An, X., Wu, Z., Qin, H., Liu, X., He, Y., Xu, X., Li, T., Yu, B., 2021. Integrated co-pyrolysis and coating for the synthesis of a new coated biochar-based fertilizer with enhanced slow-release performance. J. Clean. Prod. 283, 124642. https://doi.org/10.1016/j.jclepro.2020.124642

An, X., Wu, Z., Yu, J., Cravotto, G., Liu, X., Li, Q., Yu, B., 2020. Copyrolysis of Biomass, Bentonite, and Nutrients as a New Strategy for the Synthesis of Improved Biochar-Based Slow-Release Fertilizers. ACS Sustain. Chem. Eng. 8, 3181–3190. https://doi.org/10.1021/acssuschemeng.9b06483

Andelkovic, I.B., Kabiri, S., Tavakkoli, E., Kirby, J.K., McLaughlin, M.J., Losic, D., 2018. Graphene oxide-Fe(III) composite containing phosphate – A novel slow release fertilizer for improved agriculture management. J. Clean. Prod. 185, 97–104. https://doi.org/10.1016/j.jclepro.2018.03.050

Ayawei, N., Ebelegi, A.N., Wankasi, D., 2017. Modelling and Interpretation of Adsorption Isotherms. J. Chem. 1–11. https://doi.org/10.1155/2017/3039817

Baty, F., Ritz, C., Charles, S., Brutsche, M., Flandrois, J.-P., Delignette-Muller, M.-L., 2015. A toolbox for nonlinear regression in R: The package nlstools. J. Stat. Softw. 66, 1–21.

https://doi.org/10.18637/jss.v066.i05

Bavariani, M.Z., Ronaghi, A., Ghasemi, R., 2019. Influence of Pyrolysis Temperatures on FTIR Analysis, Nutrient Bioavailability, and Agricultural use of Poultry Manure Biochars. Commun. Soil Sci. Plant Anal. 50, 402–411. https://doi.org/10.1080/00103624.2018.1563101

Bekiaris, G., Bruun, S., Peltre, C., Houot, S., Jensen, L.S., 2015. FTIR-PAS: A powerful tool for characterising the chemical composition and predicting the labile C fraction of various organic waste products. Waste Manag. 39, 45–56. https://doi.org/10.1016/j.wasman.2015.02.029

Bekiaris, G., Peltre, C., Jensen, L.S., Bruun, S., 2016. Using FTIR-photoacoustic spectroscopy for phosphorus speciation analysis of biochars. Spectrochim. Acta - Part A Mol. Biomol. Spectrosc. 168, 29–36. https://doi.org/10.1016/j.saa.2016.05.049

Bishnoi, A., Kumar, S., Joshi, N., 2017. Wide-Angle X-ray Diffraction (WXRD): Technique for Characterization of Nanomaterials and Polymer Nanocomposites, in: Microscopy Methods in Nanomaterials Characterization. Elsevier Inc., pp. 313–337. https://doi.org/10.1016/b978-0-323-46141-2.00009-2

Bolan, N., Szogi, A., Seshadri, B., Chuasavathi, T., 2010. The management of phosphorus in poultry litter, in: 19th World Congress of Soil Science, Soil Solutions for a Changing World. Brisbane, Australia., pp. 317–320.

Borges, B.M.M.N., Strauss, M., Camelo, P.A., Sohi, S.P., Franco, H.C.J., 2020. Re-use of sugarcane residue as a novel biochar fertiliser - Increased phosphorus use efficiency and plant yield. J. Clean. Prod. 262, 121406. https://doi.org/10.1016/j.jclepro.2020.121406

Brasil, 2017. Manual de métodos analíticos oficiais para fertilizantes e corretivos. MAPA, Ministério da Agricultura Pecuária e Abastecimento/SDA, Secretaria de Defesa Agropecuária, Brasilia - DF.

Brown, P.H., Cakmak, I., Zhang, Q., 1993. Form and function of zinc plants, in: Robson, A.D. (Ed.), Zinc in Soil and Plants. Development in Plant and Soil Sciences. Springer, Dordrecht, pp. 93–102. https://doi.org/10.1007/978-94-011-0878-2

Carneiro, J.S. da S., Lustosa Filho, J.F., Nardis, B.O., Ribeiro-Soares, J., Zinn, Y.L., Melo, L.C.A., 2018. Carbon Stability of Engineered Biochar-Based Phosphate Fertilizers. ACS Sustain. Chem. Eng. 6, 14203–14212. https://doi.org/10.1021/acssuschemeng.8b02841

Carneiro, J.S. da S., Ribeiro, I.C.A., Nardis, B.O., Barbosa, C.F., Lustosa Filho, J.F., Melo, L.C.A., 2021. Long-term effect of biochar-based fertilizers application in tropical soil: Agronomic efficiency and phosphorus availability. Sci. Total Environ. 760, 143955. https://doi.org/10.1016/j.scitotenv.2020.143955

Carrier, A.J., Abdullahi, I., Hawboldt, K.A., Fiolek, B., MacQuarrie, S.L., 2017. Probing Surface Functionality on Amorphous Carbons Using X-ray Photoelectron Spectroscopy of Bound Metal Ions. J. Phys. Chem. C 121, 26300–26307. https://doi.org/10.1021/acs.jpcc.7b06311

Casagrande, J.C., Soares, M.R., Mouta, E.R., 2008. Zinc adsorption in highly weathered soils. Pesqui. Agropecu. Bras. 43, 131–139. https://doi.org/10.1590/S0100-204X2008000100017

Chen, L., Chen, X.L., Zhou, C.H., Yang, H.M., Ji, S.F., Tong, D.S., Zhong, Z.K., Yu, W.H., Chu, M.Q., 2017. Environmental-friendly montmorillonite-biochar composites: Facile production and tunable adsorption-release of ammonium and phosphate. J. Clean. Prod. 156, 648–659. https://doi.org/10.1016/j.jclepro.2017.04.050

Clemente, J.S., Beauchemin, S., Thibault, Y., Mackinnon, T., Smith, D., 2018. Differentiating Inorganics in Biochars Produced at Commercial Scale Using Principal Component Analysis. ACS Omega 3, 6931–6944. https://doi.org/10.1021/acsomega.8b00523

Cuixia, Y., Yingming, X., Lin, W., Xuefeng, L., Yuebing, S., Hongtao, J., 2020. Effect of

different pyrolysis temperatures on physico-chemical characteristics and lead(II) removal of biochar derived from chicken manure. RSC Adv. 10, 3667–3674. https://doi.org/10.1039/c9ra08199b

Delfini, J., Moda-Cirino, V., dos Santos Neto, J., Buratto, J.S., Ruas, P.M., Gonçalves, L.S.A., 2020. Diversity of nutritional content in seeds of Brazilian common bean germplasm. PLoS One 15, 1–13. https://doi.org/10.1371/journal.pone.0239263

Domingues, R.R., Trugilho, P.F., Silva, C.A., Melo, I.C.N.A. de, Melo, L.C.A., Magriotis, Z.M., Sánchez-Monedero, M.A., 2017. Properties of biochar derived from wood and high-nutrient biomasses with the aim of agronomic and environmental benefits. PLoS One 12, 1–19. https://doi.org/10.1371/journal.pone.0176884

Enders, A., Sohi, S., Lehmann, J., Singh, B., 2017. Total elemental analysis of metals and nutrients in biochars, in: Singh, B., Camps-Arbestain, M., Lehmann, J. (Eds.), Biochar: A Guide to Analytical Methods. CRC Press, Taylor & Francis Group, Australia and New Zealand, pp. 95–108.

Feitosa, S., Greiner, R., Meinhardt, A.K., Müller, A., Almeida, D.T., Posten, C., 2018. Effect of traditional household processes on iron, zinc and copper bioaccessibility in black bean (Phaseolus vulgaris L.). Foods 7, 1–12. https://doi.org/10.3390/foods7080123

Ghaffar, A., Younis, M.N., 2014. Adsorption of organic chemicals on graphene coated biochars and its environmental implications. Green Process. Synth. 3, 479–487. https://doi.org/10.1515/gps-2014-0071

Gwenzi, W., Nyambishi, T.J., Chaukura, N., Mapope, N., 2018. Synthesis and nutrient release patterns of a biochar-based N–P–K slow-release fertilizer. Int. J. Environ. Sci. Technol. 15, 405–414. https://doi.org/10.1007/s13762-017-1399-7

Henriques, A.R., Chalfun-Junior, A., Aarts, M., 2012. Strategies to increase zinc deficiency tolerance and homeostasis in plants. Brazilian J. Plant Physiol. 24, 3–8.

https://doi.org/10.1590/S1677-04202012000100002

Hertzberger, A.J., Cusick, R.D., Margenot, A.J., 2021. Maize and soybean response to phosphorus fertilization with blends of struvite and monoammonium phosphate. Plant Soil 461, 547–563. https://doi.org/10.1007/s11104-021-04830-2

Huang, D., Wang, X., Zhang, C., Zeng, G., Peng, Z., Zhou, J., Cheng, M., Wang, R., Hu, Z., Qin, X., 2017. Sorptive removal of ionizable antibiotic sulfamethazine from aqueous solution by graphene oxide-coated biochar nanocomposites: Influencing factors and mechanism. Chemosphere 186, 414–421. https://doi.org/10.1016/j.chemosphere.2017.07.154

Janu, R., Mrlik, V., Ribitsch, D., Hofman, J., Sedláček, P., Bielská, L., Soja, G., 2021. Biochar surface functional groups as affected by biomass feedstock, biochar composition and pyrolysis temperature. Carbon Resour. Convers. 4, 36–46. https://doi.org/10.1016/j.crcon.2021.01.003

Kabiri, S., Baird, R., Tran, D.N.H., Andelkovic, I., McLaughlin, M.J., Losic, D., 2018. Cogranulation of Low Rates of Graphene and Graphene Oxide with Macronutrient Fertilizers Remarkably Improves Their Physical Properties. ACS Sustain. Chem. Eng. 6, 1299–1309. https://doi.org/10.1021/acssuschemeng.7b03655

Kabiri, S., Degryse, F., Tran, D.N.H., Da Silva, R.C., McLaughlin, M.J., Losic, D., 2017. Graphene Oxide: A New Carrier for Slow Release of Plant Micronutrients. ACS Appl. Mater. Interfaces 9, 43325–43335. https://doi.org/10.1021/acsami.7b07890

Kingdom, F.A.A., Prins, N., 2016. Model Comparisons, in: Kingdom, F.A.A., Prins, N. (Eds.), Psychophysics: A Pratical Introduction. Academic press, United States of America, pp. 247–307. https://doi.org/10.1016/b978-0-12-407156-8.00009-8

Lavres Junior, J., Cabral, C.P., Rossi, M.L., Nogueira, T.A.R., Nogueira, N. de L., Malavolta, E., 2012. Deficiency symptoms and uptake of micronutrients by castor bean grown in

nutrient solution. Rev. Bras. Ciência do Solo 36, 233–242. https://doi.org/10.1590/s0100-06832012000100024

Leal, R.M., Prado, R.M., 2008. Desordens nutricionais no feijoeiro por deficiência de macronutrientes, boro e zinco. Brazilian J. Agric. Sci. 3, 301–306. https://doi.org/10.5039/agraria.v3i4a322

Lehmann, J., Joseph, S. (Eds.), 2015. Biochar for Environmental Management: Science, Technology and Implementation, 2nd ed. Routledge: Taylor and Francis group, London and New York.

Leng, L., Xiong, Q., Yang, L., Li, Hui, Zhou, Y., Zhang, W., Jiang, S., Li, Hailong, Huang, H., 2021. An overview on engineering the surface area and porosity of biochar. Sci. Total Environ. 763, 144204. https://doi.org/10.1016/j.scitotenv.2020.144204

Lenth, R., Singman, H., Love, J., Buerkner, P., Herve, M., 2019. Package 'emmeans': Estimated Marginal Means, aka Least-Squares Means. CRAN R Proj.

Li, M., Tang, Y., Ren, N., Zhang, Z., Cao, Y., 2018. Effect of mineral constituents on temperature-dependent structural characterization of carbon fractions in sewage sludge-derived biochar. J. Clean. Prod. 172, 3342–3350. https://doi.org/10.1016/j.jclepro.2017.11.090

Liu, T., Gao, B., Fang, J., Wang, B., Cao, X., 2016. Biochar-supported carbon nanotube and graphene oxide nanocomposites for Pb(II) and Cd(II) removal. RSC Adv. 6, 24314–24319. https://doi.org/10.1039/c6ra01895e

Lustosa Filho, J.F., Penido, E.S., Castro, P.P., Silva, C.A., Melo, L.C.A., 2017. Co-Pyrolysis of Poultry Litter and Phosphate and Magnesium Generates Alternative Slow-Release Fertilizer Suitable for Tropical Soils. ACS Sustain. Chem. Eng. 5, 9043–9052. https://doi.org/10.1021/acssuschemeng.7b01935

Ma, Y., Wu, L., Li, P., Yang, L., He, L., Chen, S., Yang, Y., Gao, F., Qi, X., Zhang, Z., 2021.

A novel, efficient and sustainable magnetic sludge biochar modified by graphene oxide for environmental concentration imidacloprid removal. J. Hazard. Mater. 407. https://doi.org/10.1016/j.jhazmat.2020.124777

Malavolta, E., 2006. Manual de Nutrição Mineral de Plantas, 1st ed. Editora Agronomica Ceres Ltda, São paulo.

Malavolta, E., 1980. Elementos de nutrição mineral das plantas. Agronômica Ceres, São Paulo.

Malavolta, E., Vitti, G.C., Oliveira, S.A., 1997. Avaliação do estado nutricional das plantas - Princípios e aplicações, 2nd ed. Associação Brasileira para Pesquisa da Potassa e do Fósforo, Piracicaba, SP.

Mannan, M.A., Hirano, Y., Quitain, A.T., M, K., Kida, T., 2018. Boron Doped Graphene Oxide: Synthesis and Application to Glucose Responsive Reactivity. J. Mater. Sci. Eng. 07. https://doi.org/10.4172/2169-0022.1000492

Marcano, D.C., Kosynkin, D. V., Berlin, J.M., Sinitskii, A., Sun, Z., Slesarev, A.S., Alemany, L.B., Lu, W., Tour, J.M., 2018. Correction to Improved Synthesis of Graphene Oxide. ACS Nano 12, 2078–2078. https://doi.org/10.1021/acsnano.8b00128

Marcano, D.C., Kosynkin, D. V, Berlin, J.M., Sinitskii, A., Sun, Z., Slesarev, A., Alemany, L.B., Lu, W., Tour, J.M., 2010. Improved Synthesis ofGraphene Oxide. ACS Nano 4, 4806–4814. https://doi.org/10.1021/nn1006368

Mouta, E.R., Soares, M.R., Casagrande, J.C., 2008. Copper adsorption as a function of solution parameters of variable charge soils. J. Braz. Chem. Soc. 19, 996–1009. https://doi.org/10.1590/S0103-50532008000500027

Nardis, B.O., Carneiro, J.S. da S., Souza, I.M.G. de, Barros, R.G. de, Melo, L.C.A., 2020. Phosphorus recovery using magnesium-enriched biochar and its potential use as fertilizer. Arch. Agron. Soil Sci. https://doi.org/10.1080/03650340.2020.1771699

Natarelli, C.V.L., Lopes, C.M.S., Carneiro, J.S.S., Melo, L.C.A., Oliveira, J.E., Medeiros, E.S., 2021. Zinc slow-release systems for maize using biodegradable PBAT nanofibers obtained by solution blow spinning. J. Mater. Sci. 56, 4896–4908. https://doi.org/10.1007/s10853-020-05545-y

Novais, R.F., Neves, J.C.L., Barros, N.F., 1991. Ensaio em ambiente controlado, in: Oliveira, A.J., Garrido, W.E., Araújo, J.D., Lourenço, S. (Eds.), Métodos de Pesquisa Em Fertilidade Do Solo. Embrapa-SEA, Brasília, pp. 189–253.

Penido, E.S., Melo, L.C.A., Guilherme, L.R.G., Bianchi, M.L., 2019. Cadmium binding mechanisms and adsorption capacity by novel phosphorus/magnesium-engineered biochars. Sci. Total Environ. 671, 1134–1143. https://doi.org/10.1016/j.scitotenv.2019.03.437

Pholosi, A., Naidoo, E.B., Ofomaja, A.E., 2020. Intraparticle diffusion of Cr(VI) through biomass and magnetite coated biomass: A comparative kinetic and diffusion study. South African J. Chem. Eng. 32, 39–55. https://doi.org/10.1016/j.sajce.2020.01.005

Qiu, H., Lv, L., Pan, B.C., Zhang, Q.J., Zhang, W.M., Zhang, Q.X., 2009. Critical review in adsorption kinetic models. J. Zhejiang Univ. Sci. A 10, 716–724. https://doi.org/10.1631/jzus.A0820524

R Core Team, 2019. R: A language and environment for statistical computing. R Found. Stat. Comput.

Raij, B. van, Andrade, J.C. de, Cantarella, H., Quaggio, J.A. (Eds.), 2001. Análise química para avaliação da fertilidade de solos tropicais. Instituto Agrônomico de Campinas, Campinas.

Saadi, R., Saadi, Z., Fazaeli, R., Fard, N.E., 2015. Monolayer and multilayer adsorption isotherm models for sorption from aqueous media. Korean J. Chem. Eng. 32, 787–799. https://doi.org/10.1007/s11814-015-0053-7

Sarfaraz, Q., Silva, L., Drescher, G., Zafar, M., Severo, F., Kokkonen, A., Molin, G., Shafi, M., Shafique, Q., Solaiman, Z., 2020. Characterization and carbon mineralization of biochars produced from different animal manures and plant residues. Sci. Rep. 10, 2–10. https://doi.org/10.1038/s41598-020-57987-8

Sashidhar, P., Kochar, M., Singh, B., Gupta, M., Cahill, D., Adholeya, A., Dubey, M., 2020. Biochar for delivery of agri-inputs: Current status and future perspectives. Sci. Total Environ. 703, 134892. https://doi.org/10.1016/j.scitotenv.2019.134892

Shang, M.R., Liu, Y.G., Liu, S.B., Zeng, G.M., Tan, X.F., Jiang, L.H., Huang, X.X., Ding, Y., Guo, Y.M., Wang, S.F., 2016. A novel graphene oxide coated biochar composite: Synthesis, characterization and application for Cr(VI) removal. RSC Adv. 6, 85202–85212. https://doi.org/10.1039/c6ra07151a

Shariatmadari, H., Shirvani, M., Jafari, A., 2006. Phosphorus release kinetics and availability in calcareous soils of selected arid and semiarid toposequences. Geoderma 132, 261–272. https://doi.org/10.1016/j.geoderma.2005.05.011

Shen, Y., Li, H., Zhu, W., Ho, S.H., Yuan, W., Chen, J., Xie, Y., 2017. Microalgal-biochar immobilized complex: A novel efficient biosorbent for cadmium removal from aqueous solution. Bioresour. Technol. 244, 1031–1038. https://doi.org/10.1016/j.biortech.2017.08.085

Silva, F.C., 2009. Manual de análises químicas de solos, plantas e fertilizantes, 2nd ed. Empresa Brasileira de Pesquisa Agropecuária, Embrapa Solos, Brasília, DF.

Silveira, M.L.A., Alleoni, L.R.F., 2003. Copper adsorption in tropical oxisols. Brazilian Arch. Biol. Technol. 46, 529–536. https://doi.org/10.1590/s1516-89132003000400006

Singh, B., Dolk, M.M., Shen, Q., Camps-Arbestain, M., 2017. Biochar pH, electrical conductivity and liming potential, in: Singh, B., Camps-Arbestain, M., Lehmann, J. (Eds.), Biochar: A Guide to Analytical Methods. CRC Press, Taylor & Francis Group,

Australia and New Zealand, pp. 23–38.

Sitko, R., Turek, E., Zawisza, B., Malicka, E., Talik, E., Heimann, J., Gagor, A., Feist, B., Wrzalik, R., 2013. Adsorption of divalent metal ions from aqueous solutions using graphene oxide. Dalt. Trans. 42, 5682–5689. https://doi.org/10.1039/c3dt33097d

Taherymoosavi, S., Verheyen, V., Munroe, P., Joseph, S., Reynolds, A., 2017. Characterization of organic compounds in biochars derived from municipal solid waste. Waste Manag. 67, 131–142. https://doi.org/10.1016/j.wasman.2017.05.052

Tran, H.N., You, S.J., Hosseini-Bandegharaei, A., Chao, H.P., 2017. Mistakes and inconsistencies regarding adsorption of contaminants from aqueous solutions: A critical review. Water Res. 120, 88–116. https://doi.org/10.1016/j.watres.2017.04.014

Venegas, V.H.A., Novais, R.F. de, Barros, N.F. de, Cantarutti, R.B., Lopes, A.S., 1999. Interpretação dos resultados das análises de solo, in: Ribeiro, A.C., Guimarães, P.T.G., Venegas, V.H.A. (Eds.), Recomendações Para o Uso de Corretivos e Fertilizantes Em Minas Gerais, 5ª Aproximação. Comissão de Fertilidade do Solo do Estado de Minas Gerais – CFSEMG, Viçosa, MG, Brazil, pp. 25–36.

Vikrant, K., Kim, K.H., Ok, Y.S., Tsang, D.C.W., Tsang, Y.F., Giri, B.S., Singh, R.S., 2018. Engineered/designer biochar for the removal of phosphate in water and wastewater. Sci. Total Environ. 616–617, 1242–1260. https://doi.org/10.1016/j.scitotenv.2017.10.193

Wang, H., Yuan, X., Wu, Y., Huang, H., Zeng, G., Liu, Y., Wang, X., Lin, N., Qi, Y., 2013. Adsorption characteristics and behaviors of graphene oxide for Zn(II) removal from aqueous solution. Appl. Surf. Sci. 279, 432–440. https://doi.org/10.1016/j.apsusc.2013.04.133

Wang, J., Guo, X., 2020a. Adsorption isotherm models: Classification, physical meaning, application and solving method. Chemosphere 258, 127279. https://doi.org/10.1016/j.chemosphere.2020.127279

Wang, J., Guo, X., 2020b. Adsorption kinetic models: Physical meanings, applications, and solving methods. J. Hazard. Mater. 390, 122156. https://doi.org/10.1016/j.jhazmat.2020.122156

Watts-Williams, S.J., Nguyen, T.D., Kabiri, S., Losic, D., McLaughlin, M.J., 2020. Potential of zinc-loaded graphene oxide and arbuscular mycorrhizal fungi to improve the growth and zinc nutrition of Hordeum vulgare and Medicago truncatula. Appl. Soil Ecol. 150, 103464. https://doi.org/10.1016/j.apsoil.2019.103464

Wei, T., Simko, V., 2021. R package "corrplot": Visualization of a Correlation Matrix. CRAN.R-project.org.

White, R.L., White, C.M., Turgut, H., Massoud, A., Tian, Z.R., 2018. Comparative studies on copper adsorption by graphene oxide and functionalized graphene oxide nanoparticles. J. Taiwan Inst. Chem. Eng. 85, 18–28. https://doi.org/10.1016/j.jtice.2018.01.036

Wu, F.C., Tseng, R.L., Juang, R.S., 2009. Initial behavior of intraparticle diffusion model used in the description of adsorption kinetics. Chem. Eng. J. 153, 1–8. https://doi.org/10.1016/j.cej.2009.04.042

Yuan, W., Shen, Y., Ma, F., Du, C., 2018. Application of Graphene-Oxide-Modified Polyacrylate Polymer for Controlled-Release Coated Urea. Coatings 8, 1–10. https://doi.org/10.3390/coatings8020064

Zhang, M., Gao, B., Chen, J., Li, Y., Creamer, A.E., Chen, H., 2014. Slow-release fertilizer encapsulated by graphene oxide films. Chem. Eng. J. 255, 107–113. https://doi.org/10.1016/j.cej.2014.06.023

Zhang, M., Gao, B., Yao, Y., Xue, Y., Inyang, M., 2012. Synthesis, characterization, and environmental implications of graphene-coated biochar. Sci. Total Environ. 435–436, 567–572. https://doi.org/10.1016/j.scitotenv.2012.07.038

Zhang, Y., Cao, B., Zhao, L., Sun, L., Gao, Y., Li, J., Yang, F., 2018. Biochar-supported

reduced graphene oxide composite for adsorption and coadsorption of atrazine and lead ions. Appl. Surf. Sci. 427, 147–155. https://doi.org/10.1016/j.apsusc.2017.07.237

Zhao, R., Jiang, D., Coles, N., Wu, J., 2015. Effects of biochar on the acidity of a loamy clay soil under different incubation conditions. J. Soils Sediments 15, 1919–1926. https://doi.org/10.1007/s11368-015-1143-1

APPENDIX B

Supplementary material

Biochar and graphene oxide composite matrix producing micronutrient fertilizer: a new approach towards the improvement of effectiveness in tropical soil

Jefferson Santana da Silva Carneiro[a], *Dagna Ariele da Costa Leite*[b], *Gustavo Mesquita de Castro*[a], *José Romão Franca*[c], *Lívia Botelho*[a], *Jenaina Ribeiro Soares*[c], *Juliano Elvis de Oliveira*[d], *Leônidas Carrijo Azevedo Melo*[a*]

[a]Federal University of Lavras, School of Agricultural Sciences, Soil Science Department, Lavras, 37200-900, Minas Gerais, Brazil.

[b] Federal University of Tocantins, Gurupi campus, Gurupi, 77402-970, Tocantins, Brazil.

[c]Federal University of Lavras, Institute of Natural Sciences, Physics Department, Lavras, 37200-900, Minas Gerais, Brazil.

[d] Federal University of Lavras, School of Engineering, Engineering Department, Lavras, 37200-900, Minas Gerais, Brazil.

*Corresponding author

Leônidas Carrijo Azevedo Melo,

Email: leonidas.melo@ufla.br

MATERIAL AND METHODS

Preparation of graphene oxide

Graphene oxide was prepared according to Hummers' improved method as described in Marcano et al. (2010) and Marcano et al. (2018). In summary, a concentrated 9:1 mixture of 360 mL of H_2SO_4 (98%) and 40 mL of H_3PO_4 (85%) were added to a mixture of graphite flakes (3.0 g, 1 equiv. wt.) and $KMnO_4$ (99%) (18.0 g, 6 equiv. wt.), which produced a fair exothermic reaction at 35-40 °C. This reaction generated a moss-green color. The reaction was then heated to 50 °C and stirred for 12 h, at which time it was cooled to room temperature and poured onto 400 mL of deionized water in ice form with 3 mL of 30% H_2O_2.

For workup, the mixture was sifted through a metal U.S. Standard testing sieve (300 μm), later centrifuged at 4000 rpm for 4 h whilst the supernatant was decanted away. Remaining solid material was then washed in a sequence with 200 mL of deionized water, after applying 200 mL of 30% HCl (37%) and 200 mL of ethanol (37%).

This procedure was performed twice with a goal of reaching a more effective purification of graphene oxide by removing excess precursor materials. After each wash (water, HCl or ethanol), the mixture was sifted through the U.S. Standard testing sieve, centrifuged at 4000 rpm for 4 h and the supernatant decanted away.

The material remaining after this extended, multiple-washing process was coagulated with 200 mL of ether and the resulting suspension was filtered over a PTFE (Teflon Polytetrafluoroethylene) membrane with 0.45 μm pore size. Solids obtained on the filter were vacuum-dried overnight at room temperature, which led to obtaining graphene oxide (GO).

Adsorption study

Isotherm models

Three widely used models, which were the Langmuir, Freundlich and Langmuir-Freundlich (SIPS), were applied in order to describe the adsorption equilibrium.

Langmuir:

$$Q_e = \frac{q_m K_L C_e}{1 + K_L C_e}$$

Where Q_e (mg g^{-1}) is the amount of compound adsorbed per mass unit of powders, C_e (mg L^{-1}) is the Zn and Cu concentration at equilibrium, q_m (mg g^{-1}) is the maximum adsorption capacity and K_L (L mg^{-1}) is a constant related to the affinity between the micronutrient and the adsorbent.

Freundlich:

$$Q_e = K_f C_e^{\,1/n}$$

Where K_f is the Freundlich isotherm constant (mg g^{-1}) (mg L^{-1})$^{-n}$ related to the adsorption capacity, C_e (mg L^{-1}) is the Zn and Cu concentration at equilibrium and n is a coefficient related to adsorption intensity.

Langmuir-Freundlich (SIPS):

$$Q_e = \frac{q_m K_s C_e^{n_s}}{1 + K_s C_e^{n_s}}$$

Where Q_e (mg g^{-1}) is the content of Zn or Cu adsorbed per unit of mass, C_e (mg L^{-1}) is the concentration of Zn and Cu at equilibrium, q_m (mg g^{-1}) is the maximum capacity of adsorption, K_s (L mg^{-1}) is the constant related between Zn or Cu and the adsorbent material and n_s is a coefficient related to adsorption intensity.

Kinetics models

Three models were used to describe the kinetics of Cu and Zn adsorption: pseudo first-order, pseudo second-order and intraparticle diffusion (Table S1).

Table S1 - Models tested to describe copper and zinc adsorption kinetics data of BBFs and conventional fertilizers.

Kinetics models	Parameters	Reference
Pseudo First-order: $Q_t = Q_e\ [1 - exp(-k_1\ t)]$	k_1, first order rate constant (h^{-1})	Simonin (2016)
Pseudo Second-order: $Q_t = Q_e\ [(k_2\ t)/(1+k_2\ t)]$	k_2, second order rate constant [$(mg\ g^{-1})^{-1}$]	Simonin (2016)
Intraparticle diffusion: $Q_t = K_p\ t^{1/2} + C$	K_p, intraparticle diffusion rate constant [$mg\ /(g\ h^{1/2})$] C, constant for any experiment ($mg\ g^{-1}$)	Wu et al. (2009)

In which Q_t ($mg\ g^{-1}$) is the cumulative Cu or Zn release at t time; Q_e ($mg\ g^{-1}$) is the amount of Cu or Zn release at equilibrium or maximum Cu or Zn released.

For the intraparticle diffusion R_i was calculated, which is the initial adsorption factor according to Wu et al. (2009) and Pholosi et al. (2020) using their equation parameters through the following equation:

$$R_i = \frac{q_{ref} - C}{q_{ref}}$$

Where R_i is the initial adsorption factor, q_{ref} is the solid phase concentration at time $t = t_{ref}$ for an adsorption system, and C is constant for any experiment.

q_{ref} is calculated through the following equation:

$$q_{ref} = K_p t_{ref}^{1/2} + C$$

Where t_{ref} is the longest time in the adsorption process (72 h).

Table S2- Initial adsorption factor (R_i) and kinetics behavior based on the intraparticle diffusion model.

*R_i	Initial adsorption behavior
$R_i = 1$	No initial adsorption
$1 > R_i > 0.9$	Weak initial adsorption
$0.9 > R_i > 0.5$	Intermediate initial adsorption
$0.5 > R_i > 0.1$	Strong initial adsorption
$R_i < 0.1$	Approaching complete initial adsorption

*Adapted from Wu et al. (2009) and Pholosi et al. (2020).

Kinetics models of Cu and Zn released by BBF's and conventional fertilizers

Table S3-Models tested for describing kinetics data of copper and zinc release by BBFs and conventional fertilizers.

Kinetics models	Parameters	Reference
Pseudo First-order: $Q_t = Q_e\,[1 - exp(-k_1\,t)]$	k_1, first order rate constant (h^{-1})	Simonin (2016)
Pseudo Second-order: $Q_t = Q_e\,[(k_2\,t)/(1+k_2\,t)]$	k_2, second order rate constant [$(mg\ g^{-1})^{-1}$]	Simonin (2016)
Power function: $Q_t = a\,t^b$	a, initial Cu or Zn desorption rate ($mg\ g^{-1}\ h^{-1})^b$ b, desorption rate coefficient [$(mg\ g^{-1})^{-1}$]	Shariatmadari et al. (2006)
Elovich: $Q_t = \alpha - \beta\ln(t)$	α, initial Cu or Zn desorption ($mg\ g^{-1}\ h^{-1}$) β, Cu or Zn desorption constant [$(mg\ g^{-1})^{-1}$]	Lustosa Filho et al. (2017)
Parabolic diffusion: $Q_t = Q_e + R\,t^{0.5}$	R, diffusion rate constant [$(mg\ g^{-1})^{-0.5}$]	Shariatmadari et al. (2006)

In which Q_t ($mg\ g^{-1}$) is the cumulative Cu or Zn release at t time and Q_e ($mg\ g^{-1}$) is the amount of Cu or Zn release at equilibrium or maximum Cu or Zn released.

Evaluation of isotherm and kinetics models

The mathematical models were tested and mathematically adjusted to a Cu and Zn adsorption and kinetics data set, as the quality of the fit was observed based on its standard error of estimate (SE) (Equation 1) (Shariatmadari et al., 2006) and the most-fitting model was chosen based on the Akaike information criterion (AIC) (Equation 2) (Akaike, 1974; Kingdom and Prins, 2016).

$$SE = \left[\left(Q_m - Q_p^{'}\right)^2 /(N - 2)\right]^{1/2} \quad \text{Equation 1}$$

In which Q_m and Q'_p are the measured and predicted amounts of adsorbed or released Cu or Zn at equilibrium concentration C_e or time t, respectively, and N is the number of measurements.

$$AIC = -2LL(\theta|y,M_i) + 2K_i \quad \text{Equation 2}$$

In which $LL(\theta|y,M_i)$ is the log-likelihood for model M_i using maximum likelihood estimates for its parameters θ, based on the observed data y and K_i is the number of free parameters in model M_i.

Crystallite size

XRD diffractograms were employed to determine the average crystallite size of PLB and PLB-GO. The average crystallite size (nm) was calculated according to Scherrer's equation (Bishnoi et al., 2017) through the following equation:

$$L = \frac{K\lambda}{\tau\,(cos\,\theta)}$$

Where L is the mean size of the ordered (crystalline) domains (nm); K is the Scherrer constant (0.90); λ is radiation wavelength used for analysis (CoKa = 0.178901 nm); τ is width at half the height of the diffraction peak (°) and θ is the Bragg angle (°). The width at half the height of the diffraction peak was determined using the demo version of the Match!3.12 software.

To determine the average crystallite size, data of three main peaks from each spectrum were used.

Soil characterization

Table S4 – Chemical and textural properties of soil used in plant research.

Properties and units[a]	Mean ± SE[b]
pH H_2O	4.80 ± 0.00
Available potassium – K^+ (mg kg^{-1})	18.7 ± 0.85
Available phosphorus – P (mg kg^{-1})	2.60 ± 0.70
Exchangeable calcium – Ca^{2+} ($cmol_c$ kg^{-1})	0.25 ± 0.05
Exchangeable magnesium – Mg^{2+} ($cmol_c$ kg^{-1})	0.10 ± 0.00
Exchangeable aluminum – Al^{3+} ($cmol_c$ kg^{-1})	0.10 ± 0.00
Potential acidity – H+Al ($cmol_c$ kg^{-1})	2.95 ± 0.05
Sum of bases – SB ($cmol_c$ kg^{-1})	0.40 ± 0.05
Effective cation exchange capacity – t ($cmol_c$ kg^{-1})	0.50 ± 0.05
Cation exchange capacity at pH 7 – T ($cmol_c$ kg^{-1})	3.35 ± 0.00
Base saturation index – V (%)	11.9 ± 1.49
Aluminum saturation index - m (%)	20.2 ± 2.02
Organic matter – O.M. (dag kg^{-1})	1.05 ± 0.05
Remaining phosphorus – Rem-P (mg kg^{-1})	29.4 ± 0.55
Available zinc – Zn^{2+} (mg kg^{-1})	0.15 ± 0.05
Available iron – Fe^{2+} (mg kg^{-1})	38.3 ± 0.15
Available manganese – Mn^{2+} (mg kg^{-1})	1.40 ± 0.00
Available copper – Cu^{2+} (mg kg^{-1})	0.50 ± 0.00
Available boron – B (mg kg^{-1})	0.13 ± 0.00
Available sulphur – S (mg kg^{-1})	4.05 ± 0.65
Clay content (g kg^{-1})	333
Silt content (g kg^{-1})	39
Sand content (g kg^{-1})	628

[a]Ca^{2+}, Mg^{2+} and Al^{3+}: KCl extractor (1 mol L^{-1}); P, K^+, Fe^{2+}, Zn^{2+}, Mn^{2+} and Cu^{2+}: Mehlich-1 extractor; H+Al: SMP extractor; B: Hot water extractor; S: monocalcium phosphate in acetic acid extractor; O.M.: organic matter by $Na_2Cr_2O_7$ 4 mol L^{-1} + H_2SO_4 10 mol L^{-1} oxidation; SB: sum of bases (Ca^{2+} + Mg^{2+} + K^+); T: cation exchange capacity at pH 7 (SB + H+Al); t: effective cation exchange capacity (SB + Al^{3+}); V: base saturation index [(SB / T) * 100]; and m%: aluminum saturation index [(Al^{3+} / t) * 100]; [b]Standard error of the mean - SE (n = 2).

RESULTS

Adsorption research

Table S5 – Comparison of Copper and Zinc sorption by different biochars reported in literature.

Feedstock material	Pyrolysis temperature (°C)	Biochar dosage (g L^{-1})	Maximum sorption capacity (q_m)	Reference
Copper (Cu) adsorption				
Banana stalks	500	2	134.9	Deng et al. (2020)
Chicken manure	450	33	81.3	Rodríguez-Vila et al. (2018)
Cedar wood	450	33	17.7	Rodríguez-Vila et al. (2018)
Farmyard manure	450	33	35.8	Rodríguez-Vila et al. (2018)
Horse chestnut leaves	450	33	56.5	Rodríguez-Vila et al. (2018)
Cedar wood	550	33	27.2	Rodríguez-Vila et al. (2018)
Cedar wood	600	33	30.6	Rodríguez-Vila et al. (2018)
Cedar wood	650	33	23.9	Rodríguez-Vila et al. (2018)
Cedar wood	700	33	28.7	Rodríguez-Vila et al. (2018)
Corn straw	600	5	12.5	Chen et al. (2011)
Hardwood	450	5	6.8	Chen et al. (2011)
Apple tree[c]	500	5	11.4	Zhao et al. (2020)
Spent mushroom[d]	500	10	364.2	Abdallah et al. (2019)
Poultry litter	600	1	60.6	This paper
Poultry litter + GO[a]	600	1	70.3	This paper
Zinc (Zn) adsorption				
Banana stalks	500	2	108.1	Deng et al. (2020)
Chicken manure	450	33	31.9	Rodríguez-Vila et al. (2018)
Cedar wood	450	33	10.7	Rodríguez-Vila et al. (2018)
Farmyard manure	450	33	26.0	Rodríguez-Vila et al. (2018)
Horse chestnut leaves	450	33	35.2	Rodríguez-Vila et al. (2018)
Cedar wood	550	33	13.9	Rodríguez-Vila et al. (2018)
Cedar wood	600	33	13.5	Rodríguez-Vila et al. (2018)
Cedar wood	650	33	15.2	Rodríguez-Vila et al. (2018)
Cedar wood	700	33	15.1	Rodríguez-Vila et al. (2018)
Corn straw + MNT[b]	200	2	7.74	Song et al. (2020)
Corn straw + MNT	350	2	8.16	Song et al. (2020)
Corn straw + MNT	500	2	7.32	Song et al. (2020)
Corn straw + MNT	700	2	5.74	Song et al. (2020)
Corn straw	600	5	11.0	Chen et al. (2011)
Hardwood	450	5	4.54	Chen et al. (2011)
Apple tree	500	5	10.2	Zhao et al. (2020)
Spent mushroom	500	10	333.2	Abdallah et al. (2019)

Poultry litter	600	1	48.0	This paper
Poultry litter + GO	600	1	56.5	This paper

[a]GO = graphene oxide; [b]MNT = calcium-montmorillonite; [c]Apple tree branches and cutoffs; [d]Spent mushroom compost.

SEM-EDS mapping and SEM-EDX spectra

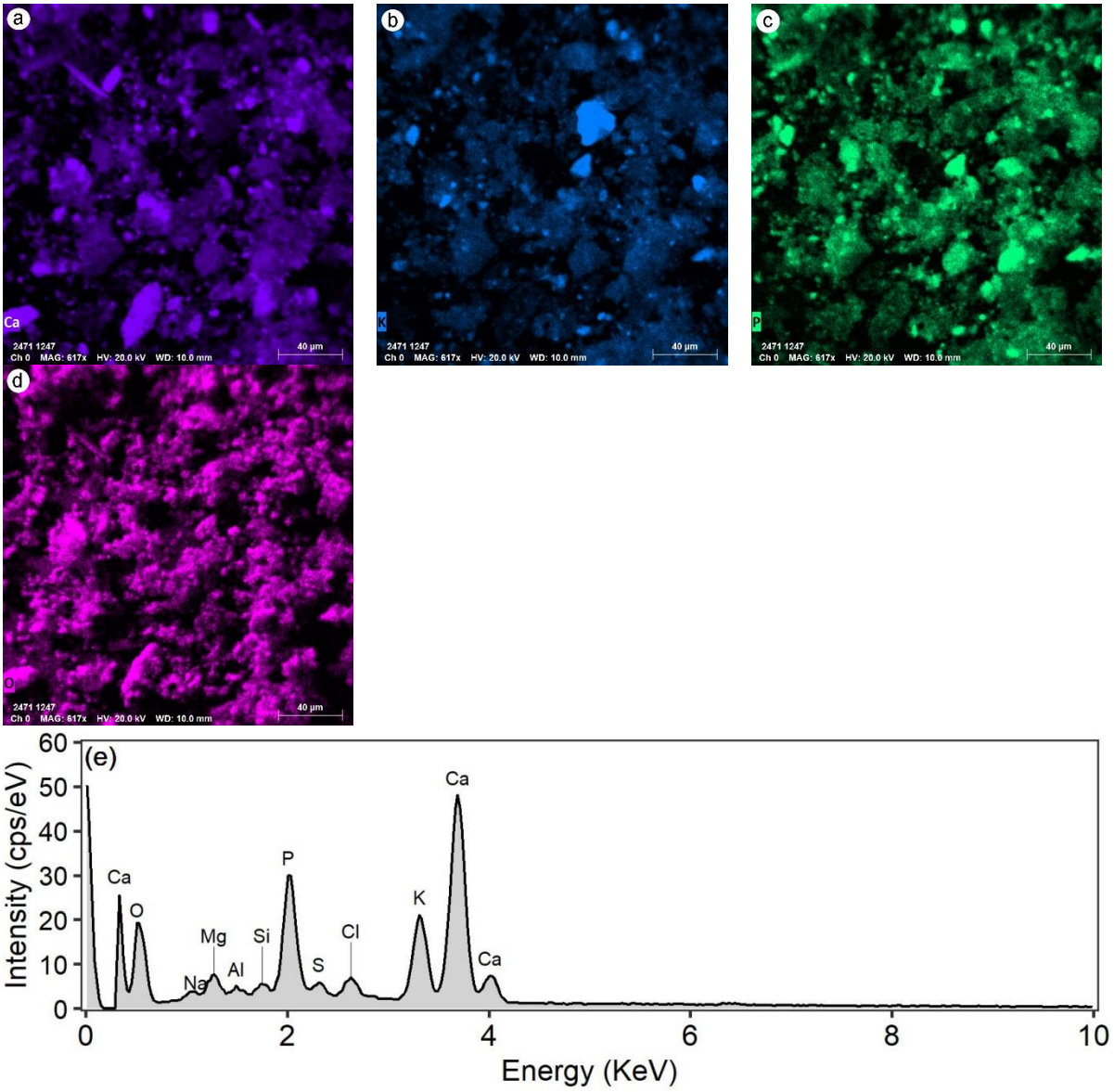

Figure S1 – SEM-EDS mapping for Ca (a), K (b), P (c) and O (d) and SEM-EDX spectrum (e) for poultry litter biochar (PLB).

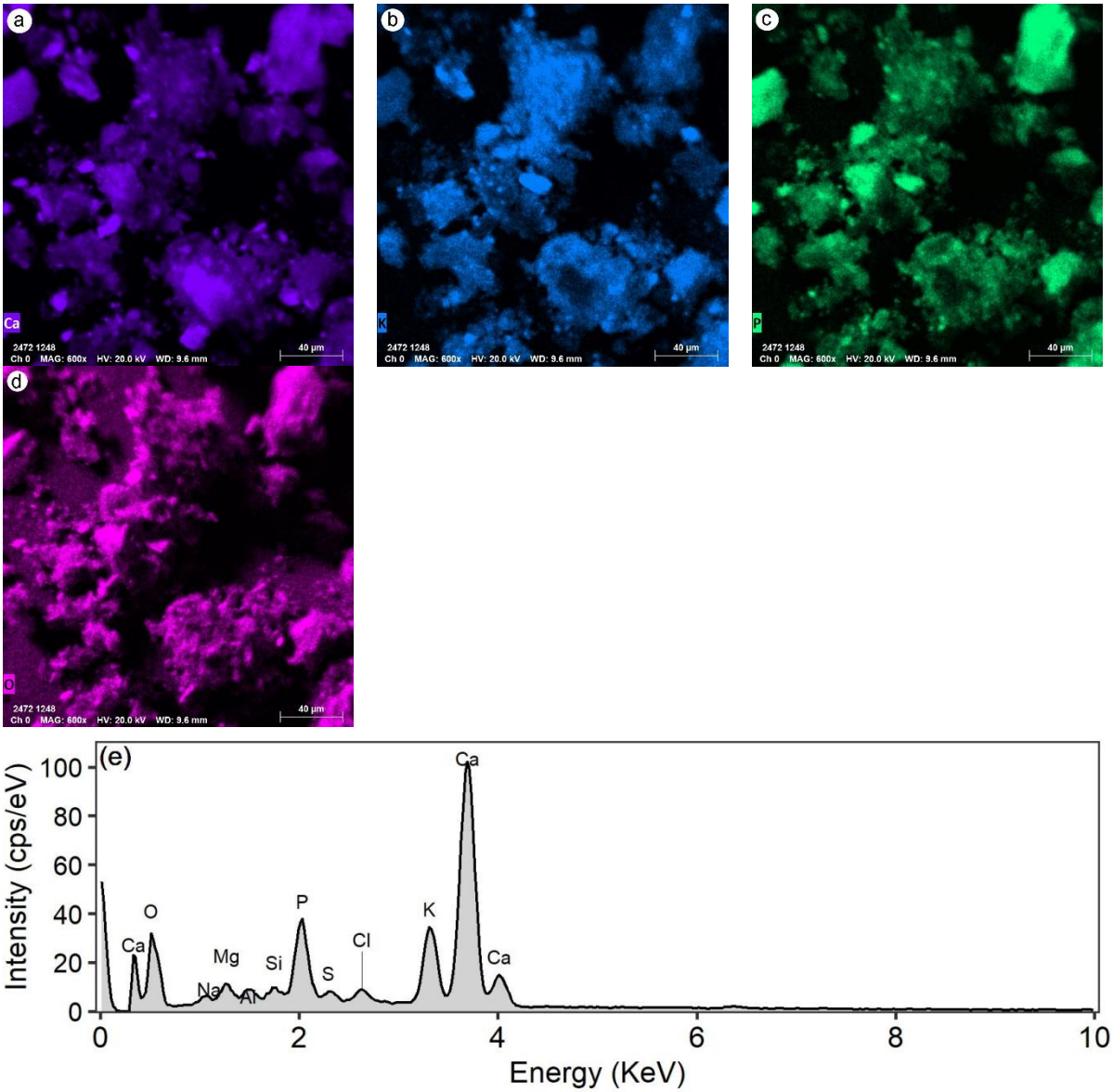

Figure S2 – SEM-EDS mapping for Ca (a), K (b), P (c), and O (d) and SEM-EDX spectrum (e) for graphene oxide enriched poultry litter biochar (PLB-GO).

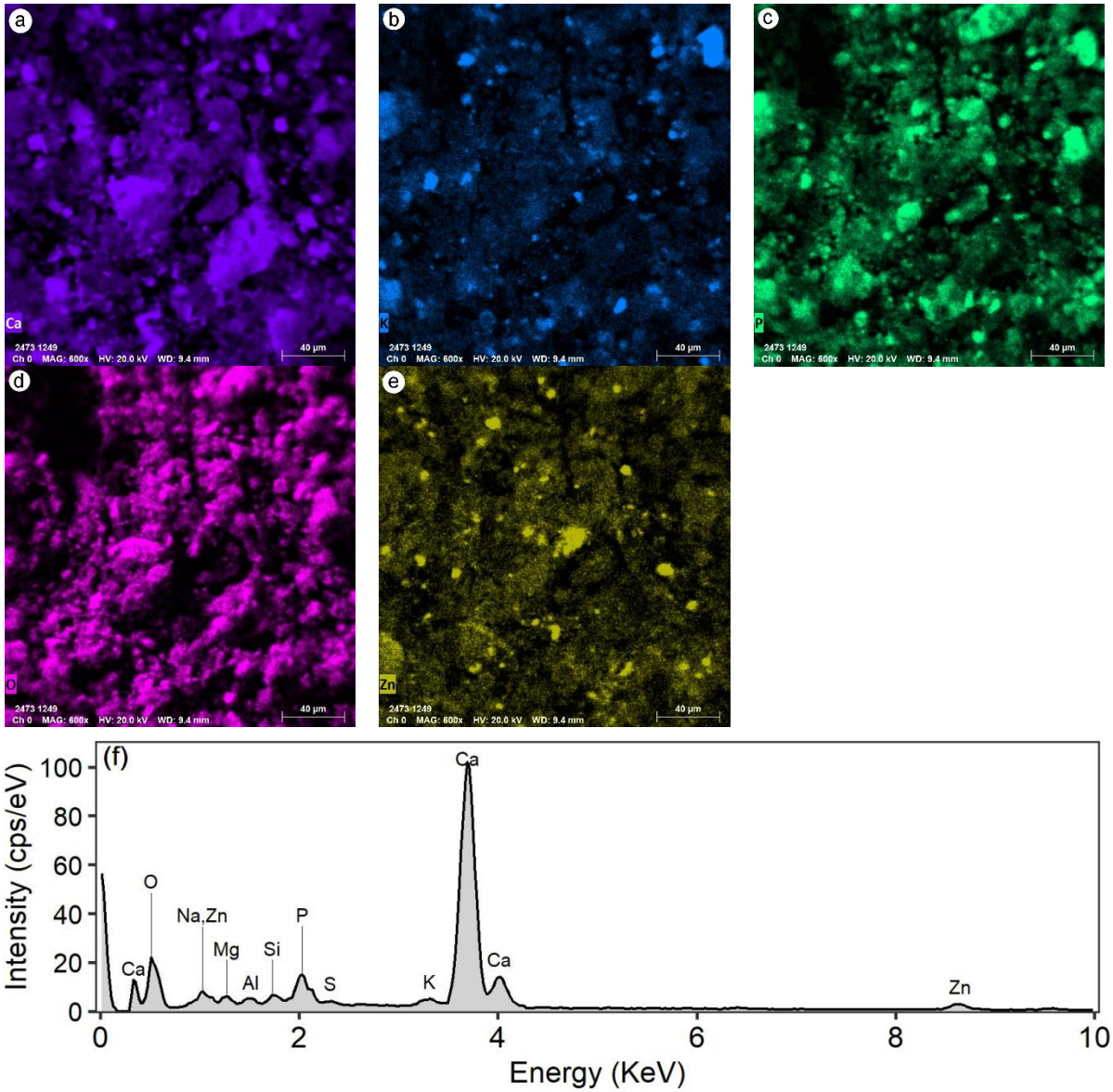

Figure S3 – SEM-EDS mapping for Ca (a), K (b), P (c), O (d), Zn (e) and SEM-EDX spectrum (f) for poultry litter biochar zinc fertilizer (PLB-Zn).

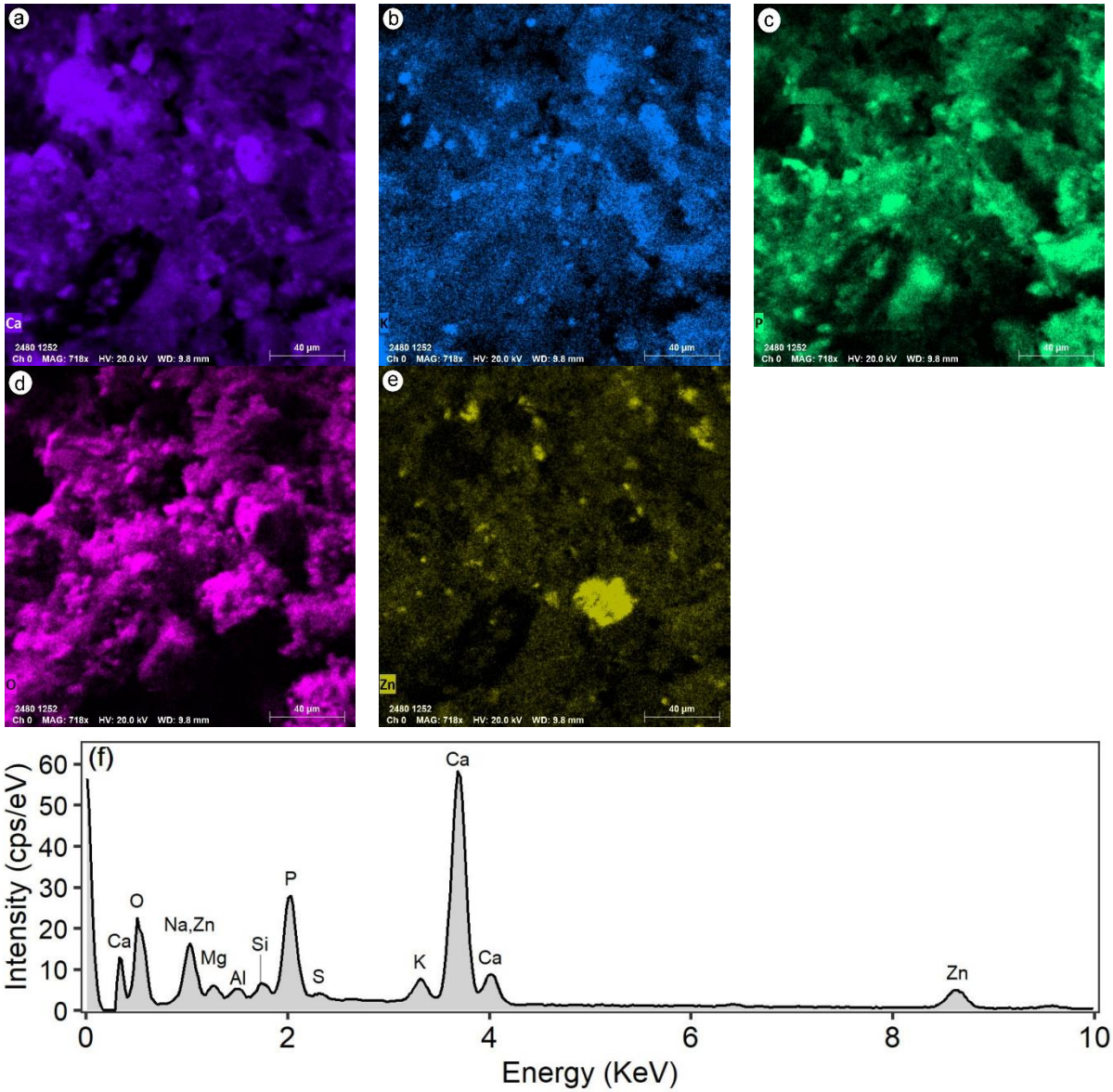

Figure S4 – SEM-EDS mapping for Ca (a), K (b), P (c), O (d), Zn (e), and SEM-EDX spectrum (f) for graphene oxide enriched poultry litter biochar zinc fertilizer (PLB-GO-Zn).

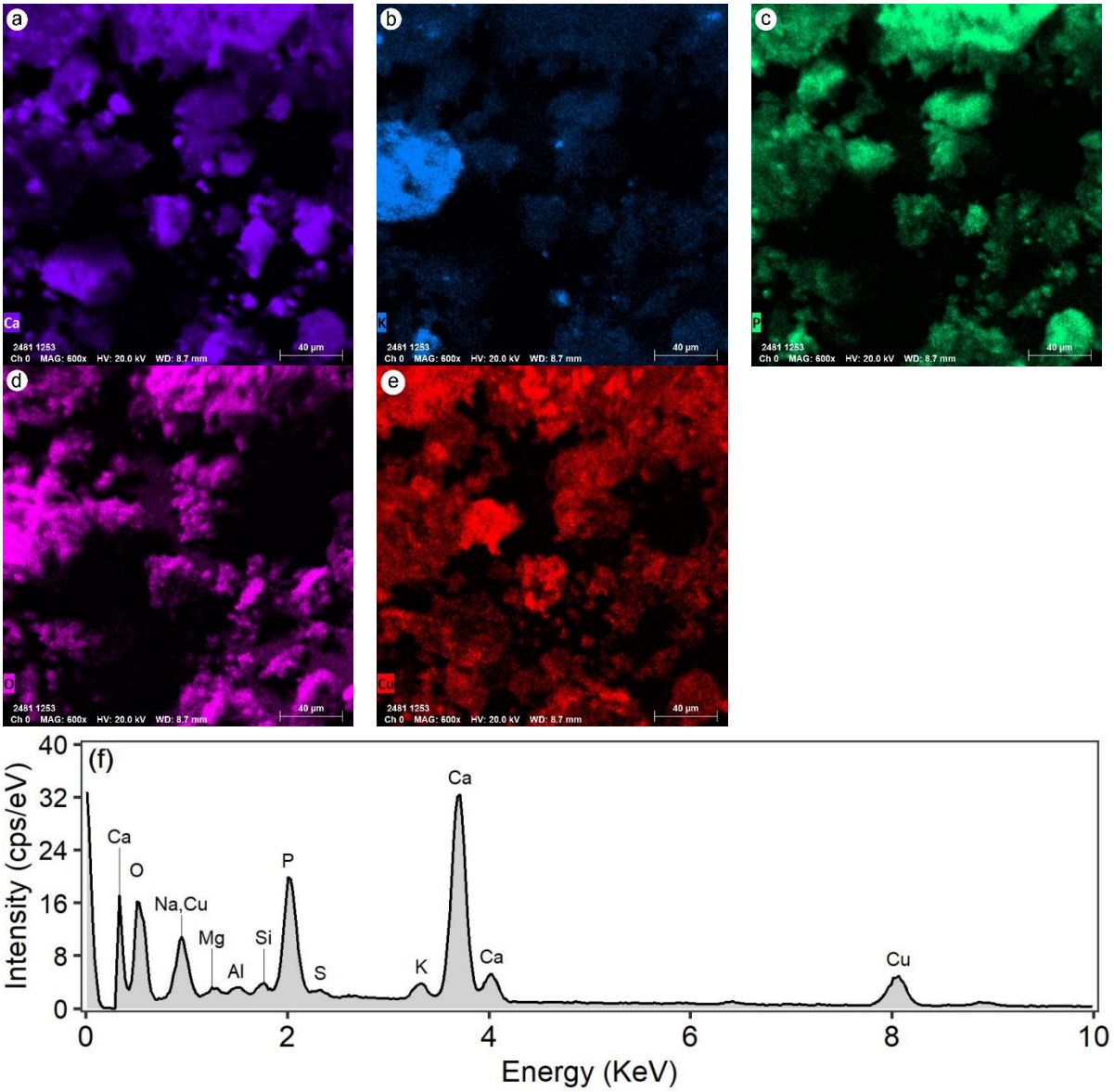

Figure S5 – SEM-EDS mapping for Ca (a), K (b), P (c), O (d), Cu (e) and SEM-EDX spectrum (f) for poultry litter biochar copper fertilizer (PLB-Cu).

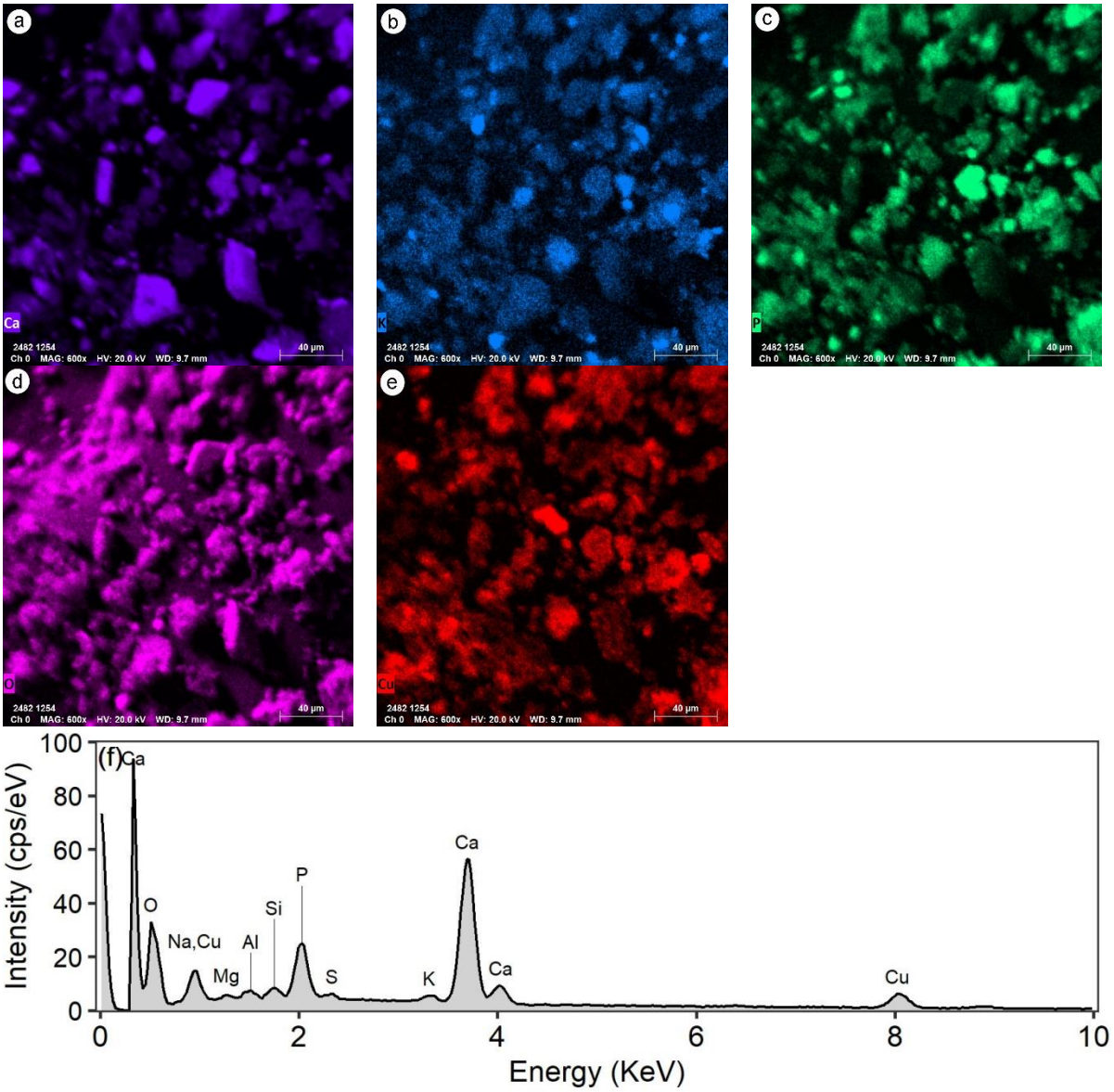

Figure S6 – SEM-EDS mapping for Ca (a), K (b), P (c), O (d), Cu (e), and SEM-EDX spectrum (f) for graphene oxide enriched poultry litter biochar copper fertilizer (PLB-GO-Cu).

Biochar-based micronutrient fertilizer properties

Table S6 – Total nutrient content, C content, pH, EC and copper and zinc solubility (g kg^{-1}) of biochar-based micronutrient fertilizers (BBF).

BBFs	Phosphorus (P[a])	Potassium (K)	Calcium (Ca)	Magnesium (Mg)	Sulphur (S)
PLB-Zn	57.0±0.58	18.8±0.18	247±1.78	9.49±0.07	5.12±0.02
PLB-GO-Zn	56.2±0.96	14.1±0.17	243±3.06	8.58±0.14	5.57±0.06
PLB-Cu	54.7±0.29	10.1±0.14	243±1.66	6.52±0.08	5.76±0.03
PLB-GO-Cu	53.2±0.11	9.53±0.15	252±1.19	6.12±0.07	6.80±0.00
	Copper (Cu)	Zinc (Zn)	Manganese (Mn)	Iron (Fe)	
PLB-Zn	0.11±0.00	42.3±0.55	0.96±0.01	6.06±0.05	
PLB-GO-Zn	0.11±0.00	50.2±0.87	0.90±0.02	5.74±0.09	
PLB-Cu	43.8±0.39	0.83±0.06	0.85±0.02	5.88±0.02	
PLB-GO-Cu	42.6±0.14	0.63±0.01	0.77±0.01	5.62±0.04	
	C content[c] (%)	pH[c] (1:2.5)	EC[c] (mS cm^{-1})		
PLB-Zn	22.2±0.32	8.04±0.00	0.29±0.00		
PLB-GO-Zn	22.0±0.16	7.82±0.01	0.32±0.01		
PLB-Cu	22.1±0.60	7.54±0.02	0.51±0.01		
PLB-GO-Cu	21.9±0.46	7.45±0.02	0.42±0.00		
	Solubility[b] (g kg^{-1})	Water	Citric acid	NAC+Water[d]	
PLB-Zn	Zinc	0.01	42.5	39.5	
PLB-GO-Zn	(Zn)	0.08	51.0	47.9	
PLB-Cu	Copper	0.05	40.8	44.5	
PLB-GO-Cu	(Cu)	0.05	42.1	44.6	

[a] Mean ± SEM (n = 3); [b] According to Brasil (2017); [c] Mean ± SEM (n = 2); [d] Neutral ammonium citrate; EC = Electric conductivity; C = Carbon.

Copper and Zinc release kinetics

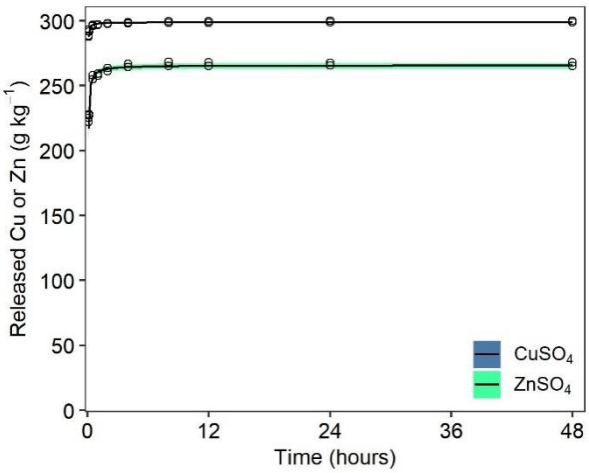

Figure S7 – Kinetics of copper and zinc release in water from conventional micronutrient fertilizers. Notes: points are experimental data; color shading indicates 95% confidence interval), and lines are data predicted by the best-fitting model.

Plant height and total dry mass

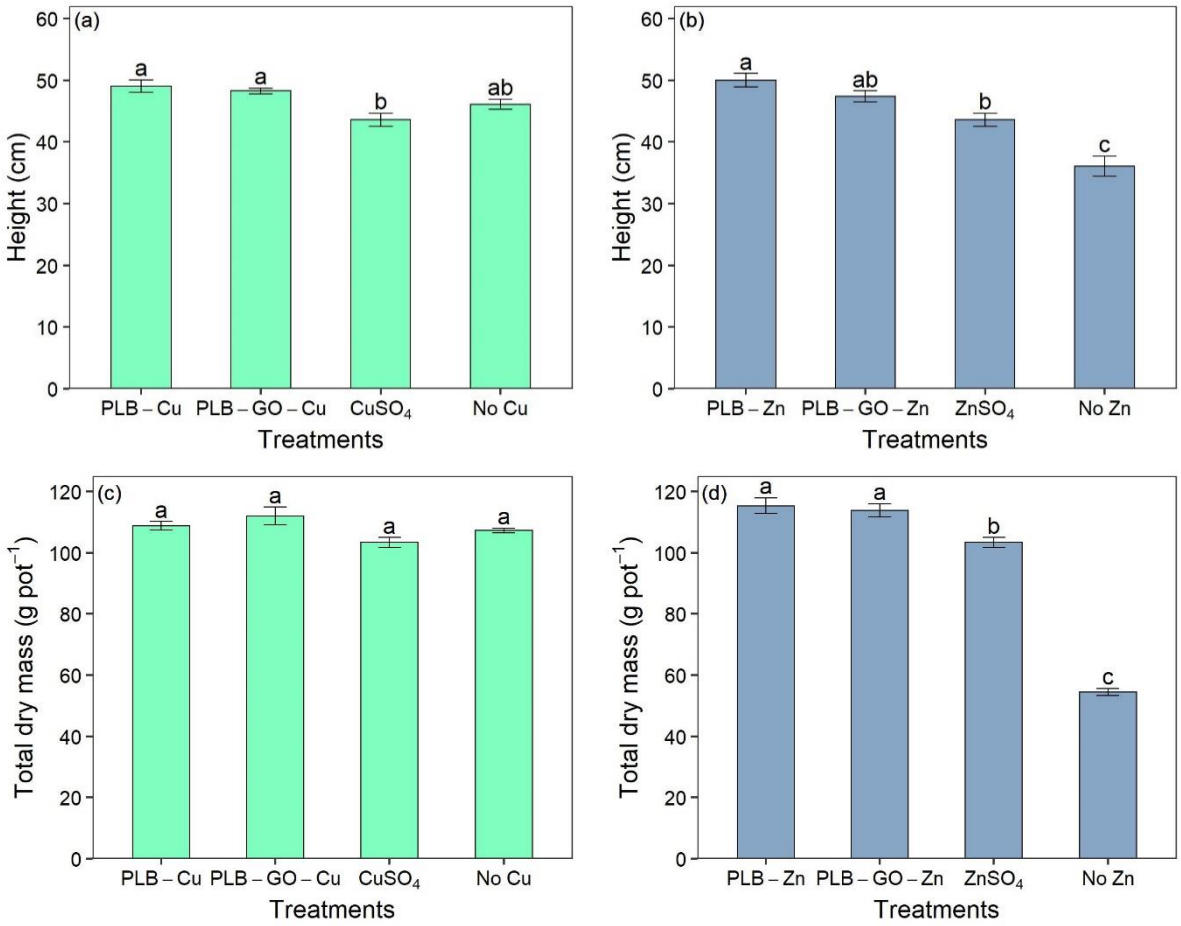

Figure S8 – Plant height (a and b) and total dry mass (c and d) of common bean plants for copper and zinc fertilization, respectively, using BBFs and conventional fertilizers. Means followed by the same letters in the bars do not differ from each other according to the Tukey test ($p< 0.05$); Error bars represent standard error of the mean (n = 4).

Total Copper and Zinc uptake

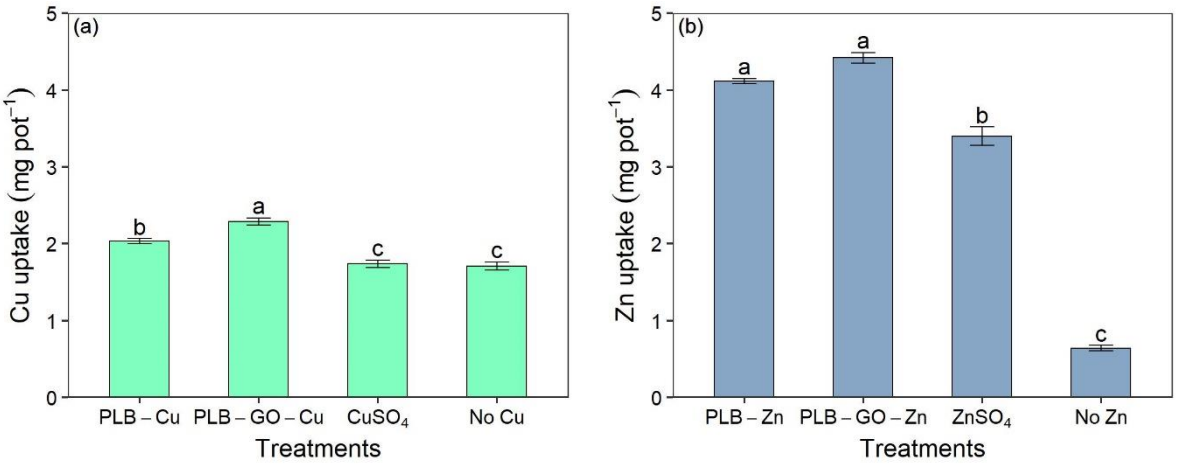

Figure S9 – Total copper (a) and zinc (c) uptake of common bean plants for copper and zinc fertilization, using BBFs and conventional fertilizers. Means followed by the same letters in the bars do not differ from each other according to the Tukey test ($p< 0.05$); Error bars represent standard error of the mean (n = 4).

Copper and Zinc content in plants and grains

Table S7 – Copper and zinc content (g kg^{-1}) [mean ± standard error of the mean (n = 4)] in plants and grains.

Treatments	Shoot dry mass	Grains
Copper fertilization	Copper content (mg kg^{-1})	
No Cu	15.4 ± 0.52 b	16.7 ± 0.44 b
PLB-Cu	17.1 ± 0.43 b	20.8 ± 0.54 a
PLB-GO-Cu	21.5 ± 0.95 a	19.4 ± 0.68 ab
$CuSO_4$	15.2 ± 0.33 b	18.5 ± 0.39 ab
Zinc fertilization	Zinc content (mg kg^{-1})	
No Zn	9.87 ± 0.24 c	17.8 ± 0.77 c
PLB-Zn	33.3 ± 1.06 a	38.8 ± 0.27 b
PLB-GO-Zn	35.5 ± 1.63 a	43.5 ±0.86 a
$ZnSO_4$	26.7 ± 0.68 b	40.1 ± 0.81 ab

*Means followed by the same letters in the columns do not differ from each other according to the Tukey test ($p < 0.05$).

Soil pH

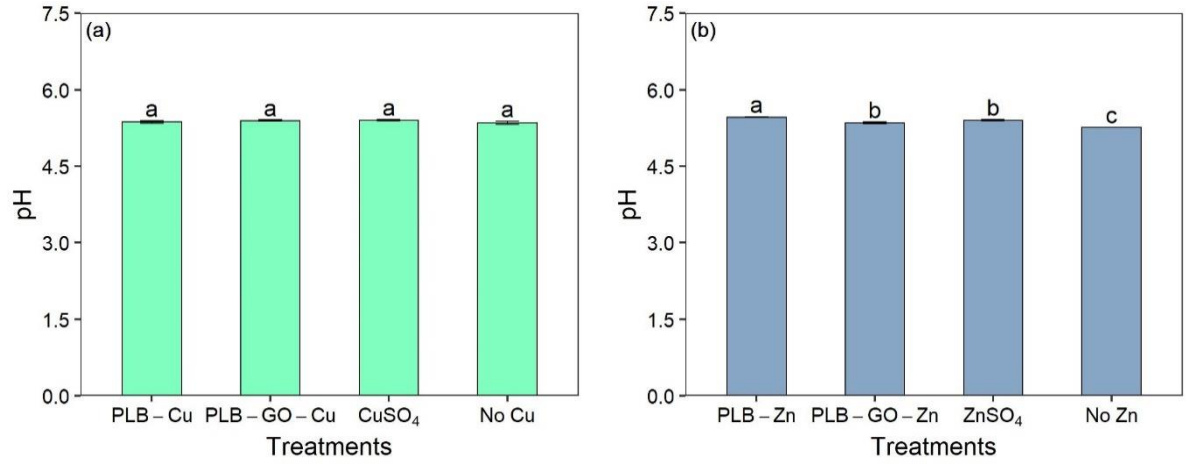

Figure S10 – Soil pH in water after common bean plants grown under copper (a) and zinc fertilization (b), using BBFs and conventional fertilizers. Notes: Means followed by the same letters in the bars do not differ from each other according to the Tukey test ($p < 0.05$); Error bars represent standard error of the mean (n = 4).

Plant growth in some different development stages under Cu and Zn fertilization

Figure S11 – Common bean plants grown under copper fertilization, 30 days after emergence.

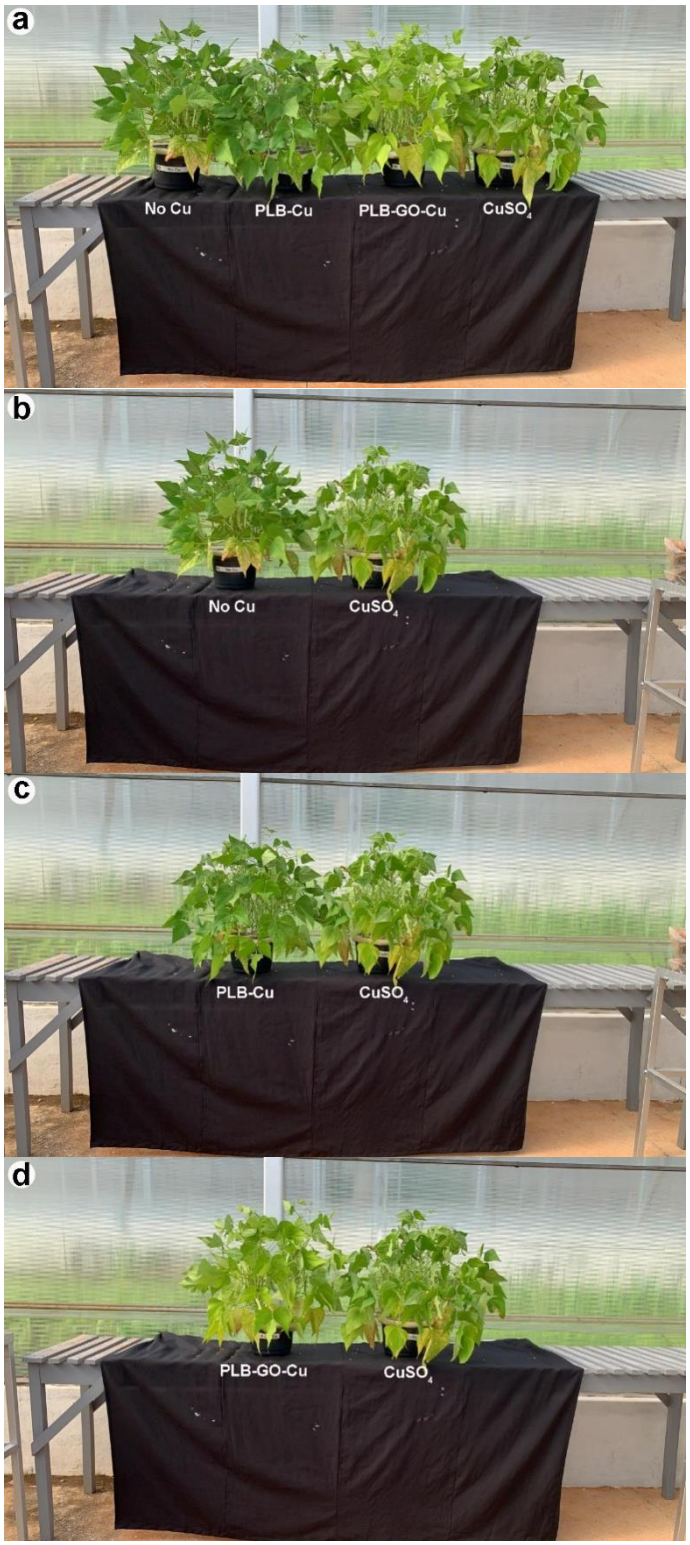

Figure S12 – Common bean plants grown under copper fertilization, 50 days after emergence.

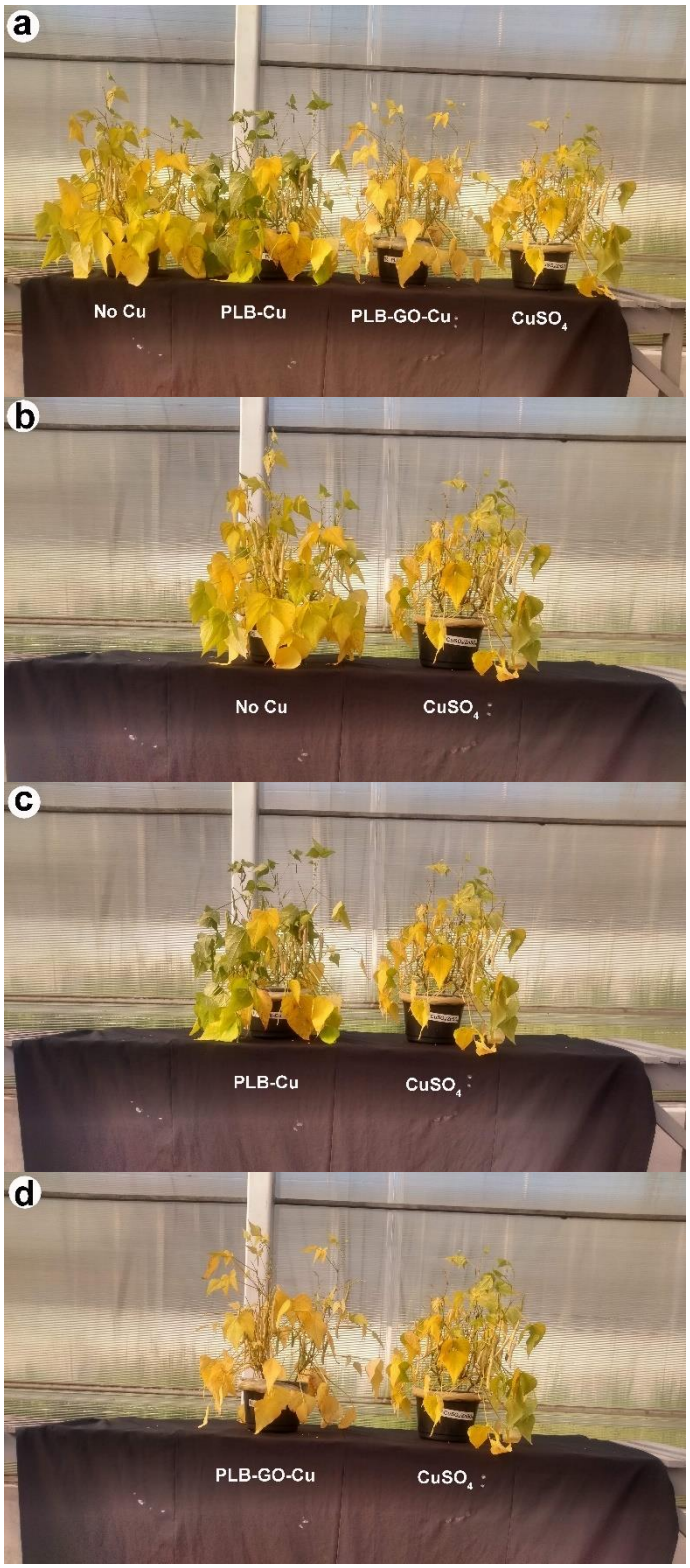

Figure S13 – Common bean plants grown under copper fertilization, 60 days after emergence.

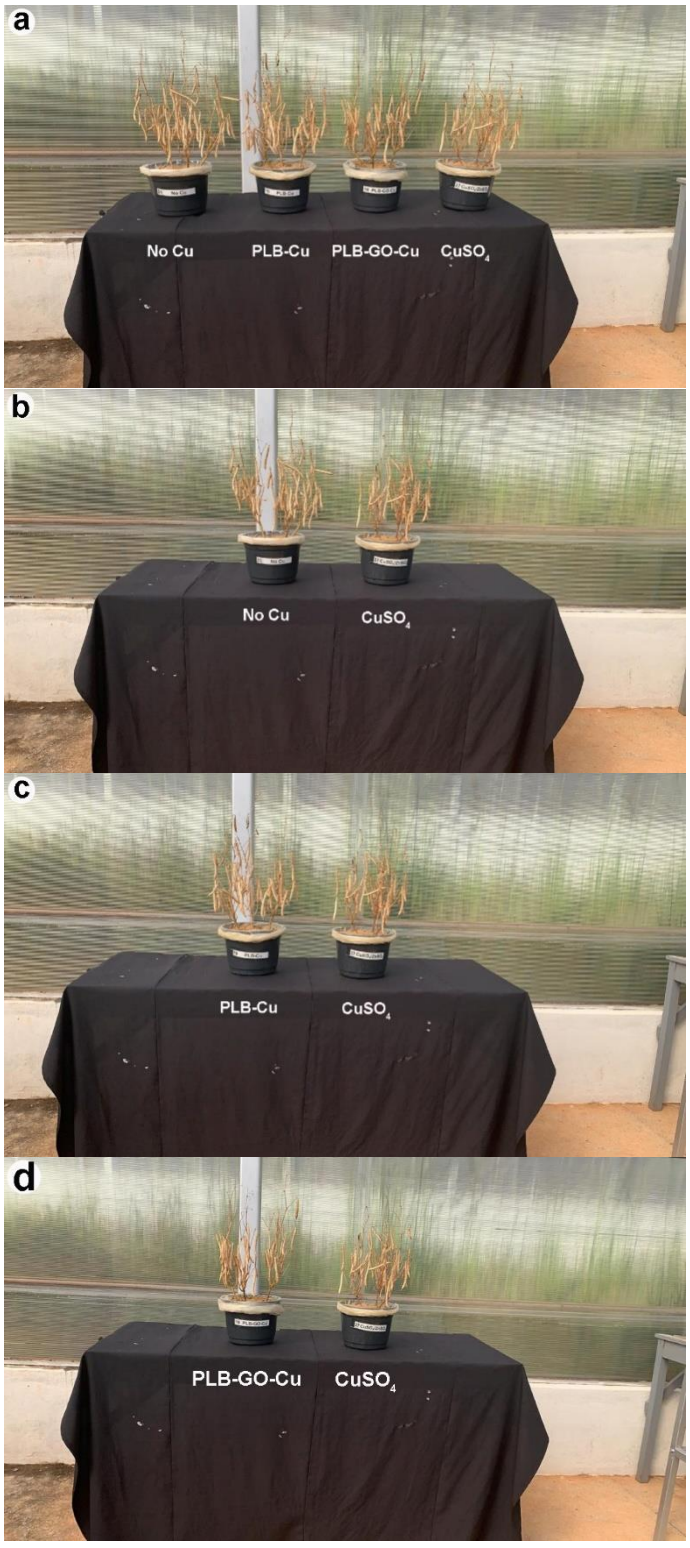

Figure S14 – Common bean plants grown under copper fertilization, 80 days after emergence.

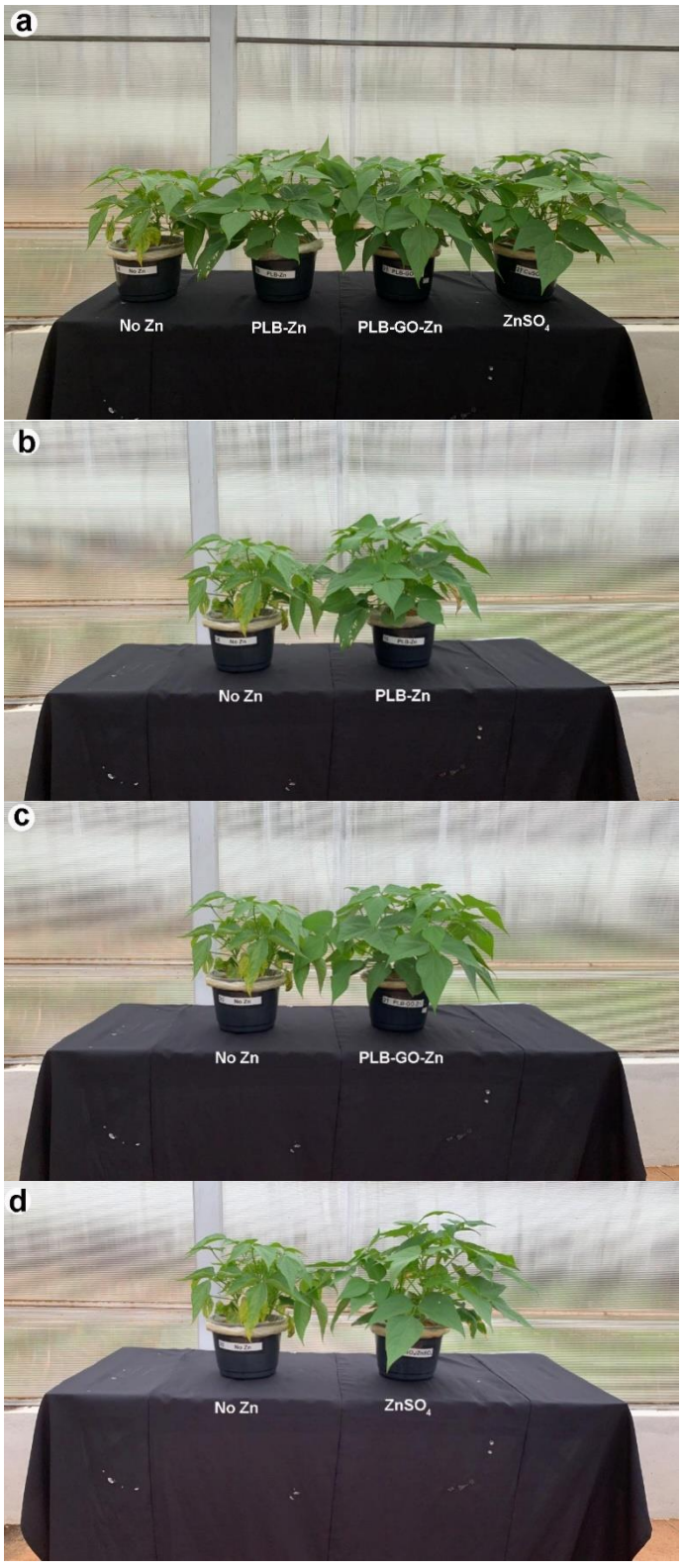
a
No Zn
PLB-Zn
PLB-GO-Zn
ZnSO4
b
No Zn
PLB-Zn
c
No Zn
PLB-GO-Zn
d
No Zn
ZnSO4

Figure S15 – Common bean plants grown under zinc fertilization, 30 days after emergence.

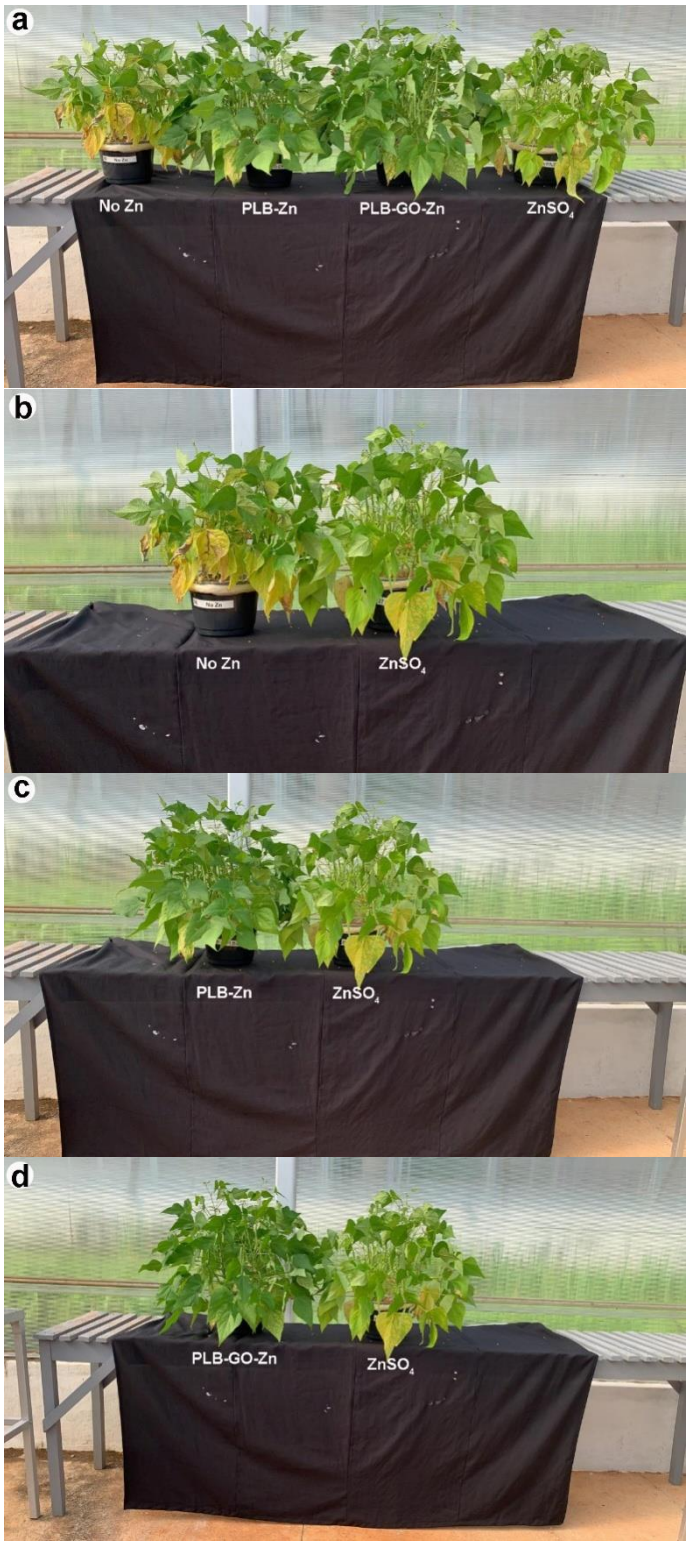

Figure S16 – Common bean plants grown under zinc fertilization, 50 days after emergence.

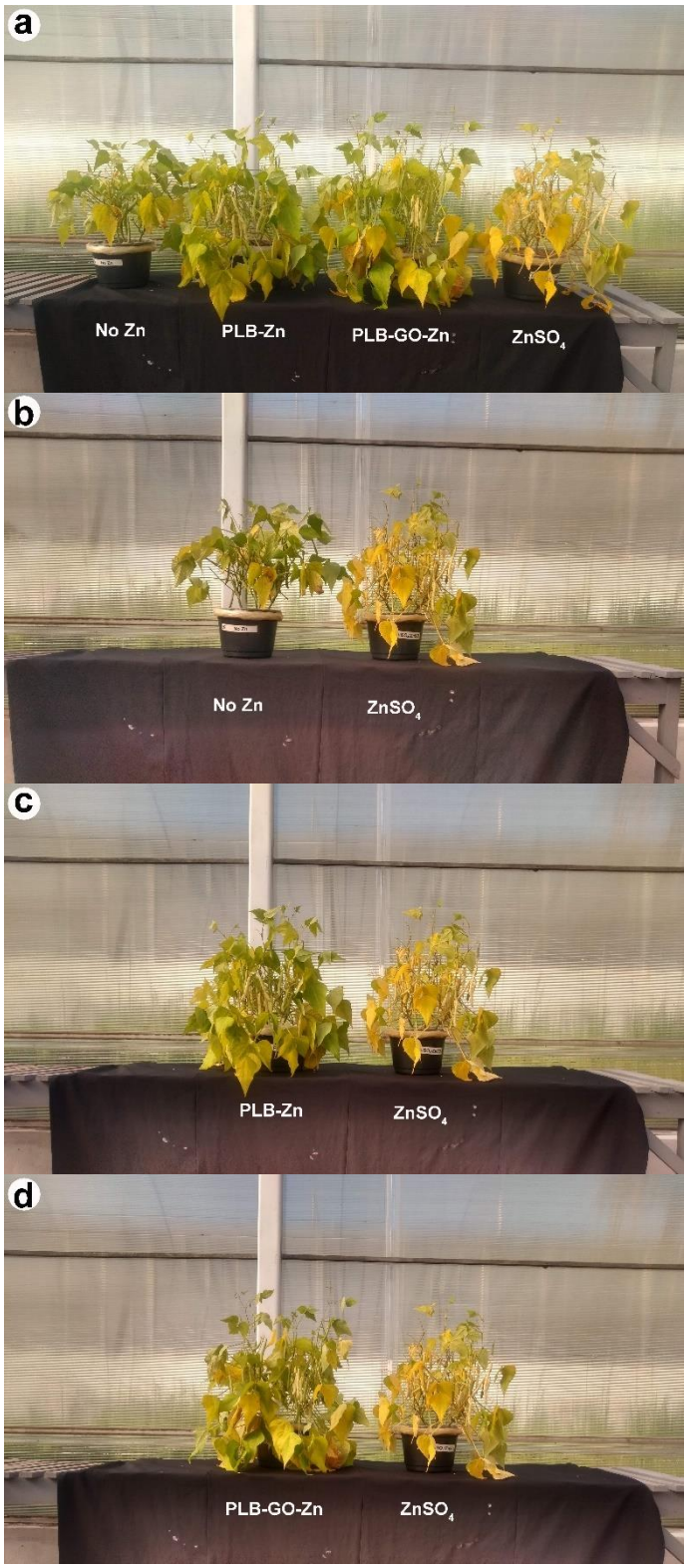

Figure S17 – Common bean plants grown under zinc fertilization, 60 days after emergence.

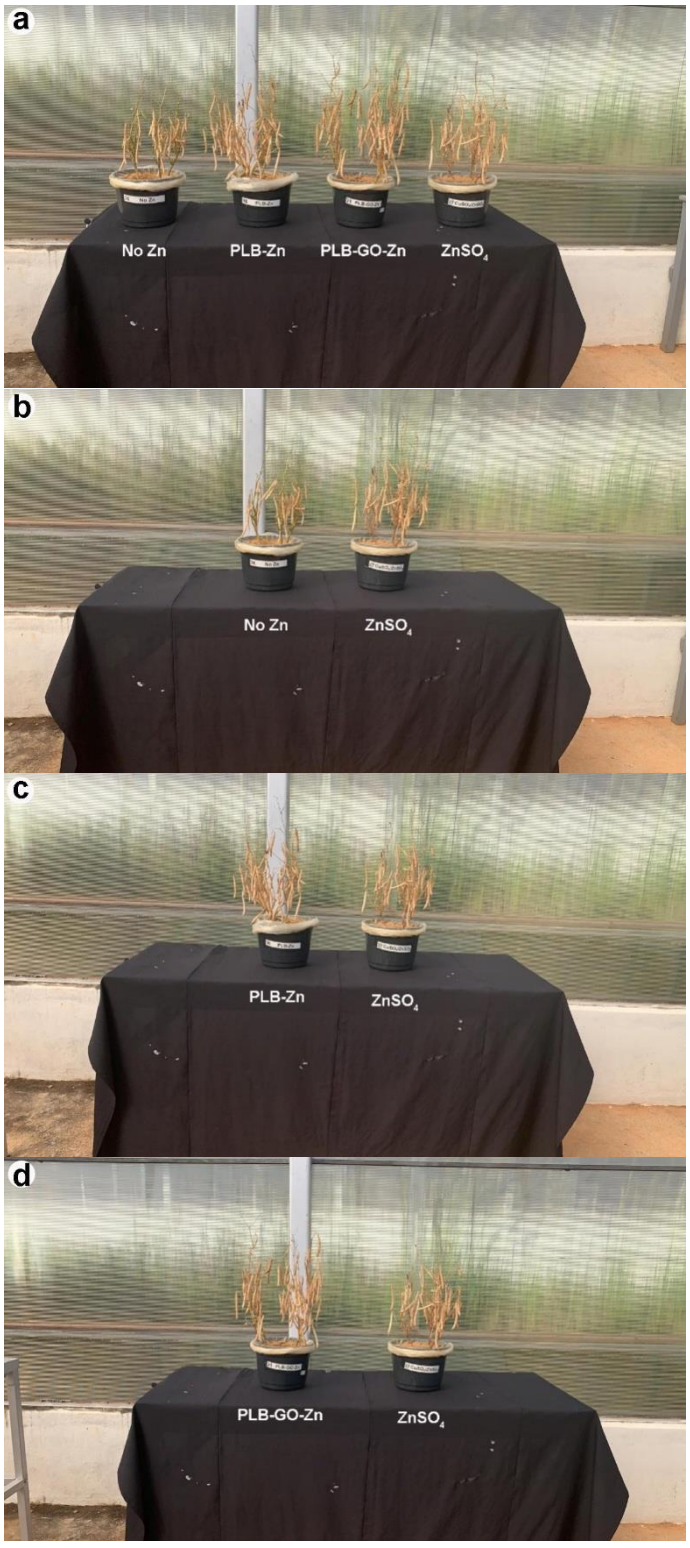

Figure S18 – Common bean plants grown under zinc fertilization, 80 days after emergence.

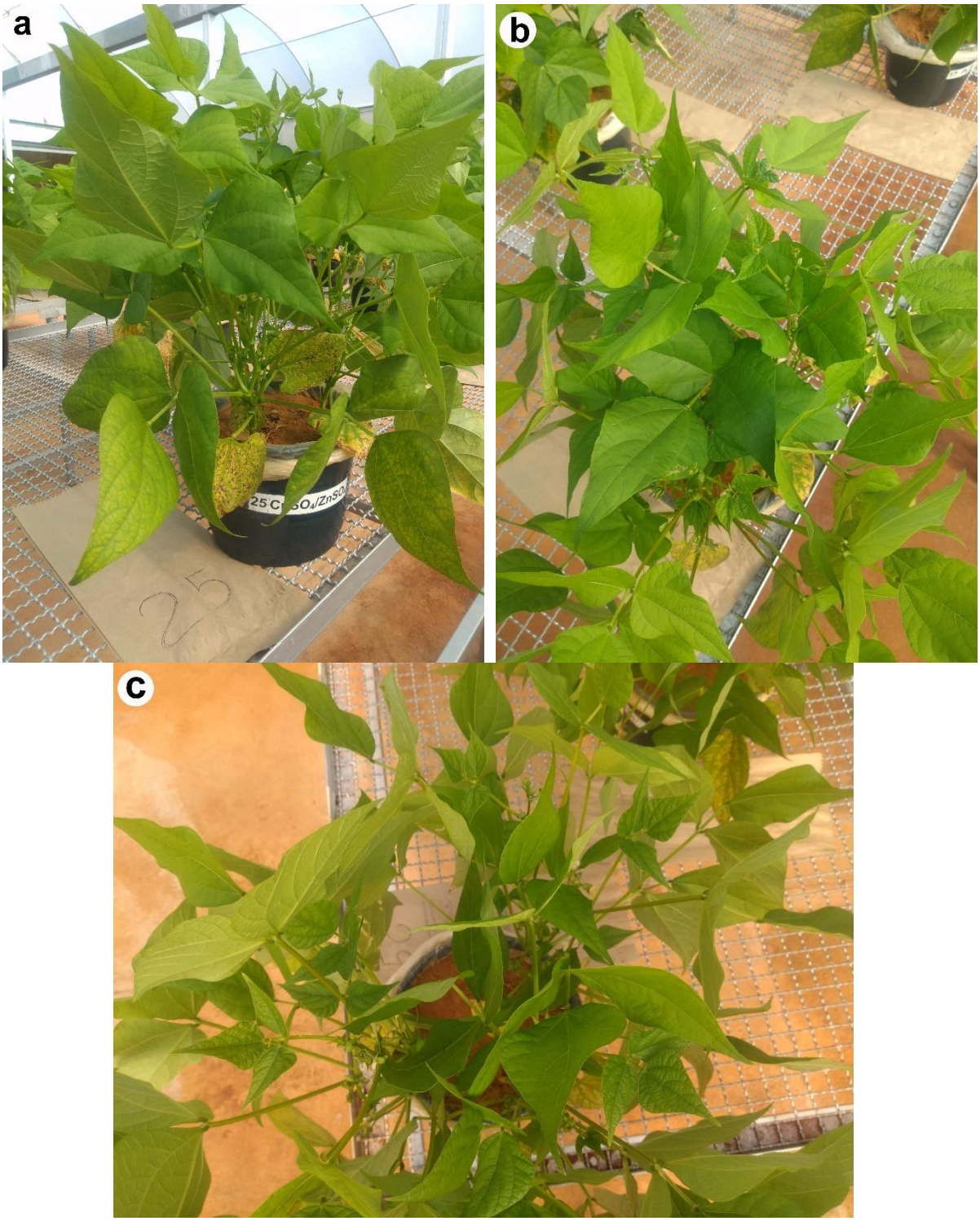
a
b
c


d
e

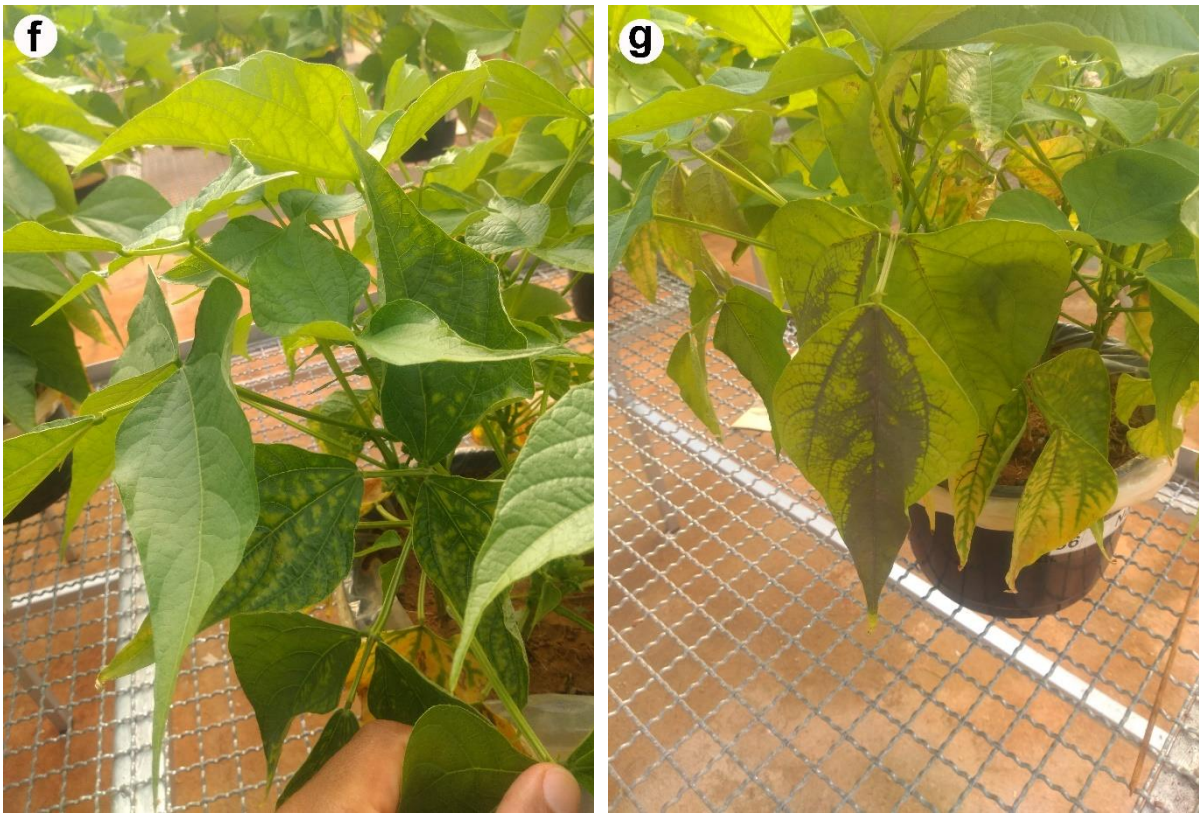

Figure S19 – Common bean plants grown under copper and zinc fertilization (a and b), no copper fertilization (c and d) and no zinc fertilization (e and f), 37 days and 47 days (g) after emergence.

References

Abdallah, M.M., Ahmad, M.N., Walker, G., Leahy, J.J., Kwapinski, W., 2019. Batch and Continuous Systems for Zn, Cu, and Pb Metal Ions Adsorption on Spent Mushroom Compost Biochar. Ind. Eng. Chem. Res. 58, 7296–7307. https://doi.org/10.1021/acs.iecr.9b00749

Akaike, H., 1974. A New Look at the Statistical Model Identification. IEEE Trans. Automat. Contr. 19, 716–723. https://doi.org/10.1109/TAC.1974.1100705

Bishnoi, A., Kumar, S., Joshi, N., 2017. Wide-Angle X-ray Diffraction (WXRD): Technique for Characterization of Nanomaterials and Polymer Nanocomposites, in: Microscopy Methods in Nanomaterials Characterization. Elsevier Inc., pp. 313–337. https://doi.org/10.1016/b978-0-323-46141-2.00009-2

Brasil, 2017. Manual de métodos analíticos oficiais para fertilizantes e corretivos. MAPA, Ministério da Agricultura Pecuária e Abastecimento/SDA, Secretaria de Defesa Agropecuária, Brasilia - DF.

Chen, X., Chen, G., Chen, L., Chen, Y., Lehmann, J., McBride, M.B., Hay, A.G., 2011. Adsorption of copper and zinc by biochars produced from pyrolysis of hardwood and corn straw in aqueous solution. Bioresour. Technol. 102, 8877–8884. https://doi.org/10.1016/j.biortech.2011.06.078

Deng, H., Li, Q., Huang, M., Li, A., Zhang, J., Li, Y., Li, S., Kang, C., Mo, W., 2020. Removal of Zn(II), Mn(II) and Cu(II) by adsorption onto banana stalk biochar: Adsorption process and mechanisms. Water Sci. Technol. 82, 2962–2974. https://doi.org/10.2166/wst.2020.543

Kingdom, F.A.A., Prins, N., 2016. Model Comparisons, in: Kingdom, F.A.A., Prins, N. (Eds.), Psychophysics: A Pratical Introduction. Academic press, United States of America, pp. 247–307. https://doi.org/10.1016/b978-0-12-407156-8.00009-8

Lustosa Filho, J.F., Penido, E.S., Castro, P.P., Silva, C.A., Melo, L.C.A., 2017. Co-Pyrolysis of Poultry Litter and Phosphate and Magnesium Generates Alternative Slow-Release Fertilizer Suitable for Tropical Soils. ACS Sustain. Chem. Eng. 5, 9043–9052. https://doi.org/10.1021/acssuschemeng.7b01935

Marcano, D.C., Kosynkin, D. V., Berlin, J.M., Sinitskii, A., Sun, Z., Slesarev, A.S., Alemany, L.B., Lu, W., Tour, J.M., 2018. Correction to Improved Synthesis of Graphene Oxide. ACS Nano 12, 2078–2078. https://doi.org/10.1021/acsnano.8b00128

Marcano, D.C., Kosynkin, D. V, Berlin, J.M., Sinitskii, A., Sun, Z., Slesarev, A., Alemany, L.B., Lu, W., Tour, J.M., 2010. Improved Synthesis ofGraphene Oxide. ACS Nano 4, 4806–4814. https://doi.org/10.1021/nn1006368

Pholosi, A., Naidoo, E.B., Ofomaja, A.E., 2020. Intraparticle diffusion of Cr(VI) through biomass and magnetite coated biomass: A comparative kinetic and diffusion study. South African J. Chem. Eng. 32, 39–55. https://doi.org/10.1016/j.sajce.2020.01.005

Rodríguez-Vila, A., Selwyn-Smith, H., Enunwa, L., Smail, I., Covelo, E.F., Sizmur, T., 2018. Predicting Cu and Zn sorption capacity of biochar from feedstock C/N ratio and pyrolysis temperature. Environ. Sci. Pollut. Res. 25, 7730–7739. https://doi.org/10.1007/s11356-017-1047-2

Shariatmadari, H., Shirvani, M., Jafari, A., 2006. Phosphorus release kinetics and availability in calcareous soils of selected arid and semiarid toposequences. Geoderma 132, 261–272. https://doi.org/10.1016/j.geoderma.2005.05.011

Simonin, J.P., 2016. On the comparison of pseudo-first order and pseudo-second order rate laws in the modeling of adsorption kinetics. Chem. Eng. J. 300, 254–263. https://doi.org/10.1016/j.cej.2016.04.079

Song, J., Zhang, S., Li, G., Du, Q., Yang, F., 2020. Preparation of montmorillonite modified biochar with various temperatures and their mechanism for Zn ion removal. J. Hazard.

Mater. 391, 121692. https://doi.org/10.1016/j.jhazmat.2019.121692

Wu, F.C., Tseng, R.L., Juang, R.S., 2009. Initial behavior of intraparticle diffusion model used in the description of adsorption kinetics. Chem. Eng. J. 153, 1–8. https://doi.org/10.1016/j.cej.2009.04.042

Zhao, S., Ta, N., Wang, X., 2020. Absorption of Cu(II) and Zn(II) from aqueous solutions onto biochars derived from apple tree branches. Energies 13. https://doi.org/10.3390/en13133498

FOURTH PART

FINAL REMARKS

Two studies were carried out under greenhouse conditions, and showed the ability of BBF to nutrient use efficiency by plants when compared with conventional fertilizer sources. The first study was carried out with P, which is considered one of the most limiting nutrients for agricultural production in tropical regions. Cultivated areas in Brazil generally requires the application of large amounts of this nutrient, aiming at obtaining high levels of crop productivity due to the high soil P fixing capacity. Thus, alternative technologies must be developed to ensure agricultural sustainability.

Phosphorus biochar-based fertilizers (BBF), through the pyrolysis of P-enriched feedstock has shown promising results, but studies that evaluate the residual effect of the fertilization were lacking. Thus, in this first study we evaluated the long-term effect of P-containing biochar fertilizers using three successive crops (grass, maize, and common beans) compared with conventional fertilizer (triple superphosphate – TSP). Despite the slow P release profile of BBF when compared with TSP, similar or higher crop yields were observed, either in the short- or long-term using different crops. The novelty of this BBF was the incorporation of MgO present, that contributed to the synergistic effect with P, increasing the performance of BBFs as phosphate fertilizers. Either the BBF application alone or in combination with TSP is recommended and showed that BBF can replace partially or totally the conventional fertilizer source. The effect of BBF in the short-term is due to its lower P release and protection against fast adsorption in the soil components. The BBFs effect was more related to plant growth and P uptake than TSP fertilizer, showing their considerable effect on plant development and nutrition. BBFs application increases the P reserves in the soil due to its insoluble forms, such as Ca/Mg-pyrophosphate.

Despite the positive results, the P-containing BBFs were produced using phosphoric acid (H_3PO_4) as P source, which can increase the production cost. Therefore, alternative sources of P for the enrichment of biomass should be considered, such as phosphate rocks, bone meal, etc. using a bio-augmentation approach. In addition, studies under field conditions should be carried out to confirm the results obtained under controlled conditions, both in the short- and long-term. Since P has a complex dynamic due to its great interaction with soil components, evaluating the effect of these BBFs in different soils could be an alternative to elucidate questions regarding its plant use efficiency.

Similarly, to P, copper (Cu) and zinc (Zn) have naturally a low availability in tropical soils and present a complex interaction with soil components. The main fertilizer sources used to supply these micronutrients have high solubility and fast release, which favors their low plant use efficiency when applied to highly weathered soils due to the rapid interaction with mineral and organic soil constituents. Considering the importance of these micronutrients for plants and humans, we seek to develop a material with potential for use as a fertilizer from the combination of biochar and graphene oxide (GO) loaded with these two elements. Biochar is known for its ability to adsorb metals as well as GO. Graphene oxide has several the capacity to improve either chemical and physical properties of fertilizers, but its high cost and difficult scalability make it unfeasible as an additive for fertilizer industries. Thus, we combined a small amount of GO (0.5%, w/w) with biochar with the objective of enhancing the biochar adsorption properties at an affordable cost.

This low amount of GO was sufficient to increase the biochar adsorption capacity of Cu and Zn by the developed materials, which were also tested as nutrient carriers. Copper and Zn adsorbed by biochars present low solubility in water, and when used as fertilizer increases common bean production and micronutrient uptake, especially Zn, that increased even more than the conventional soluble fertilizer. Higher micronutrient use efficiency was attributed to the protection of the adsorption reactions that cationic metals had with soil components due to the functional organic matrix that caused their slow-release and favored plant uptake and nutrient availability after cultivation.

Despite the promising results, more in depth understanding of the micronutrient interactions in the rhizosphere is needed in order to design efficient and cost-effective novel fertilizers with a matrix carrier. Other approaches, such as coating/encapsulating should also be researched and comprehended in more details. As this study was carried out with only one concentration of graphene oxide, the evaluation of different proportions of this material for biochar enrichment should be studied, including other biomasses as feedstock. In addition, an economic study of the production of this BBF can be carried out in order to verify the feasibility of using GO. Finally, research on the residual effect of fertilization in the medium- to long-term as well as research under field conditions must be carried out prior to large scale recommendation.

ABOUT THE AUTHOR

Born in São Félix do Xingu city, in the Para state – Brazil on July 27, 1992. He attended high school integrated to the vocational course Agriculture and Livestock Technician between 2008 and 2010 at the Federal Institute of Education, Science and Technology of Tocantins State – Araguatins *Campus*, Araguatins city, Tocantins – Brazil, formerly known as Federal Agrotechnical School of Araguatins. He studied Agronomy at the Federal University of Tocantins – Gurupi *Campus*, Gurupi city, Tocantins – Brazil between 2011 and 2016, graduating in the first semester of 2016. During this period, he participated in several academic and scientific activities. He was a scholarship of scientific initiation. In addition, he participated in other research related to Soil Science - Soil Fertility and Plant Nutrition, mainly with soil acidity correction, fertilization and nutrition, and use of residues in agriculture. He obtained a Master degree in Soil Science in the area of Soil Fertility and Plant Nutrition by the Graduate Program in Soil Science of the School of Agricultural Sciences, Federal University of Lavras in 2018. The Master Thesis was entitled "Carbon stability of engineered biochar-based phosphate fertilizers". He submitted to obtain the Doctor degree in Soil Science in the area of Soil Fertility and Plant Nutrition by the Graduate Program in Soil Science of the School of Agricultural Sciences, Federal University of Lavras in February 24th, 2022. During his Doctorate he served as a substitute professor in the courses of Agronomy, Animal Science, and Forest Engineering, teaching subjects related to Soil Science at the Federal Rural University of the Amazon – Parauapebas *Campus*, Parauapebas city, Para – Brazil. During the Doctorate he also co-authored more than 10 peer-reviewed articles in scientific journals.